DOE/JPL-1024-78/1
Distribution Category UC-59a

A Fixed Tilt Solar Collector Employing Reversible Vee-Trough Reflectors and Evacuated Tube Receivers for Solar Heating and Cooling Systems

Final Report - Phase II Data Acquisition

M. Kudret Selcuk

October 15, 1978

Prepared for

U.S. Department of Energy
Southwest District Office

by

Jet Propulsion Laboratory
California Institute of Technology
Pasadena, California

(JPL PUBLICATION 78-106)

DISCLAIMER

DOE/JPL-1024-78/1
Distribution Category UC-59a

A Fixed Tilt Solar Collector Employing Reversible Vee-Trough Reflectors and Evacuated Tube Receivers for Solar Heating and Cooling Systems

Final Report - Phase II Data Acquisition

M. Kudret Selcuk

October 15, 1978

Prepared for
U.S. Department of Energy
Southwest District Office
by
Jet Propulsion Laboratory
California Institute of Technology
Pasadena, California
(JPL PUBLICATION 78-106)

Prepared by the Jet Propulsion Laboratory, California Institute of Technology, for the U.S. Department of Energy by agreement with the National Aeronautics and Space Administration.

ABSTRACT

The objective of the Vee-Trough/Evacuated Tube Collector (VTETC) Project, undertaken for the DOE Solar Heating and Cooling Branch, was to show how vee-trough concentrators could improve the heat collection capability and reduce the cost of collectors consisting of evacuated tube receivers. The work was carried out in two phases:

During the first phase, the VTETC was analyzed rigorously and various mathematical models were developed to calculate the optical performance of the vee-trough concentrators and the thermal performance of the evacuated tube receivers. A test bed was constructed to verify the mathematical analyses and compare reflectors made of back-silvered glass mirror, Alzak, Aluminized Teflon, and Kinglux (an electro polished aluminum reflector). Testing was conducted and data was obtained for the months of April to August 1977. The results of the mathematical analyses, as well as the results from 1977, were reported in DOE/JPL/1024-1, published in January 1978.

In the second phase, additional tests were run at temperatures ranging from 80 to 190°C (176 - 374°F) during the months of April, May, June and July 1978.

The results obtained compared well with theoretical predictions. For the glass mirror reflectors, peak efficiencies, based on aperture area and operating temperatures of 125°C (257°F), were over 40%. Efficiencies of about 40% were observed at temperatures of 150°C (302°F) and 30% at 175°C (347°F).

Test data covering a complete day are presented for selected dates throughout the test season. Predicted daily useful heats collected and efficiency values are presented for a full year. These theoretical values are then compared with actual data points for the same temperature range.

The study conducted did not examine a system incorporating an energy storage subsystem and a load. Instead, its purpose was to determine the quasi-steady-state performance of the evacuated tube receiver with and without vee-trough concentrators.

Recommendations are made for the continuation of data acquisition through the winter months to identify year-round performance in an actual solar heating and cooling system, with thermal storage and varying load conditions.

THIS PAGE

WAS INTENTIONALLY

LEFT BLANK

FOREWORD

This report is submitted to the United States Department of Energy, Division of Solar Energy R&D Branch, and covers work conducted by the National Aeronautics and Space Administration, Jet Propulsion Laboratory under Interagency Agreement No. E(49-26)-1024. The work was performed under the direction of Dr. Stephen Sargent, Program Manager from the DOE R&D Branch, Heating and Cooling Office, and Dr. R. Kirk Collier, the Contract Monitor from the Los Alamos Scientific Laboratories.

ACKNOWLEDGEMENT

This project was conducted by members of the Jet Propulsion Laboratory (JPL) Technical Staff, with Dr. M. Kudret Selcuk as Principal Investigator.

Mr. Alan Aghan was the key person in operating the test setup and evaluating the data acquired.

Instrumentation for temperature and flow measurements were calibrated by the JPL Instrumentation Section, headed by Mr. Daniel C. Griffin, Jr. The assistance of Mr. James A. Bryant is gratefully acknowledged.

During this second phase of the project, the analytical tools developed and the test setup built during the first phase were used extensively for experimentation. Contributors to the first phase, in alphabetical order were: Mr. Nabil El Gabalawi of JPL; Dr. Frances P. Fehlner of Corning Glass Works (CGW); Mr. Eugene W. Noller and Mr. Edward L. Noon of JPL; Dr. Kemal Onat of Istanbul Technical University; Dr. Ugur Ortabasi (CGW); Mr. Donald D. Schneider and Dr. Burton Zeldin of JPL.

Dr. V. C. Truscello was the Program Manager for JPL.

CONTENTS

CONTENTS (Continued)

Tables

NOMENCLATURE

Symbol	Item	Unit
A	area	m^2 (ft^2)
A_c	collector area	m^2 (ft^2)
A_p	absorber plate area	m^2 (ft^2)
CR	concentration ratio	dimensionless
C_p	specific heat	kJ/kg ^oC (Btu/lb ^oF)
d	density	kg/m^3 (lb/gal.)
F_R	heat removal factor	dimensionless
I_t	total radiation intensity	W/m^2 (Btu/hr-ft^2)
L	length	m (ft)
$\dot{m}$	mass flow rate	kg/hr (lb/hr)
N	day number	dimensionless
Q_{in}	incident heat	Watts (Btu/hr)
Q_u	useful heat	Watts (Btu/hr)
Q_L	lost heat	Watts (Btu/hr)
T	temperature	^oC (^oF)
T_a	ambient temperature	^oC (^oF)
T_{fi}	fluid inlet temperature	^oC (^oF)
T_{fo}	fluid outlet temperature	^oC (^oF)
ΔT	temperature difference	deg.C. (deg.F)
U_L	heat loss coefficient	W/m^2 ^oC (Btu/hr-ft^2 ^oF)
V	wind speed	m/sec (mph)

Greek Symbols

α	absorptivity	dimensionless
ε	emissivity	dimensionless
η	efficiency	dimensionless

NOMENCLATURE (Continued)

Symbol	Item	Unit
ρ	reflectivity	dimensionless
$(T\alpha)_e$	effective transmittance absorptance product	dimensionless
T	transmittance	dimensionless
σ_o	Stephan-Boltzmann constant	$W/m^2\ {}^oK^4$ (Btu/hr ft^2R^4)
ϕ	latitude	degrees

Subscripts

a	ambient
c	collector
d	diffuse
f	fluid
g	glass
i	inlet
o	outlet
p	plate

SECTION 1

INTRODUCTION

This report discusses the analyses and the experiments conducted on vee-trough concentrators to demonstrate their usefulness in improving the heat collection capability and reducing the cost of solar collectors consisting of evacuated tube receivers. This work was performed at the Jet Propulsion Laboratory (JPL) during a contract period from October 1977 to October 1978. Preliminary work on this project was started in June 1976 under the sponsorship of the Department of Energy, Solar Heating and Cooling Branch, with contract extensions to October 1978.

Optical performance analyses were undertaken for asymmetric vee-troughs at various angles of reflector tilt and aperture sizes. Thermal performance analyses of evacuated tube receivers with a flat plate absorber was also carried out with and without the vee-trough concentrators. These evacuated glass tube receivers were developed by the Corning Glass Works, Corning, New York.

Analytical results were verified with data acquired using an experimental setup designed specifically for this purpose. Test temperatures ranged from 90 to 190°C (194 to 374°F) and data were collected during the spring and summer of 1978 at different temperatures.

1.1 VEE-TROUGH COLLECTOR CONFIGURATION

The experimental setup used flat plate absorbers enclosed in evacuated glass tubes. Four such tubes were used in the setup and each tube was nested between two fixed tilt concentrators as shown in Figures 1-1 and 1-2. The alternate positions of the concentrators for winter and summer operation are also shown. The angles on the reflectors are changed twice a year on the seasonal equinoxes by simply reversing the lightweight triangular reflector assemblies. This vee-trough collector configuration eliminates the tilt adjustments necessary with a collector box assembly, or the complications of a sun tracking system. The plumbing lines are stationary; no flexible fluid lines or movable joints are used, thus eliminating leakage problems. System installation, operation and maintenance costs are correspondingly reduced. Figures 1-3 through 1-6 show photographs of the actual test setup.

The copper heat transfer tubes that run through the evacuated glass tubes are connected in series and a heat transfer fluid, Therminol 44*, is pumped through the system. A series arrangement assures an identical mass flow rate for each tube. Although the fluid inlet temperature varies from tube to tube, the effects of this variation are bypassed by evaluating the performance of the individual tube at its inlet/outlet temperature.

*Heat transfer oil provided by Monsanto Chemicals, Properties in Appendix C.

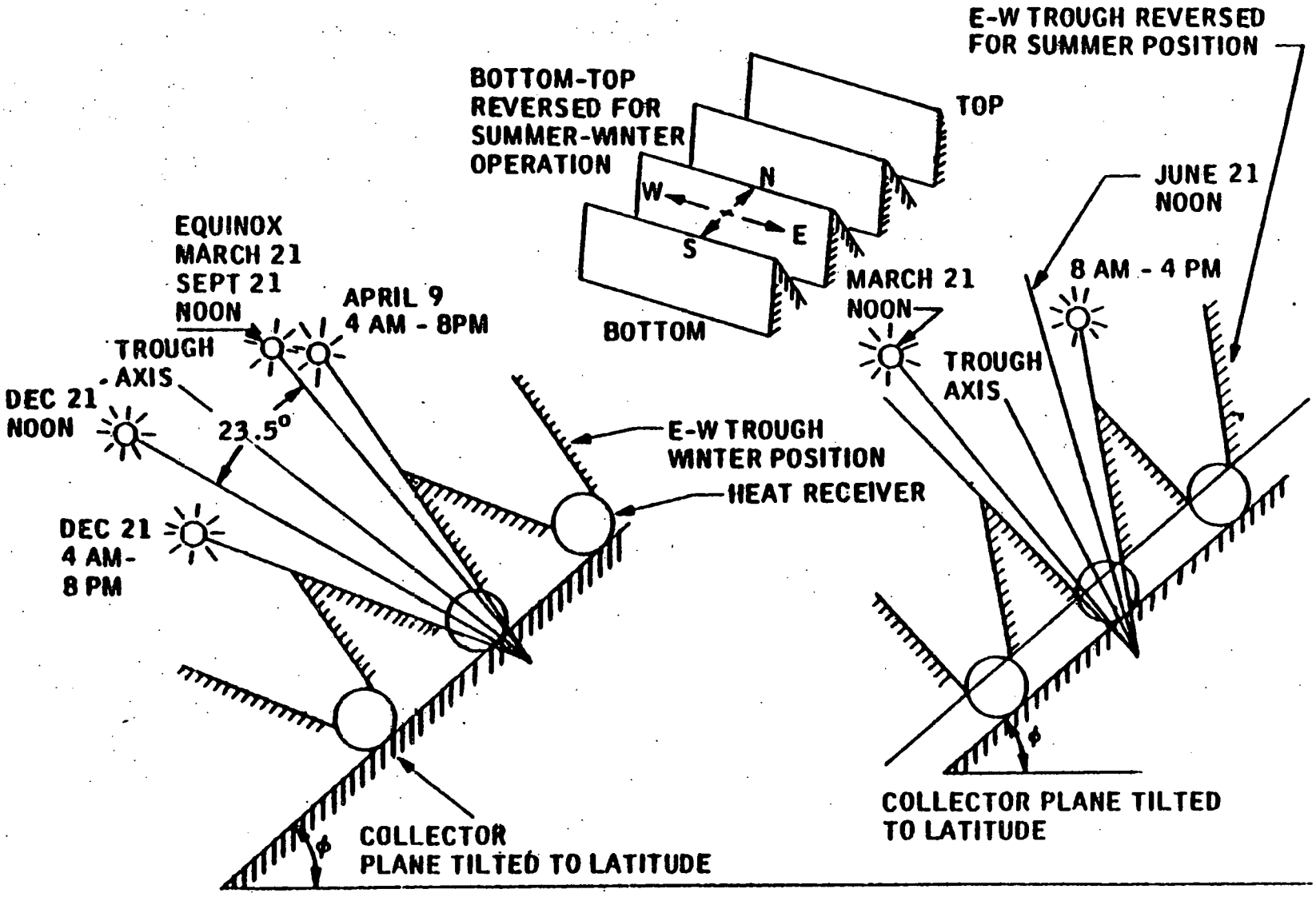

Figure 1-1. Vee-Trough /Concentrator Concept

Dimensions of vacuum tube receiver courtesy of Corning Glass Works, Corning, N.Y.

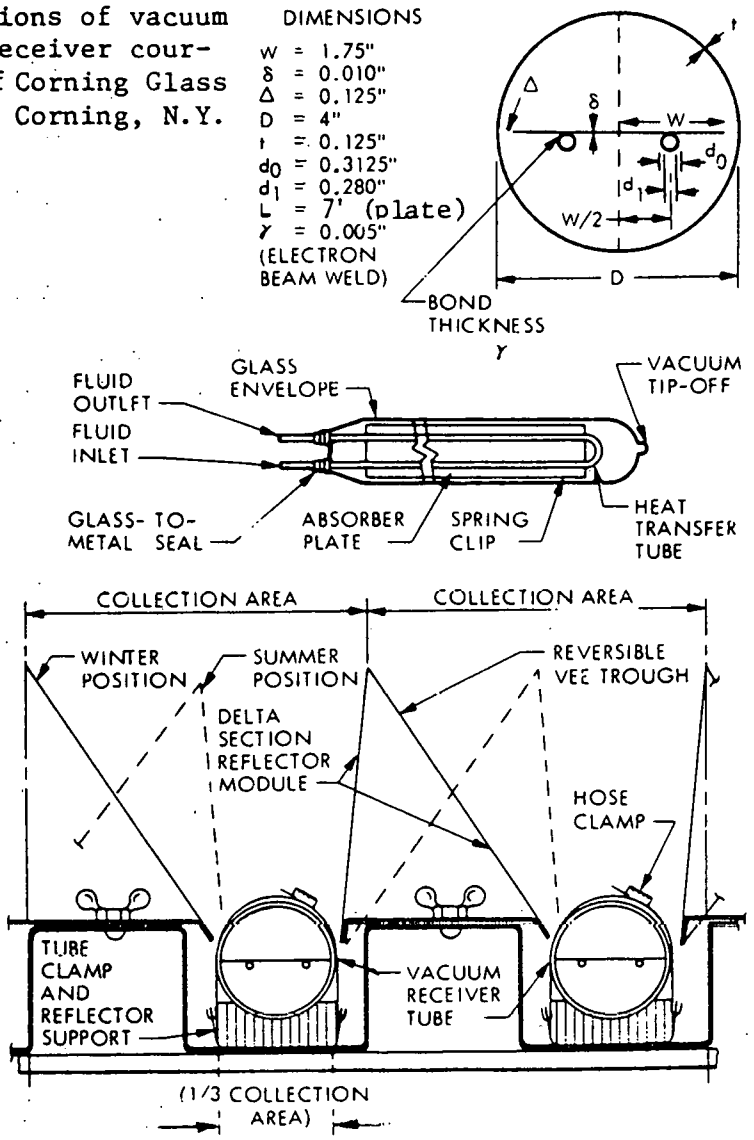

Figure 1-2. Reversible, Asymmetric Vee-Trough Concentrator and Evacuated Tube Collector

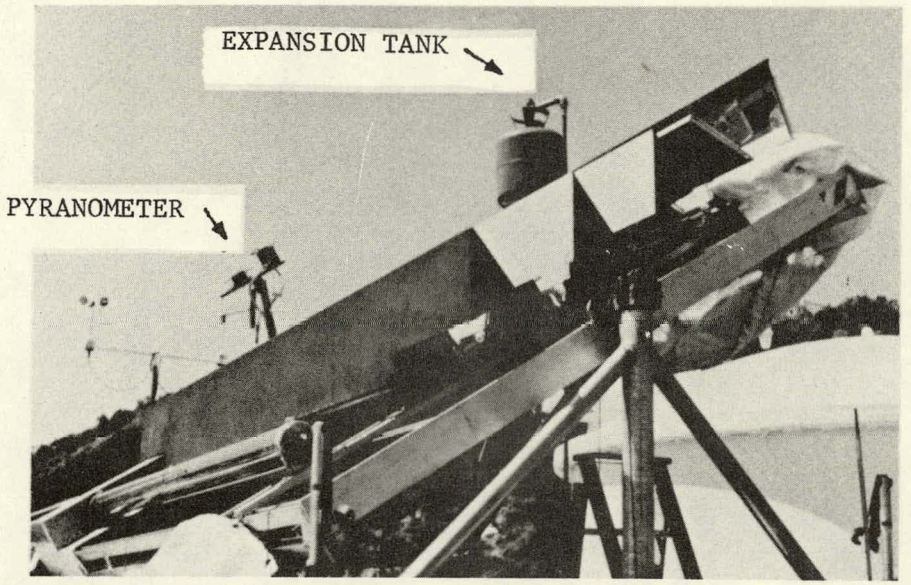

Figure 1-3. Evacuated Tube Receivers With and Without Vee-Trough Reflectors

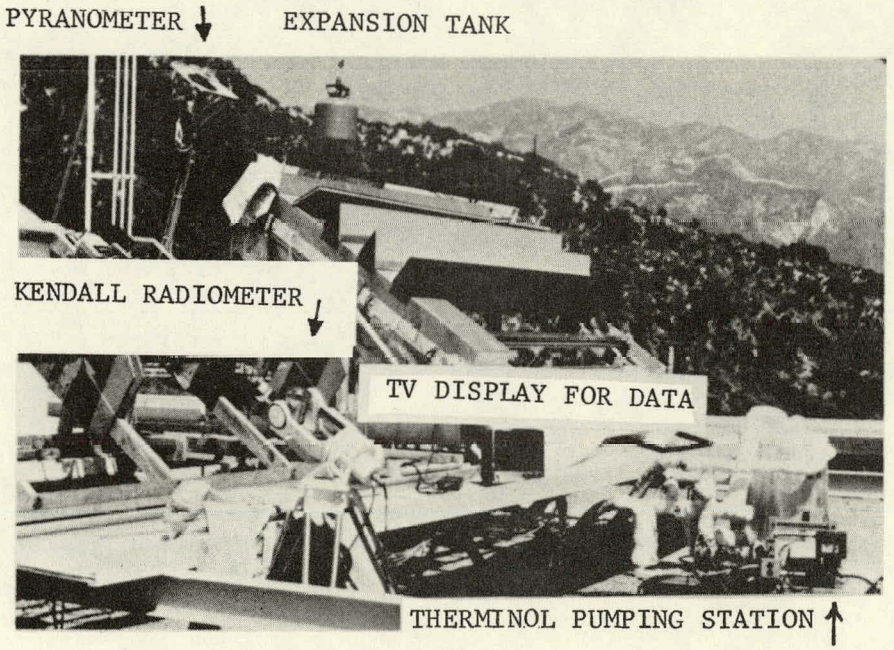

Figure 1-4. Test Bed and Pumping Station

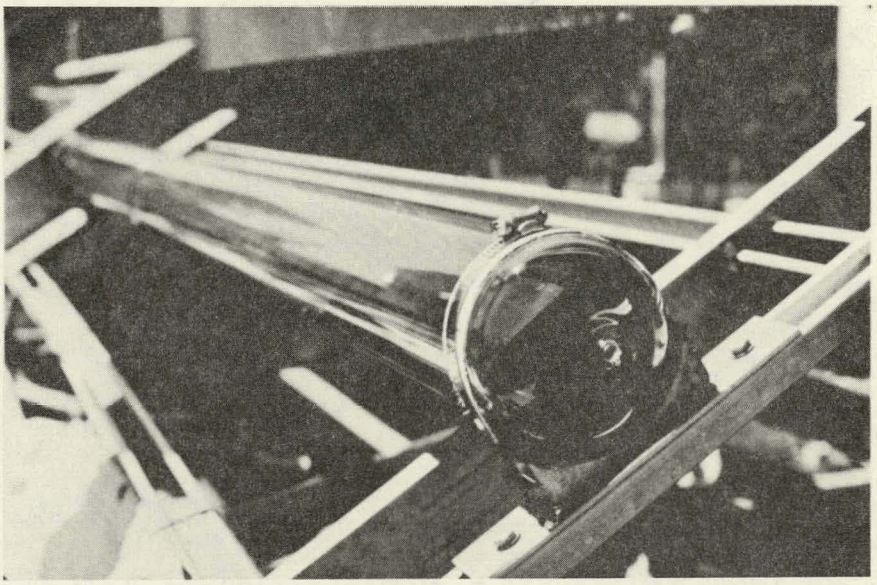

Figure 1-5. Evacuated Tube Receiver

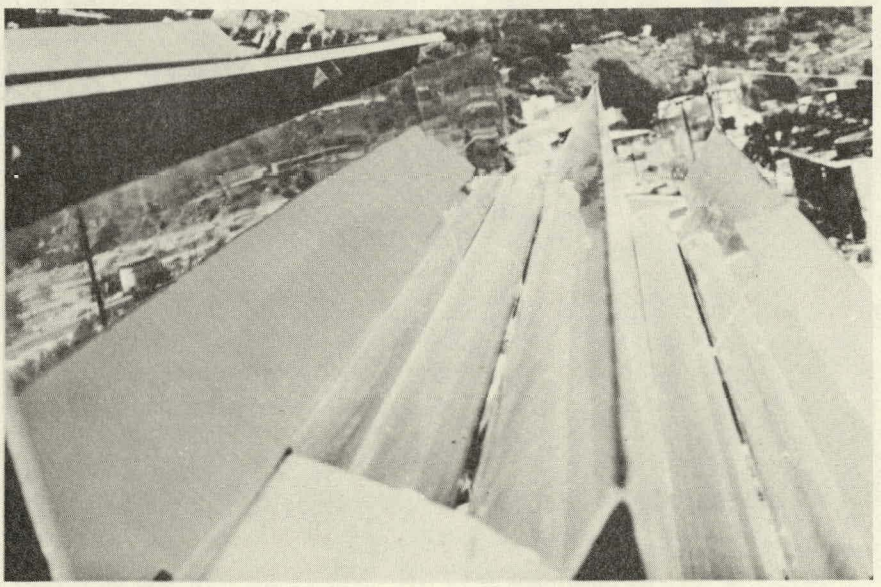

Figure 1-6. Top view of Vee-Trough Concentrators and Evacuated Tubes

SECTION 2

MATHEMATICAL ANALYSIS RESULTS

2.1 METHODOLOGY

The analysis used in this project was based on a mathematical model of the Vee-Trough/Evacuated Tube Collector (VTETC) incorporating an optical model of the vee-trough concentrator and a thermal model of the evacuated tube receiver. Variable solar flux and ambient conditions were considered, and computer codes were generated to solve each mathematical model. Details of the modelling are discussed in DOE/JPL/1024-1, published in January 1978.

2.2 THE OPTICAL MODEL

The optical model of the concentrator predicts the optical performance of the vee-trough reflectors by dividing the mirror surfaces into finite strips to obtain an accurate flux map at the bottom of the vee-trough. This model considers end effects and secondary reflections from the mirrors. The following assumptions were used in the formulations:

(1) The solar beam is specularly reflected from the mirror surface and all the reflected specular beam is captured by the receiver provided that the beam is within the acceptance angle and does not reflect back to space. Reference 1 indicates this assumption is valid for silvered surfaces.

(2) The diffuse radiation intensity at the bottom of the vee-trough is assumed to be about 80% of the diffuse radiation incident on the aperture plane (collection area). This assumption is based on data in Reference 2 and was verified experimentally.

(3) Glass transmittance is taken to be dependent upon the angle of incidence as given in Reference 3. Change of transmittance with wavelength is neglected.

2.3 THE THERMAL MODEL

The thermal model identifies the thermal performance of the evacuated tube receiver. References 4 and 5 give the derivation of the useful heat and efficiency relations of the evacuated tube receiver with or without the concentrator. The following assumptions were made in the formulation of this model:

(1) The flux intensity on the absorber plate is considered to be uniform.

(2) Since the evacuated tubes are spaced 3 diameters apart, the tubes are assumed to have no effect on each other.

(3) Convection inside the evacuated tube is completely eliminated. Studies in Reference 6 reveal that under a vacuum level of $P < 1.33 \times 10^{-2}$ Pa (10^{-4} Torr), convection losses become negligible. The tubes are evacuated to a vacuum level of $P < 5.33 \times 10^{-3}$ Pa (0.4×10^{-4} Torr). Therefore, only conduction and radiation losses are significant in the energy balance of the absorber plate.

(4) Conduction losses through the contact points between the absorber and the glass tube are neglected.

(5) Conduction through the manifolding is significant. Its magnitude was of the order of 5 to 12% for temperatures from 100 to 150°C (212 - 302°F), respectively.

2.4 THE VTETC THERMAL MODEL

The model, which defines the collector performance, combines the optical model with the evacuated tube receiver thermal model. The results of the formulation are as follows:

$$Q_u = F_R A_p \quad CR \; I_t \; (T\alpha)e - U_L \; (T_{fi} - Ta) \tag{2.1}$$

$$Q_{in} = I_t \; A_c \tag{2.2}$$

$$\eta = \frac{Q_u}{Q_{in}} \tag{2.3}$$

Where:

Q_u = rate of useful heat collected by the working fluid; Watts (Btu/hr)

F_R = heat removal factor (dimensionless). A correction factor to take into consideration the two-dimensional heat flow in the copper absorber plate; i.e., heat transfer along the tube length and across the absorber plate due to the temperature difference of the incoming and outgoing fluid lines. F_R is calculated according to the procedure described in Reference 6.

A_p = absorber plate surface area; m^2 (ft^2)

CR = the flux concentration ratio; (dimensionless)

$$CR = \frac{\text{Total energy incident on the absorber plate with vee-trough}}{\text{Total energy incident on the absorber plate without vee-trough}}$$

I_t = total rate of incident solar flux on a unit collector area; W/m^2 (Btu/hr - ft^2)

$(T\alpha)e$ = the effective transmittance - absorptance product of the receiver tube; (dimensionless)

U_L = overall heat transfer coefficient between the absorber plate and the abmient; W/m^2 ^oK (Btu/hr - ft^2 ^oF)

$T_{f,i}$ = fluid inlet temperature; ^oC (^oF)

T_a = ambient air temperature; ^oC (^oF)

Q_{in} = incident solar heat; Watts (Btu/hr)

A_c = collection area, or aperture area; m^2 (ft^2)

η = overall thermal efficiency of VTETC

The theoretical calculation of the heat loss coefficient, $U_{L\ Theo}$ is given by the following experssion:

$$U_{L\ Theo} = \frac{8.482 \times 10^7}{(T_p + T_g)(T_p^2 + T_g^2) C_c} + \frac{0.279}{5.7 + 3.8V + 2.495 \times 10^{-8} \frac{(Tg^4 - Ts^4)}{(Tg - Ta)}} \quad (2.4)$$

Where

T_p = absorber plate temperature; ^oK

T_g = surface temperature of the glass tube; ^oK

T_s = equivalent sky temperature; ^oK

T_a = ambient air temperature; ^oK

C_c = conduction loss factor (1.05 to 1.2)

V = wind velocity; m/sec.

Section 4.2 discusses U_L in more detail and Section 4.3 presents the calculation procedure and a sample calculation for the theoretical U_L.

Because of basic assumptions made for formulating the mathematical model, the resulting theoretical calculations will have uncertainties. The sources of these uncertainties include:

(1) Assuming plate temperature, T_p, is equal to the mean fluid temperature, T_m. This assumption is valid because the flow tubes are spaced only 5 cm (2 in.) apart on the absorber plate and are metallurgically bonded to the plate. For operating temperatures of above 150°C (302°F) the difference between T_p and T_m (based on T_m) is less than 3%.

(2) Inaccuracies in T_{sky} and T_{glass}.

(3) Other assumptions made for the optical and thermal models, as mentioned in Sections 2.2 and 2.3.

(4) Assuming a negligible radiation heat loss from the back of the glass tube to surrounding structures.

2.5 SOLUTION OF THE MODEL

Using equations (2.1) to (2.4), together with computer routines to calculate F_R, CR and U_L, the efficiency of the collector with and without concentrators can be calculated. Figure 2-1 represents the results of these calculations. Efficiencies are plotted against ΔTi, fluid inlet temperature minus the ambient temperature. The top set of curves give the efficiency of the receiver tube, without concentrators, based on the solar flux incident on the absorber plate area. The lower curves are based on the aperture plane area for tubes with concentrators.

At best, fluxes of up to 1110 W/m^2 (350 $Btu/hr\text{-}ft^2$) are attainable without a vee-trough concentrator. The purpose of the concentrators is to increase the flux on the absorber to levels of around 2500 W/m^2 (800 $Btu/hr\text{-}ft^2$). This is equivalent to a flux concentration ratio of about 2.2. Figure 2-2 shows the variation of actual concentration ratios for several days. Near the solstices, the concentration ratio varies from about 1.2 to a peak of 2.3; during equinoxes it is constant around 1.4.

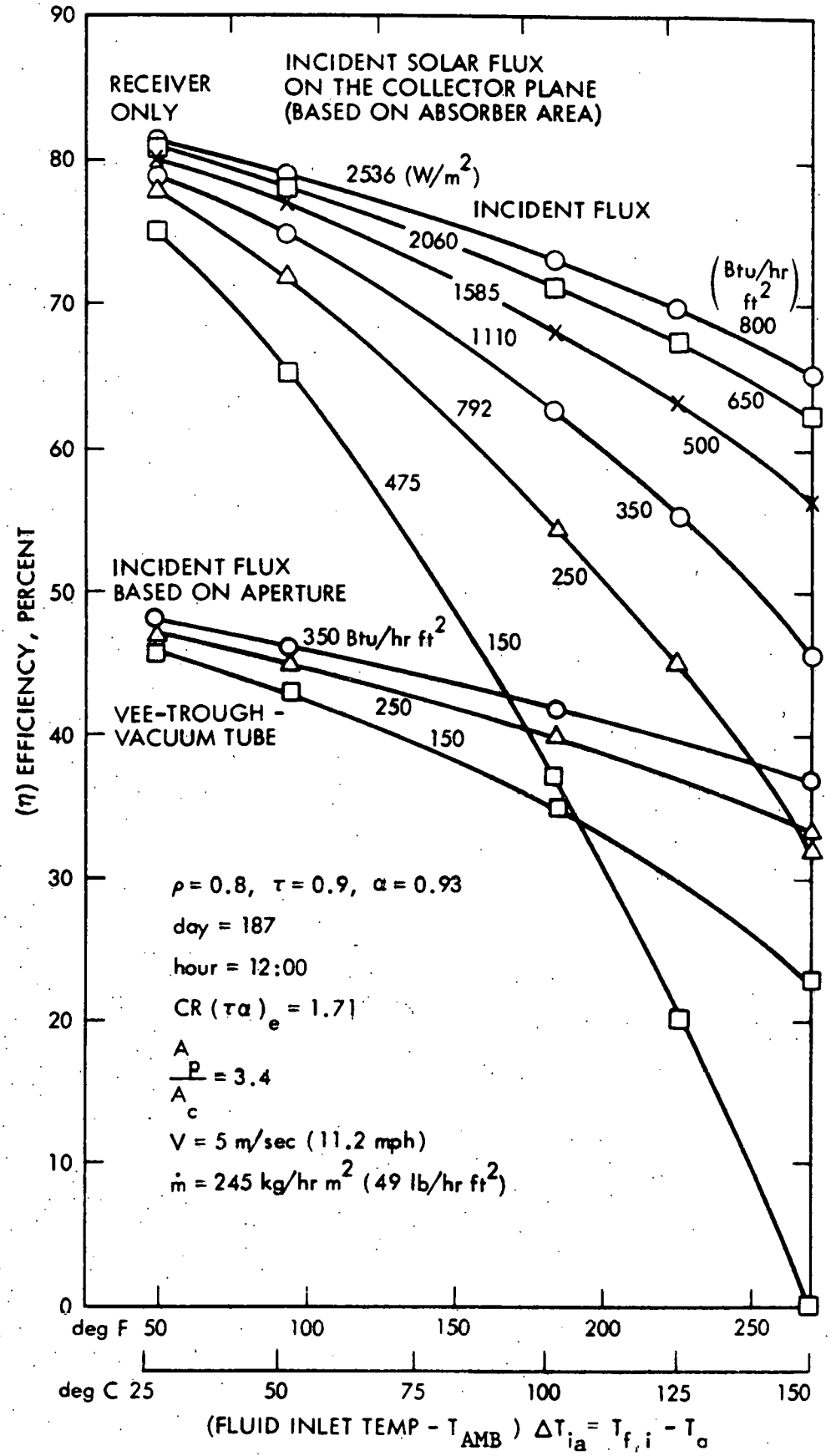

Figure 2-1. Results of the Thermal Model for the Receiver and Collector

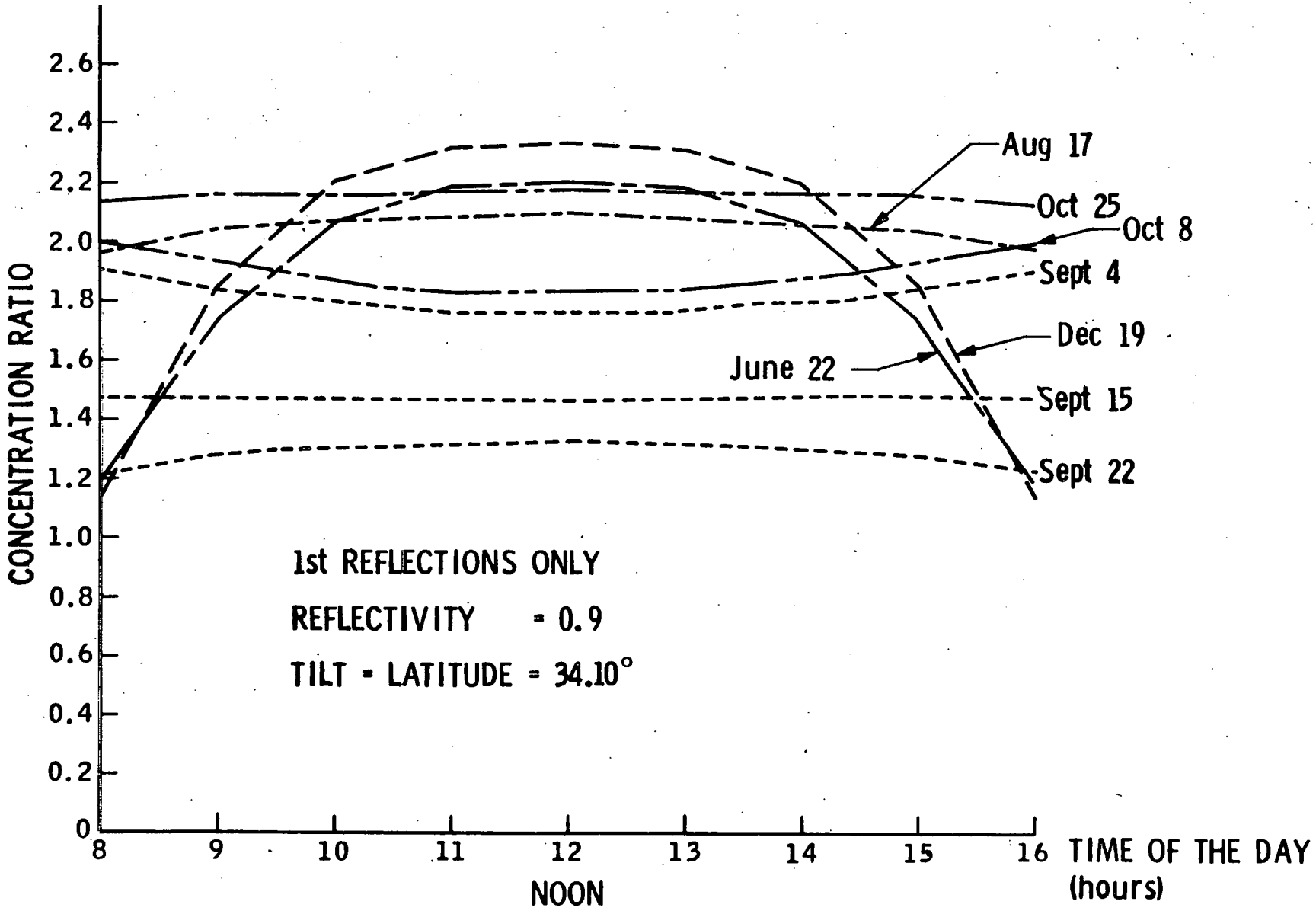

Figure 2-2. Day Long Variation of Flux, Concentration Ratio for the Vee Trough Concentrator

The actual flux concentration ratio is lower than the geometric concentration because of reflection losses from the mirror surfaces and loss due to some reflected rays missing the target (absorber plate). The former is a function of the reflector surface, material, finish and the angle of incidence. Change of reflectance with the angle of incidence for values of practical interest ($<80^{o}$) is not as significant as the effects of the beams missing the target. Although some loss of performance is noticed during the equinoxes, the simplicity of the design and operation of the fixed-tilt asymmetric triangular sections justifies their use.

SECTION 3

TEST BED AND INSTRUMENTATION DESIGN

This section presents a summary of the test bed design and instrumentation used for data acquisition. Further details regarding the design and instrumentation may be obtained from DOE/JPL/1024-1, published in January 1978.

3.1 THE TEST BED

The test bed used for evaluating the performance of the evacuated tubes with or without reflectors consisted of the following subsystems:

(1) Collector Stand

The main frame used as the mounting for the evacuated tubes, reflectors and manifolding. The collector stand is tilt adjustable but, for this project, all tests were run at a fixed tilt of 35°, which is the latitude of Los Angeles, CA. The triangular reflectors and evacuated tubes are 3.05 m (10 ft) long. The pair of reflectors serving the lowermost tube is 2.44 m (8 ft) long.

(2) Pumping Station

This subsystem is connected to the collector stand with insulated lines. The working, fluid Therminol 44, is circulated through the evacuated tubes by a gear pump. Figure 3-1 shows various components of the test bed as well as the instrumentation. Before entry into the collector loop, the fluid is preheated in a holding tank. The preheating simulates additional collector tubes that would otherwise heat the fluid, thus allowing operating temperatures of up to 190°C (374°F).

(3) Expansion Tank

The test bed is equipped with an expansion tank to accommodate the thermal expansion of Therminol 44. It also eliminates gas or air bubbles trapped in the tubes and manifolding through the use of bleed lines that connect the highest point of the collector loop to the expansion tank.

Both the fluid lines connecting pumping station to the collector stand and the manifolding for the tubes were insulated to minimize heat loss.

Therminol 44 flows through the receiver tubes entering at the lowermost tube (Tube 4) and leaving at the top (Tube 1).

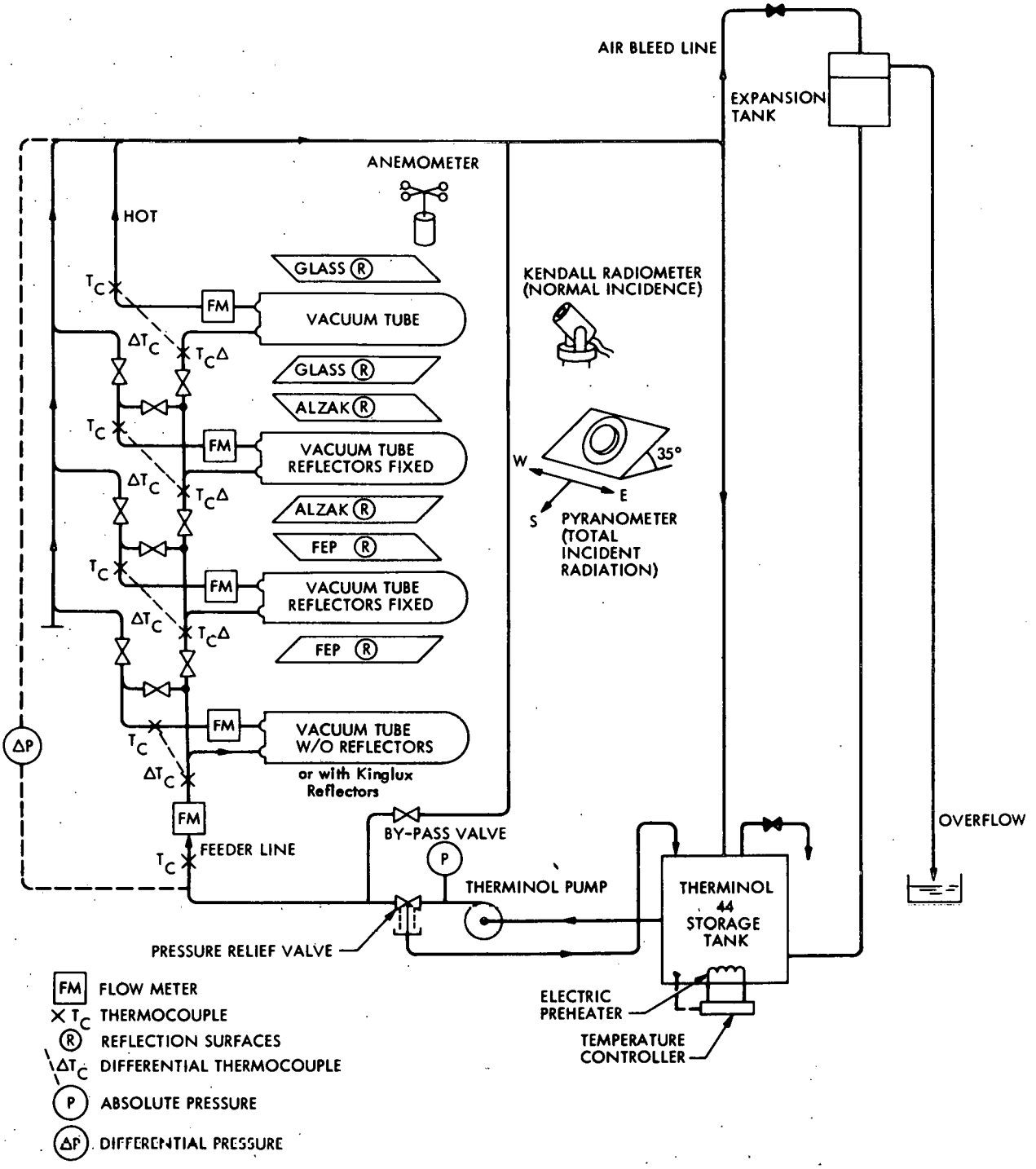

Figure 3-1. Test Arrangement for Evacuated Tube Receivers

3.2 INSTRUMENTATION AND DATA ACQUISITION SUBSYSTEM

The vee-trough collector test bed was fully instrumented to determine the receiver performance. The flow rate of the Therminol 44 was measured by turbine-type flow meters. Absolute and differential temperatures were monitored on each evacuated tube using chromel-constantan thermocouples. Differential thermocouples were made from three series elements to improve the resolution of readings. Total solar radiation, diffuse solar radiation, absolute pressures and pressure drops in the flow circuit, and ambient temperature, were also measured and recorded.

All data acquired from the vacuum tube test bed were fed into an automated data acquisition and processing system. The data was then displayed on a TV screen and recorded permanently on photosensitive paper.

SECTION 4

TESTING AND EVALUATION

Tests were run under clear day conditions for daytime efficiency determination and at night for heat loss experiments. Procedures for data acquisition and some sample data are presented and discussed in this section. Appendix A and B include additional data and processed values. Appendix C includes information about the properties of Therminol 44, the heat transfer fluid used in this experiment.

Useful heat calculations and efficiency determination require the following basic data:

(1) Mass flow rate of the working fluid, $\dot{m}$, which consists of d (density) and $\dot{V}$ (volumetric flow) rate terms.

(2) Specific heat of the working fluid, C_p

(3) Temperature rise of the working fluid in the evacuated tube, ΔT

(4) Solar flux intensity at the tilted collector plane, I_t.

Items (1), (3), and (4) were determined using calibrated instrumentation. The specific heat of Therminol 44 was taken from the manufacturer's data. These figures were also verified by tests performed at JPL. Property changes due to a slight color change of the Therminol after several runs, was not significant. These data were used in calculations either using linear interpolation techniques or by curve fitting.

All instruments used for the measurement of temperature, flow rate, and solar radiation were calibrated. Differential thermocouples were accurate to ±0.08°C (0.14°F) whereas absolute temperatures were measured within 0.1°C (0.18°F). Errors due to the measurements in the millivolt range were less than 0.02°C (0.04°F) for the differential and 0.1°C for the absolute temperature measurements. The combination of these two errors still yielded ±0.1°C for the differential temperatures and ±0.4°C (0.07°F) for the absolute temperature measurements. Volumetric flow of the working fluid, Therminol 44, was measured to within ±3%. The effect of the viscosity on the calibration factor for the flow meters was found to be negligible in the range of temperatures between 65 to 205°C (149 to 401°F). Total solar radiation measurements were made using a Spectran precision pyranometer, having an accuracy of ±1%. Therefore, the net error in the measured efficiency, due to instrument uncertainties, is ±6%. However, this ±6% is not an indication of how closely the measured values correlate with the theoretically calculated values. The actual difference between the measured and theoretical values will be a result of the combination of instrument uncertainties, simplifications made in the mathematical model, and uncertainties in determining U_L and conduction losses.

The following sections discuss procedures in data acquisition and evaluation. Generally, daytime tests were run during clear days for a period of ±4 hours around noon. Night tests were run after sunset to determine U_L values.

4.1 DAYTIME TESTS

Before starting data acquisition and removing the shading over the glass tubes, electric heaters were turned on and the heat transfer fluid was preheated to the operating temperature selected for the day. Preheating the fluid to operating temperature served two purposes:

(1) Production of high inlet temperatures, otherwise unattainable using only 4 tubes in series. Fluid inlet temperatures of up to 180°C (356°F) were achieved.

(2) Achieving a shorter warm-up time. Although lower temperature levels such as 120°C (248°F) could be attained without preheating, this process would take hours and, as a result, morning data would be lost.

Usually, tests were started at lower temperature levels, i.e., about 90°C (194°F) for the first day, then raised to 120°C (248°F), 150°C (302°F) and higher on subsequent days.

After preheating, the tubes were exposed to the sun and the circulation pump was started. After flow was set to a nominal value, the readings could be started within a few minutes since the thermal capacity of the evacuated tubes was quite small. The measured variables were absolute and differential temperatures, flow rates, pressures and solar flux intensity. These were recorded on photosensitive paper at selected intervals, normally 10 minutes.

The inlet temperature of the working fluid gradually rose during the day since the heat gain of the collector test bed was more than the losses of the system through lines and tank insulation. However, this temperature rise for the test period was small enough to justify the assumption of quasi-steady state operating conditions. This assumption was based on the fact that the input temperature increase rate was 14 deg.C (25 deg.F)/hr and the system had a small thermal capacity (i.e., temperature response time was short). In addition, the fluid transit time through the flow tubes was about 35 seconds, small enough to justify the quasi-steady state evaluation.

The test data obtained was later processed by transferring the optically printed figures on to punch cards and performing the computations with a computer. The useful heat collected by each tube was calculated from:

$$Q_u = \dot{m}\, C_p\, \Delta T \qquad (4.1)$$

where $\dot{m}$ is the mass flow rate of the fluid in (kg/hr), ΔT is the temperature rise in deg. C for each receiver tube, and C_p is the specific heat of the fluid in (kJ/kg°C), as given in Appendix C.

The efficiency of the tubes was then found by $\eta = Q_u / IA$ where I is the total solar insolation in W/m^2 and A is the aperture area. The aperture area is equal to 0.65 m^2 (7 ft^2) when the reflectors are placed on the tube. However, when the reflectors are removed, the aperture area becomes equivalent to the absorber plate area and is equal to 0.19 m^2 (2.04 ft^2). The results from the experimental data were then compared with the theoretically calculated values for the same operating conditions.

4.2 NIGHT TESTS

To determine the overall heat transfer coefficient for heat lost from the working fluid to the ambient, heat losses were measured without any heat gain during the night. Experimentally, the fluid was preheated and circulated through tubes. The fluid temperature drop (ΔT) for each tube was measured. The overall heat transfer coefficient was determined from:

$$U_L = \frac{\dot{m} C_p \Delta T}{A_p (T_{fi} - T_a)} \qquad (4.2)$$

where A_p is the absorber plate area (m^2) and $\Delta T_{fa} = (T_{fi} - T_a)$ is the difference between fluid inlet temperature and ambient air temperature. Other variables are as previously defined.

The experimental values of U_L obtained using the present preheaters correspond to fluid temperatures of about 120°C (248°F). For such temperatures, there was a good correlation between the experimentally obtained values of U_L and those calculated by Equation (2.4).

To get values for U_L at higher temperatures, the measured values were curve-fitted with a third degree polynomial as a function of temperature. A third degree polynomial was used for two reasons: First, U_L is strongly dependent on the radiative heat loss and the radiative heat loss coefficient, h_{RAD} is proportional to the cube of temperature, as defined by $Q_{RAD} = h_{RAD} \Delta T_{fa} = \sigma_o \varepsilon (T + T_a)(T^2 + T_a^2)(T - Ta)$. Second, the third degree polynomial gave good agreement between theoretical U_L and measured U_L at low temperatures.

Figures 4-1 to 4-4 show the plots of measured U_L values and the polynomial curve fits for the four tubes. The dashed lines indicate the polynomial extrapolation for measured U_L at higher temperatures. The data for these plots were taken on different nights. The scatter observed in the value of U_L is due to different sky conditions and wind conditions on different nights. Tables 4-1 to 4-7 show the measured U_L values computed using Equation (4.2). These tables also show the theoretically calculated U_L derived from Equation (2.4). At temperatures

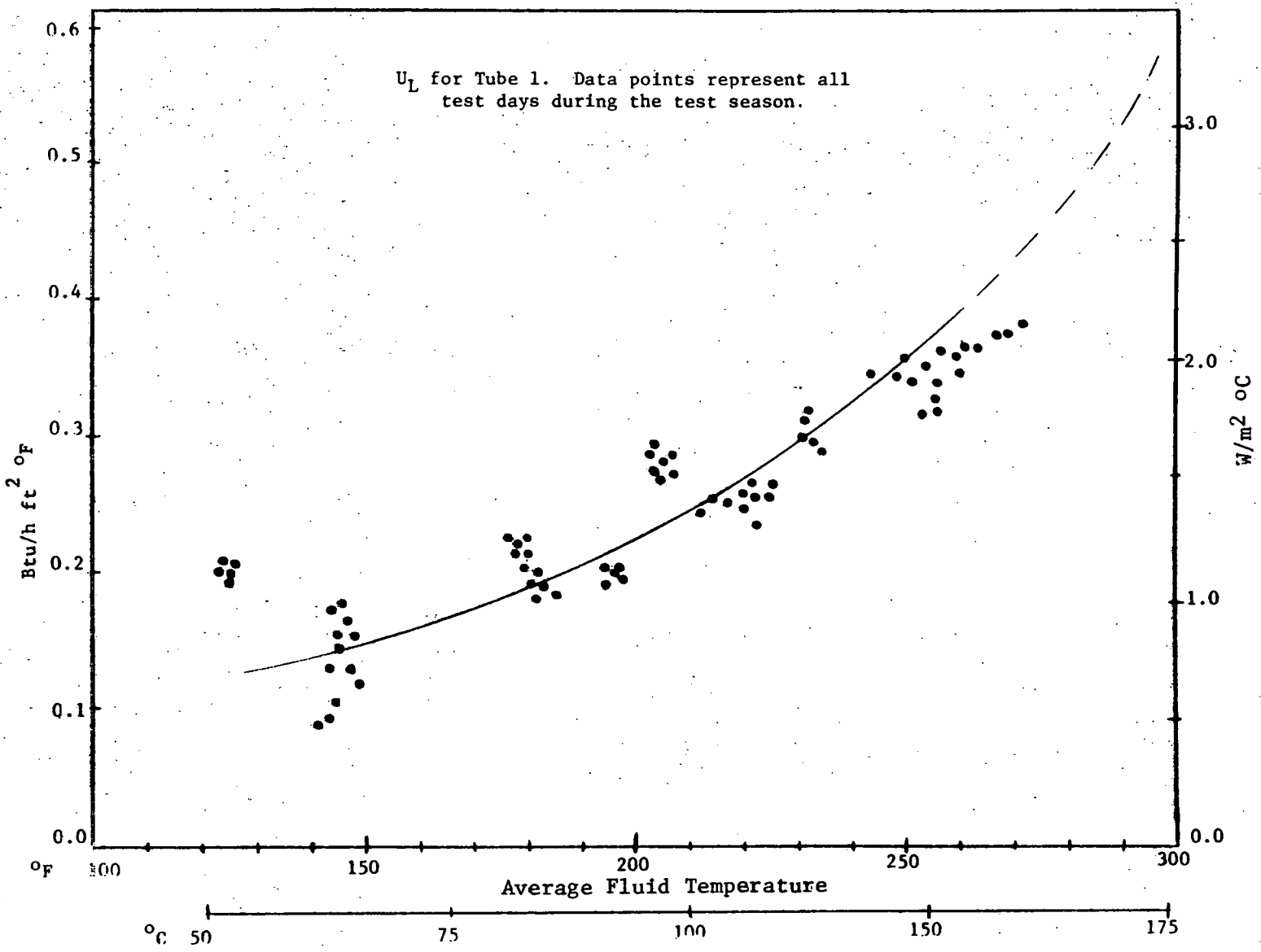

Figure 4-1. Heat Loss Coefficient and Estimated Polynomial Curve Fit

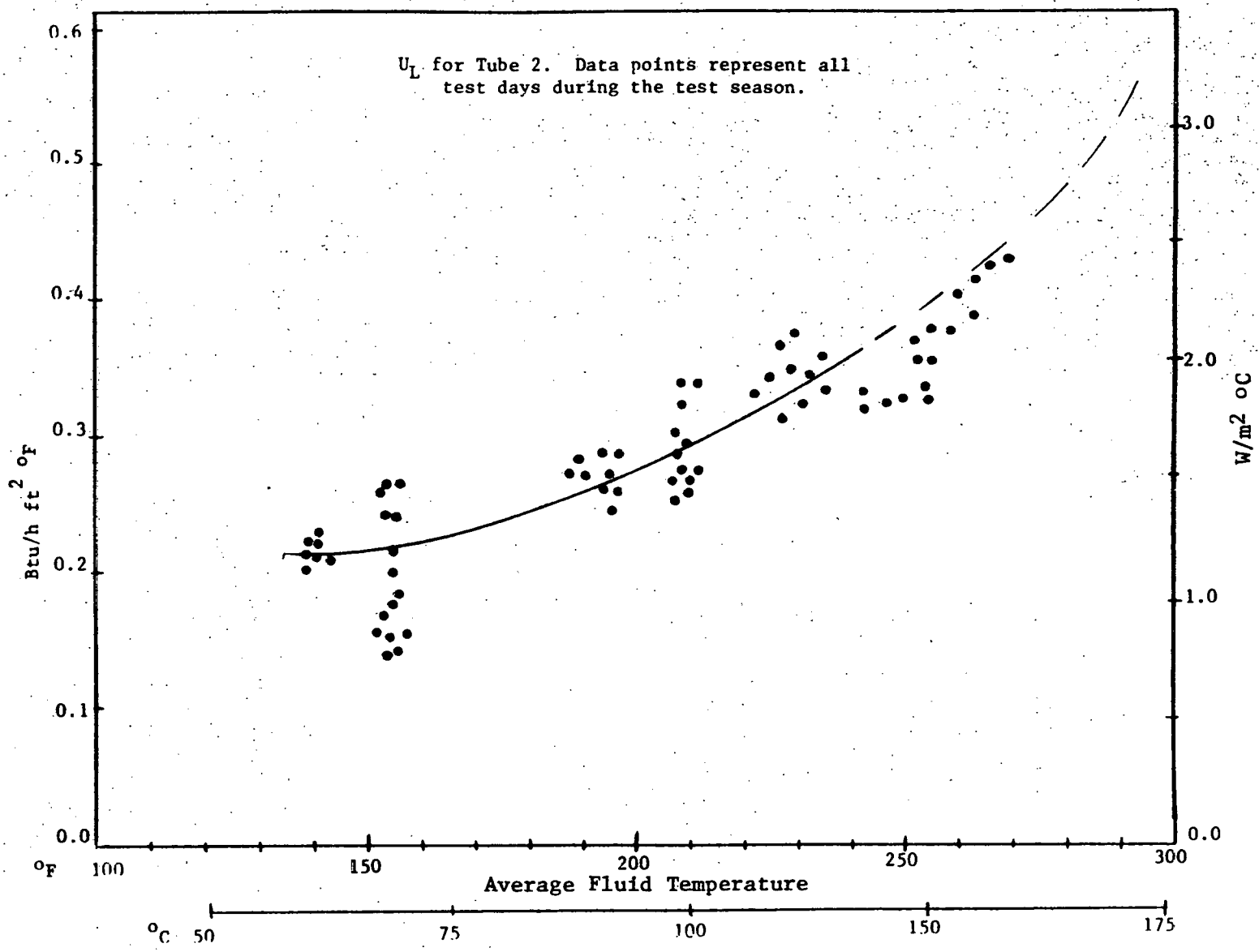

Figure 4-2. Heat Loss Coefficient and Estimated Polynomial Curve Fit

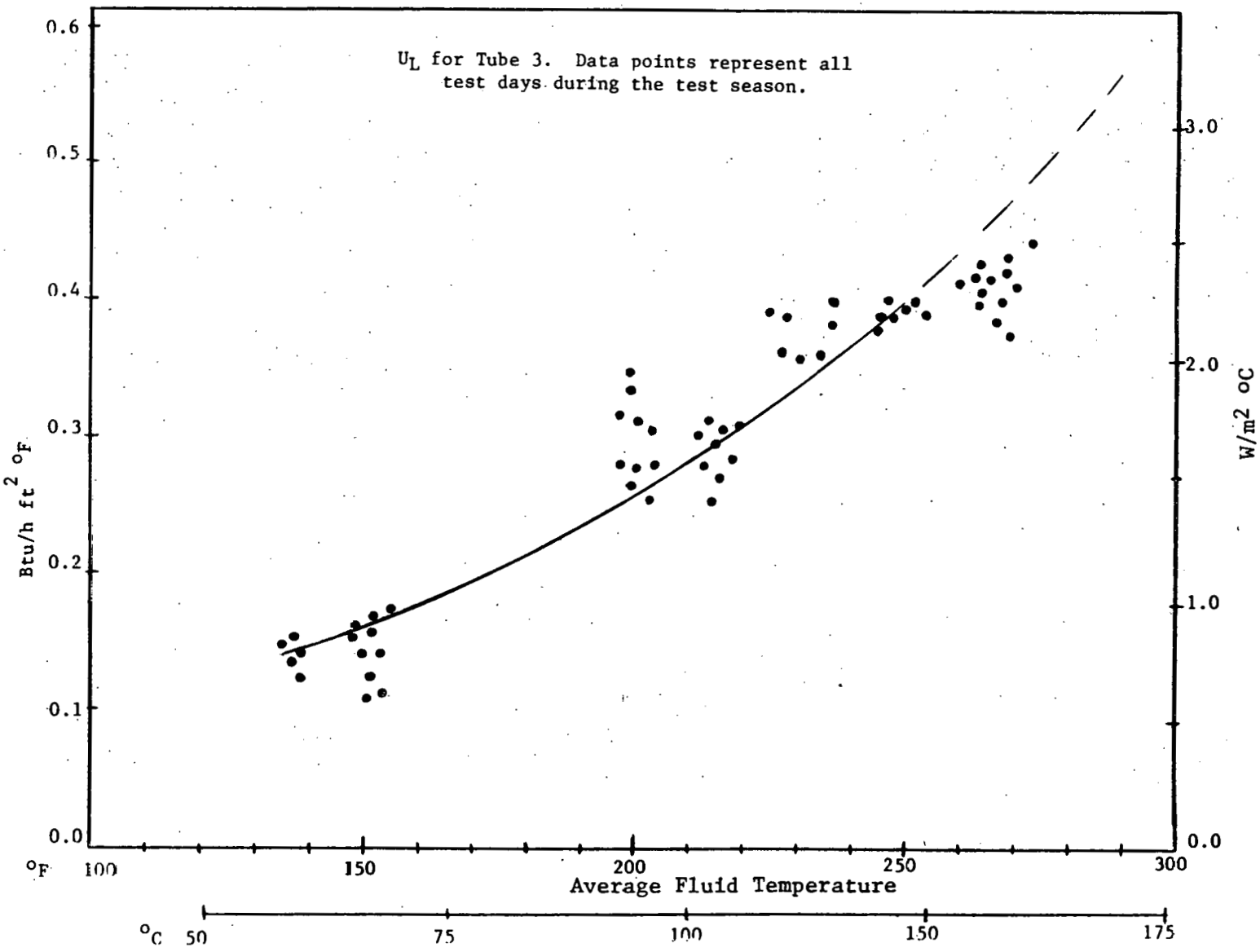

Figure 4-3. Heat Loss Coefficient and Estimated Polynomial Curve Fit

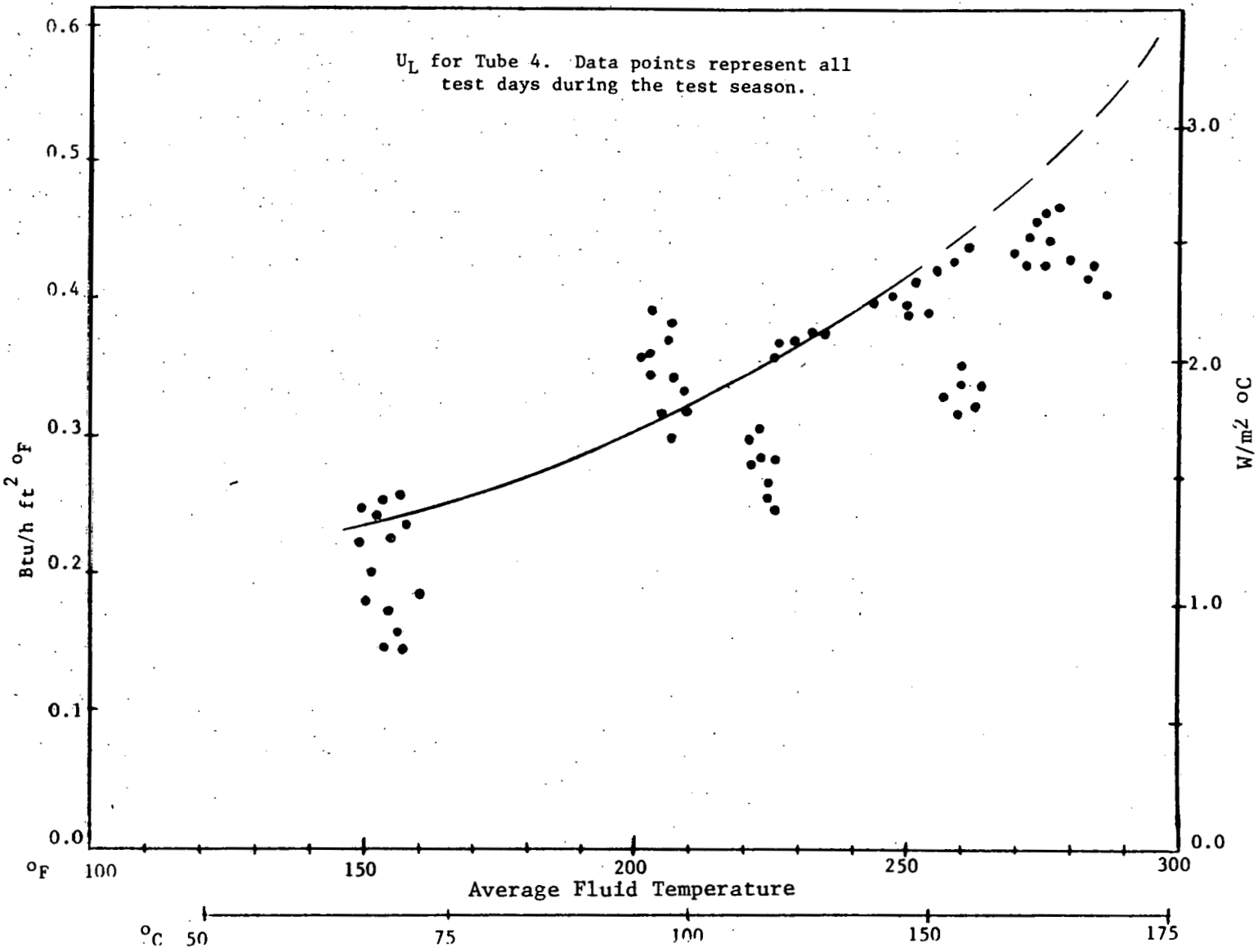

Figure 4-4. Heat Loss Coefficient and Estimated Polynomial Curve Fit

Table 4-1. Test Data Evaluation

May 9, 1978 11:55 am PST	TUBES			
	1	2	3	4
Reflector Type	GLASS	ALZAK	TEFLON	KINGLUX
Tube Outlet Temp (°C)	138.1	138.6	131.1	117.5
ΔT, Temp. rise (deg C)	14.0	13.5	12.9	12.6
Mass Flow Rate $\dot{m}$ (kg/hr)	25.8	25.8	25.8	25.8
Specific Heat C_p (KJ/kg °C)	2.24	2.23	2.21	2.17
Useful Heat $Qu = \dot{M} C_p \Delta T$ (Watts)	223.7	214.8	203.2	195.4
Qu Theoretical (Watts)	262.5	233.6	252.7	253.6
Solar Flux I (W/m^2)	907	907	907	907
Solar Input Qin = I·Area (Watts)	494.6	589.8	585.7	589.8
(%) Efficiency $\eta = \frac{Qu}{Qin}$	45.2	36.4	34.7	33.1
η Theoretical (%)	53.1	39.6	43.2	43.0
Ambient Air Temp. Ta (°C)	29.6	29.6	29.6	29.6
Theoretical Heat Loss Coeff. U_L Theo (W/m^2 - °C)	2.40	2.35	2.26	2.12
Measured Heat Loss Coefficient U_L (W/m^2 - °C)	2.42	2.46	2.07	2.12

Table 4-2. Test Data Evaluation

May 17, 1978 12:00 noon PST	TUBES			
	1	2	3	4
Reflector Type	GLASS	ALZAK	TEFLON	KINGLUX
Tube Outlet Temp (°C)	146.1	133.1	122.7	104.1
ΔT, Temp. rise (deg C)	18.3	15.9	17.4	15.8
Mass Flow Rate $\dot{m}$ (kg/hr)	23.6	23.6	23.6	23.6
Specific Heat C_p (KJ/kg °C)	2.24	2.21	2.21	2.14
Useful Heat $Qu = \dot{M} C_p \Delta T$ (Watts)	268.3	229.8	248.0	221.0
Qu Theoretical (Watts)	259.5	234.8	256.3	258.8
Solar Flux I (W/m^2)	917	917	917	917
Solar Input Qin = I·Area (Watts)	500.1	596.3	592.0	596.3
(%) Efficiency $\eta = \frac{Qu}{Qin}$	53.7	38.5	41.9	37.1
η Theoretical (%)	51.9	39.4	43.3	43.4
Ambient Air Temp. Ta (°C)	31.2	31.2	31.2	31.2
Theoretical Heat Loss Coeff. U_L Theo (W/m^2 - °C)	2.42	2.28	2.16	1.98
Measured Heat Loss Coefficient U_L (W/m^2 - °C)	2.39	2.29	1.84	1.83

Table 4-3. Test Data Evaluation

May 19, 1978 11:34 am PST	TUBES			
	1	2	3	4
Reflector Type	GLASS	ALZAK	TEFLON	KINGLUX
Tube Outlet Temp (°C)	183.7	177.9	171.1	161.6
ΔT, Temp. rise (deg C)	14.4	14.1	12.7	12.1
Mass Flow Rate $\dot{m}$ (kg/hr)	23.0	23.0	23.0	23.0
Specific Heat C_p (KJ/kg °C)	2.34	2.32	2.31	2.29
Useful Heat $Qu = \dot{M}\ C_p\ \Delta T$ (Watts)	213.7	208.4	186.1	175.7
Qu Theoretical (Watts)	227.6	200.8	220.0	220.4
Solar Flux I (W/m^2)	922	922	922	922
Solar Input Qin = I·Area (Watts)	502.8	600.0	595.3	600.0
(%) Efficiency $\eta = \frac{Qu}{Qin}$	42.5	34.8	31.3	29.3
η Theoretical (%)	45.3	33.5	36.9	36.8
Ambient Air Temp. Ta (°C)	32.4	32.4	32.4	32.4
Theoretical Heat Loss Coeff. U_L Theo (W/m^2 - °C)	2.95	2.87	2.79	2.66
Measured Heat Loss Coefficient U_L (W/m^2 - °C)	3.96	3.85	3.64	3.31

Table 4-4. Test Data Evaluation

June 9, 1978 12:10 pm PST	TUBES			
	1	2	3	4
Reflector Type	GLASS	ALZAK	TEFLON	KINGLUX
Tube Outlet Temp (°C)	176.2	172.7	171.1	167.6
ΔT, Temp. rise (deg C)	6.9	6.4	6.6	6.6
Mass Flow Rate $\dot{m}$ (kg/hr)	40.7	40.7	40.7	40.7
Specific Heat C_p (KJ/kg °C)	2.33	2.32	2.32	2.31
Useful Heat $Qu = \dot{M} C_p \Delta T$ (Watts)	181.5	169.4	172.8	170.3
Qu Theoretical (Watts)	203.6	177.3	191.7	188.2
Solar Flux I (W/m^2)	855	855	855	855
Solar Input Qin = I·Area (Watts)	466.3	556.0	552.1	556.0
(%) Efficiency $\eta = \frac{Qu}{Qin}$	38.9	30.5	31.3	30.6
η Theoretical (%)	43.7	31.9	34.7	33.9
Ambient Air Temp. Ta (°C)	33.1	33.1	33.1	33.1
Theoretical Heat Loss Coeff. $U_{L\ Theo}$ (W/m^2 - °C)	2.90	2.86	2.83	2.79
Measured Heat Loss Coefficient U_L (W/m^2 - °C)	3.77	3.79	3.82	3.62

Table 4-5. Test Data Evaluation

June 21, 1978 12:00 noon PST	TUBES			
	1	2	3	4
Reflector Type	GLASS	ALZAK	TEFLON	KINGLUX
Tube Outlet Temp (°C)	185.5	181.3	180.3	176.2
ΔT, Temp. rise (deg C)	7.7	7.3	7.5	7.3
Mass Flow Rate $\dot{m}$ (kg/hr)	37.0	37.0	37.0	37.0
Specific Heat C_p (KJ/kg °C)	2.35	2.34	2.34	2.33
Useful Heat $Qu = \dot{M} C_p \Delta T$ (Watts)	184.4	176.2	179.3	173.8
Qu Theoretical (Watts)	194.5	169.3	183.1	180.3
Solar Flux I (W/m^2)	852	852	852	852
Solar Input Qin = I·Area (Watts)	464.6	554.1	550.1	554.1
(%) Efficiency $\eta = \frac{Qu}{Qin}$	39.7	31.8	32.6	31.4
η Theoretical (%)	41.9	30.6	33.3	32.5
Ambient Air Temp. Ta (°C)	34.3	34.3	34.3	34.3
Theoretical Heat Loss Coeff. U_L Theo (W/m^2 - °C)	3.04	2.98	2.97	2.91
Measured Heat Loss Coefficient U_L (W/m^2 - °C)	4.22	4.18	4.42	3.92

Table 4-6. Test Data Evaluation

June 22, 1978 11:50 am PST	TUBES			
	1	2	3	4
Reflector Type	GLASS	ALZAK	TEFLON	KINGLUX
Tube Outlet Temp (°C)	178.9	175.5	174.1	169.9
ΔT, Temp. rise (deg C)	7.1	6.8	6.9	7.1
Mass Flow Rate $\dot{m}$ (kg/hr)	36.7	36.7	36.7	36.7
Specific Heat C_p (KJ/kg °C)	2.34	2.33	2.32	2.31
Useful Heat $Qu = \dot{M} C_p \Delta T$ (Watts)	167.0	160.0	164.1	167.7
Qu Theoretical (Watts)	211.5	181.6	196.3	193.5
Solar Flux I (W/m^2)	879	879	879	879
Solar Input Qin = I·Area (Watts)	479.4	571.6	567.6	571.6
(%) Efficiency $\eta = \frac{Qu}{Qin}$	34.8	28.0	28.9	29.3
η Theoretical (%)	44.1	31.8	34.6	33.9
Ambient Air Temp. Ta (°C)	33.5	33.5	33.5	33.5
Theoretical Heat Loss Coeff. U_L Theo (W/m^2 - °C)	2.94	2.90	2.88	2.82
Measured Heat Loss Coefficient U_L (W/m^2 - °C)	3.90	3.91	4.00	3.69

Table 4-7. Test Data Evaluation

July 12, 1978 12:00 noon PST	TUBES			
	1	2	3	4
Reflector Type	GLASS	ALZAK	TEFLON	KINGLUX
Tube Outlet Temp (°C)	190.4	185.9	184.1	179.9
ΔT, Temp. rise (deg C)	8.9	8.4	8.6	7.7
Mass Flow Rate $\dot{m}$ (kg/hr)	33.5	33.5	33.5	33.5
Specific Heat C_p (KJ/kg °C)	2.36	2.35	2.34	2.34
Useful Heat $Qu = \dot{M}\ Cp\ \Delta T$ (Watts)	195.0	185.0	187.9	167.5
Qu Theoretical (Watts)	200.0	174.0	189.2	185.8
Solar Flux I (W/m^2)	889	889	889	889
Solar Input Qin = I·Area (Watts)	484.8	578.1	574.0	578.1
(%) Efficiency $\eta = \frac{Qu}{Qin}$	40.2	32.0	32.7	29.0
η Theoretical (%)	41.2	30.1	33.0	32.1
Ambient Air Temp. Ta (°C)	32.9	32.9	32.9	32.9
Theoretical Heat Loss Coeff. U_L Theo (W/m^2 - °C)	3.09	3.03	3.00	2.95
Measured Heat Loss Coefficient U_L (W/m^2 - °C)	4.45	4.39	4.66	4.06

of under 120°C (248°F), the theoretical and measured values of U_L agreed closely, such as in Tables 4-1 and 4-2. However, at higher temperatures, the polynomial curve fits the predicted high heat loss coefficients, as shown in Tables 4-3 to 4-7.

In calculating the theoretical heats and efficiencies for Tables 4-1 to 4-7, the theoretical value of U_L was used. Section 4.3 presents a sample calculation for finding the theoretical U_L

4.3 TEST DATA EVALUATION

Test data was obtained for evaluating the hourly heat collection and efficiency of each receiver tube. Table 4-1 shows the experimental results together with the theoretically calculated values for a temperature range of about 120-140°C (248-284°F). The heat transfer fluid is flowing through the system from Tube 1 to Tube 4; therefore, the outlet temperature of Tube 1 is greater than that of Tube 2, etc. Tables 4-2 through 4-7 present collected and processed test data for different temperatures and different days. Theoretical calculated useful heats are compared with the experimental results in these tables. The discrepancies between the experimental and calculated values are caused by conduction losses from the manifold and contact points, variation of $\dot{m}$ and the resulting heat removal efficiency, F_R, wind velocity, relative humidity of the air (which affects the equivalent sky temperature), and changes in mirror reflectivity because of dust. The data shows that, in most cases, the theoretical value of Q_u is greater than the experimental. This is attributed to the effect of the overall heat transfer coefficient, U_L, in Equation (2.1), where the value of U_L used is calculated by Equation (2.4). In obtaining the theoretical values, a 10% conduction loss (conduction factor $C_c = 1.1$ in Equation [2.4]), and a wind velocity of 1.8 m/sec (4 mph) were used. The values for the flux concentration ratio, CR, were derived for a latitude of 34.1°, from data for Burbank, California, 1962, as explained in Appendix B. The reflectivities of the mirrored surfaces were taken to be $\rho = 0.87$ for the glass mirror, $\rho = 0.76$ for Alzak, $\rho = 0.8$ for the aluminized Teflon, and 0.78 for Kinglux. The calculational procedure for theoretical U_L is as follows:

(1) Heat loss equations are written for heat lost from the absorber plate to the glass tube and for heat lost from the glass tube to the surroundings:

$$Q_{p-g} = C_c h_{rp-g} A_p (T_p - T_g) \tag{4.3}$$

$$Q_{g-s} = A_g h (T_g - T_a) + (\tfrac{1}{2}A_g) h_{g-s} (T_g - T_s) \tag{4.4}$$

The ½ factor appearing with A_g is a result of the assumption that there is negligible radiation heat loss from the back of the glass tube to the back surroundings. Therefore, only radiation heat loss from the top half of the tube is considered.

In these equations,

Q_{p-g} = heat lost from absorber plate to glass tube

Q_{g-s} = heat lost from glass tube to surroundings

C_c = conduction loss factor, estimated at 1.10

h_{rp-g} = radiation heat loss coefficient from plate to glass

A_p = absorber plate area = 0.19 m^2 (0.97 ft^2)

T_p = plate temperature = $\frac{1}{2}(T_{fo} - T_{fi})$, where T_{fo} and T_{fi} are the measured fluid outlet and inlet temperatures.

h = convection heat loss from glass tube, considering wind effect. For a 1.8 m/sec (4 mph) wind h = 12.54 W/m^2 °C. This is given in Reference 3.

h_{rg-s} = radiation heat loss coefficient from glass to surroundings

A_g = total glass surface area = 0.68 m^2 (7.3 ft^2)

T_a = measured ambient air temperature

T_g = glass temperature, unknown

The radiation heat loss coefficients are given by

$$h_{rp-g} = \varepsilon \sigma_o (T_p + T_g)(T_p^2 + T_g^2) \qquad (4.5)$$

$$h_{rg-s} = \varepsilon \sigma_o (T_g + T_{sky})(T_g^2 + T_{sky}^2) \qquad (4.6)$$

where,

ε = the effective emissivity between the plate and glass. This is a function of the plate emissivity, at both the front and back, the glass emissivity, and temperature.

σ_o = Stephan-Boltzman Constant = 5.669×10^{-3} W/m^2 °K^4

ε_g = glass emissivity, taken to be constant at 0.88

T_{sky} = sky temperature, taken to be 5.5°K less than ambient air temperature

(2) The two equations for heat loss, Q_{p-g} and Q_{g-s}, should be equal for a given glass temperature, T_g. To find T_g, these two equations are iterated using the bisection method. The function for the bisection iteration is $f(T_g) = Q_{p-g} - Q_{g-s}$ and a search is made until $f(T_g)$ is appreciably small.

(3) Then the overall heat loss coefficient is:

$$U_{L\ Theo} = \left[\frac{1}{C_c h_{rp-g}} + \frac{A_p/A_g}{h + \frac{1}{2} h_{rg-s}} \right]^{-1} \qquad (4.7)$$

This result is expressed in more detail in Equation (2.4).

A sample calculation is done for the data collected on May 9, 1978 at 11:55 a.m. (Table 4-1). For Tube 1:

T_{fi} = 131.2°C = 404.2°K

T_{fo} = 145.2°C = 418.2°K

T_a = 29.6°C = 302.6°K

T_p = ½(404.2 + 418.2) = 411.2°K

ε = 0.212

ε_g = .88

$T_s = T_a$ - 5.5°K = 297.1°K

Then: $h_{rp-g} = (0.212)(5.669 \times 10^{-8})(411.2 + T_g)$

$= (411.2^2 + T_g^2)$

And: $h_{rg-s} = (0.88)(5.669 \times 10^{-8})(T_g + 297.1)$

$= (T_g^2 + 297.1^2)$

Substituting these into Equations (4.3) and (4.4) gives:

$$Q_{p-g} = 2.512 \times 10^{-9} \ (411.2^4 - T_g^4)$$

$$Q_{g-s} = 8.53 \ (T_g - 302.6) + 1.696 \times 10^{-8} \ (T_g^4 - 297.1^4)$$

Let: $f(T_g) = Q_{p-g} - Q_{g-s}$

Iterating this equation till $f(T_g) < .05$

gives $T_g = 306.42°K = 33.42°C$

Therefore: $h_{rp-g} = (1.2 \times 10^{-8})(411.2 + 307.9)$

$= (411.2^2 + 307.9^2) = 2.28 \ W/m \ °C$

and: $h_{rg-s} = (4.99 \times 10^{-8})(307.9 + 297.1)$

$= (307.9^2 + 297.1^2) = 5.53 \ W/m^2 \ °C$

From Equation (4.7):

$$U_{L_{Theo}} = \left[\frac{1}{(1.1)(2.28)} + \frac{0.19/0.68}{12.54 + 5.53/2} \right]^{-1}$$

$$= 2.398 \ W/m^2 \ °C$$

Having estimated U_L, the useful heat and the efficiency can be calculated.

From Equation (2.1), for May 9, 1978, 11:55 a.m., Tube 1:

$$Q_{u_{Theo}} = F_R A_p CR(\tau\alpha)_e I_t - U_L (T_{fi} - T_a)$$

$$= (0.946)(.19)\ 1.879(907) - 2.4\ (131.2 - 29.6)$$

$$= 262.5 \text{ Watts}$$

And from Equation (2.3), the theoretical efficiency is found:

$$\eta_{Theo} = \frac{Q_{u_{Theo}}}{Q_{in}} = \frac{262.5W}{494.6W} = 0.531$$

In the above equations, the value of F_R was determined by the methods of Reference 6. The term CR $(\tau\alpha)_e$ is the product of flux concentration ratio, CR, and the effective transmittance-absorptance product. CR is found by analyzing the optics of the vee-trough system using a computer program. The values calculated above are shown in Table 4-1.

Figure 4-5 shows the trend followed by measured efficiencies plotted against the difference between the fluid inlet temperature and ambient temperature, $(T_{fi} - T_a)$. This same trend is also shown in Figure 2-1, which represents the theoretical values.

The hourly performance of the vee-trough system over a period of one day is presented in Appendix A for selected days. The plotted values are fluid temperature at the tube outlet, temperature rise in each receiver tube, and collector module efficiency. Here, the term "module" applies to a receiver tube and the vee-trough concentrator combination. Sometimes, the reflectors were removed from Tube 4 to compare the receiver tube performance with and without the concentrators. This is demonstrated in the temperature difference plot by a sharp drop in performance for Tube 4. However, in the efficiency plot, Tube 4 efficiency takes a sharp rise when the reflectors are removed. The reason for this behavior is that the efficiency is based on the aperture area for the collector module, whereas for the tube without reflectors the efficiency is based on the absorber plate area. These results are presented in Tables 4-9 through 4-11. In each table, the data for an additional tube is presented for comparison. Table 4-8 shows Tube 4 with the reflectors in position on July 17 and with the reflectors off on July 19. Table 4-9 makes a similar comparison for May 12, but for a time interval of 10 minutes.

Daily total heats collected and average daily efficiencies are given in Table 4-11 for selected days. The temperature range indicated in the table includes the lowest and highest operating temperature during the day. These overall daily values of Q_u and η are plotted in Appendix B. Figure B-1 shows the typical variation of useful heat over the period of one year. The dips in March and September represent the

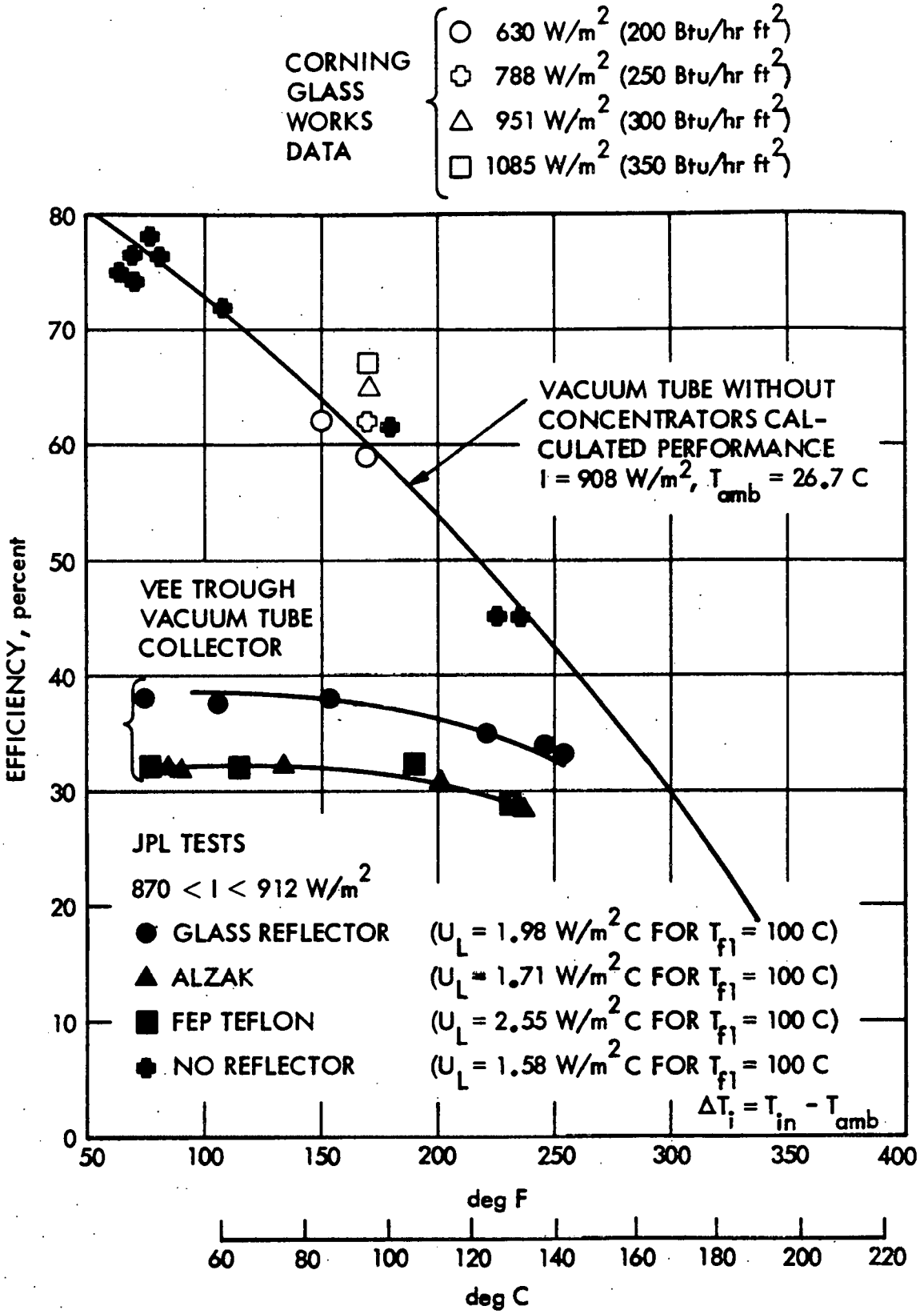

Figure 4-5. Test Data for Collector Efficiency Versus Temperature

Table 4-8. Comparison of Results for Tube 4 With and Without Reflectors

	TUBE 2		TUBE 4	
	Reflectors on		Reflec. on	Reflec. off
JULY 1978	July 17	July 19	July 17	July 19
Ambient air temp. (°C)	30.7	30.7	30.7	30.7
Solar flux, I_t (W/m^2)	873	861	873	861
Mass flow, $\dot{m}$ (kg/hr)	30.6	30.9	30.6	30.9
Specific heat (kJ/kg °C)	2.19	2.16	2.14	2.12
Useful heat Q_u (Watts)	247.0	270.5	171.6 +	86.2 +
Solar input Q_{in} = I·Area (Watts)	567.7	560.0	567.7	163.2 *
Efficiency (%)	43.5	41.7	30.3	52.8 *
Tube outlet temp. (°C)	256.5	234.5	217.1	197.6

* The efficiency and solar input of Tube 4 without the reflectors are based on the absorber plate area, which is smaller than the collector aperture area of tubes with reflectors.

+ By adding the reflectors the useful heat collected is increased by a factor of 2, in this case.

Table 4-9. Comparison of Results for Tube 4 With and Without Reflectors

	TUBE 2		TUBE 4	
	Reflectors on		Reflec. on	Reflec. off
	11:40 a.m.	11:50 a.m.	11:40 a.m.	11:50 a.m.
Ambient air temp. (°C)	35.9	36.8	35.9	36.8
Solar flux, I_t (W/m^2)	943	951	943	953
Mass flow, $\dot{m}$ (kg/hr)	24.7	24.4	24.7	24.4
Specific heat (kJ/kg °C)	2.35	2.35	2.32	2.32
Useful heat Q_u (Watts)	227.4	230.2	199.0 +	70.0 +
Solar input Q_{in} = I·Area (Watts)	613.3	618.5	613.3	180.3 *
Efficiency (%)	37.1	37.2	32.4	38.9 *
Tube outlet temp. (°C)	188.9	190.2	175.2	169.8

* The efficiency and solar input of Tube 4 without the reflectors are based on the absorber plate area, which is smaller than the collector aperture area of tubes with reflectors.

+ By adding the reflectors the useful heat collected is increased by a factor of 2.8, in this case.

Table 4-10. Comparison of Results for Tube 4 With and Without Reflectors

JUNE 1978	Tube 3		Tube 4	
	Reflectors on		Reflec. on	Reflec. off
	June 30	June 29	June 30	June 29
Ambient air temp. (°C)	28.4	26.2	28.4	26.2
Solar flux, I_t (W/m^2)	867	862	867	862
Mass flow, in (kg/hr)	22.6	22.9	22.6	22.9
Specific heat (kJ/kg °C)	2.23	2.21	2.20	2.19
Useful heat Q_u (Watts)	183.7	178.9	172.7 +	83.9 +
Solar input Q_{in} = I·Area (Watts)	559.8	556.6	563.8	163.4 *
Efficiency (%)	32.8	32.1	30.6	51.3 *
Tube outlet temp. (°C)	140.0	127.6	133.1	121.9

* The efficiency and solar input of Tube 4 without the reflectors are based on the absorber plate area, which is smaller than the collector aperture area of tubes with reflectors.

+ By adding the reflectors the useful heat collected is increased by a factor of 2.1, in this case.

Table 4-11. Daily Total Incident Fluxes, Useful Heats, and Average Efficiencies

DATE 1978	Temperature Range °C	Q_u kJ/day	Q_{in} kJ/day	η_{daily} %	Tube No.
May 3	132-170°	3650	10139	36.0	1
		3830	12082	31.7	2
		3321	12033	27.6	3
		2726 *	9270	29.4	4
May 19	145-183°	4246	10256	41.4	1
		3803	12230	31.1	2
		3408	12130	28.1	3
		3300	12222	27.0	4
June 8	120-150°	4516	10830	41.7	1
		4764	12910	36.9	2
		3419	12807	26.7	3
		3532	12138	29.1	4
June 21	135-185°	3390	9658	35.1	1
		3181	11484	27.7	2
		3090	11400	27.1	3
		3090	11490	26.9	4
June 30	120-155°	4455	9900	45.0	1
		3545	11777	30.1	2
		3280	11712	28.0	3
		3203	11776	27.2	4
July 7	127-185°	3427	9571	35.8	1
		3131	11387	27.5	2
		2927	11302	25.9	3
		2767	10644	26.0	4
July 14	120-190°	2815	7863	35.8	1
		2982	9379	31.8	2
		2897	9316	31.1	3
		2781	9364	29.7	4

* Reflectors removed in the afternoon.

equinoxes and the dip in June represents the summer solstice. Figures B-2 through B-7 show the experimental values of Q_u and η plotted with the typical performance curves, computed for various tubes and temperatures. In these figures, the theoretical predictions are evaluated for a constant fluid inlet temperature. For the test data points, the fluid inlet temperature varied over a range of temperatures throughout the day. The scatter in the data points is a result of data that was collected over a range of temperatures, rather than at a constant temperature.

SECTION 5

CONCLUSIONS AND RECOMMENDATIONS

5.1 CONCLUSIONS

This report outlines the mathematical analysis and presents the experimental results for the Vee-Trough Evacuated Tube Collector. Because of the high temperature capabilities (120-190°C) this system could be used for power generation purposes, as in an organic Rankine conversion system, as well as for solar heating and cooling. It is especially suitable for unattended pumping stations since the reflectors require reversal only once every six months.

Mathematical models of both the vee-trough concentrators and the evacuated tube receivers enable the prediction of flux concentration ratios and system performance. In this report, the concentration ratio and effective transmittance absorptance product ($CR\tau\alpha$) used in the theoretical analysis were generated from weather data for Burbank, California, which is less than 15 miles from JPL. However, the methodology developed enables use of weather data for any other locality. Necessary input data for the generation of $CR\tau\alpha$) are I_{Beam}, I_t, (horizontal), latitude, reflector flap angles, aperture angle, and receiver dimensions. Details of $CR\tau\alpha$ calculations are given in the final report of the first phase of this project (DOE/JPL/1024-1).

Test results reported represent the performance of the VTETC based on the aperture area. The data are defined for total incident flux on the collector plane, tilted 35° to the south. The combination for the instrument accuracy of data measurements is within $\pm$6%.

The tube efficiencies were determined as a ratio of useful heat collected to total solar input. Each receiver tube used reflectors made of different surfaces. Direct comparison of these reflective surfaces is not possible because the U_L values for all the tubes were not the same and the tubes operated at different temperatures for any given run. However, data taken for different runs show that Tube 1, with the glass mirror reflectors, consistently had efficiencies of about 40%, measured at 125°C (257°F) and flow rates of about 25 kg/hr (55 lb/hr). For other reflective surfaces the efficiencies were in the low 30 percent range, measured under the same conditions.

The effectiveness of the vee-trough reflectors was demonstrated by comparing the useful heat collected by a receiver tube with and without the concentrators. The results indicate an increase of heat collection by a factor of 1.8 to about 2.8, depending on time of day, time of year, cleanliness of the surfaces, and type of reflector. This magnitude of increase is substantial when considering the simplicity and low cost of the added reflectors. The merit of the collector concept is in combining the relatively expensive evacuated tube with the inexpensive concentrators to enhance tube performance by increasing solar flux.

In conclusion, this phase of the project has fulfilled its objective, which was to demonstrate the usefulness of the vee-trough concentrators in improving the heat collection per tube and reducing the cost of a solar collector. A cost study was performed and was presented in the Final Report of Phase I of this Project. It was further demonstrated that the mathematical predictions for the system agree with the test results within experimental uncertainties and theoretical assumptions.

Tests run during 1977 demonstrated the VTETC performance for various operating temperatures and for the summer months. Tests run during 1978 further confirm the conclusions reached during the first phase of the project.

Daily total heat collection follows the trend of the daily average concentration ratio. Tests were run during the vernal equinox and the summer solstice, with improved heat collection observed during May. This trend is shown in Appendix B Figures B-2 to B-7.

5.2 RECOMMENDATIONS FOR FUTURE WORK

Future work on the VTETC should include a continuation of data acquisition for winter months and further studies in applying the system to a complete solar heating, cooling, or a power generation system.

Since data acquisition to date has been only for spring and summer months, it is desirable to accumulate data for the fall and winter months to demonstrate the complete year-round performance capabilities of the VTETC.

Studies of the VTETC, so far, were aimed at predicting the system performance for quasi-steady-state conditions only without considering a complete system with an energy storage subsystem and a load. The mathematical models generated considered invariant conditions and the test data was used to verify these models for finite time intervals. Therefore, a simulation study is recommended to evaluate the collector system under actual transient conditions, incorporating an energy storage capability and a load.

Other future work should include application of the vee-trough concentrators to other types of evacuated receiver tubes, such as those developed by General Electric Company, and to heat pipe evacuated receivers developed by the Corning Glass Works.

SECTION 6

REFERENCES

1. W. I. Jacobs, "Use of Flexible Reflective Surfaces for Solar Energy Concentration," Journal of Vac. Sci. Technol., Vol. 12, No. 1, Jan/Feb 1975.

2. K. G. T. Hollands, "A Concentrator for Thin Film Solar Cells," Solar Energy, Vol. 13, page 149, 1971.

3. J. A. Duffie and W. A. Beckman, Solar Energy Thermal Processes, Wiley Interscience, New York, N.Y., 1974.

4. V. Ortabasi, "Indoor Test Methods to Determine the Effect of Vacuum on the Performance of a Tubular Flat Plate Collector," ASME Paper No. 76-WA/SOL-24.

5. S. Karaki and D. M. Frick, "Performance of an Evacuated Tube Solar Collector," paper presented at ISES 1976 Conference, Winnipeg, Manitoba, Canada.

6. S. I. Abdelkhalik, "Heat Removal Factor for a Flat Plate Solar Collector with a Serpentine Tube," Journal of Solar Energy, Vol. 18, No. 1, pp. 59-67, 1976.

APPENDIX A

DAY-LONG PERFORMANCE DATA

Collector outlet temperature, temperature rise in each receiver tube, and collector efficiencies are presented for the following days in 1978:

May 9
May 17
May 19

June 9
June 21
June 22
June 26
June 29

July 12
July 17

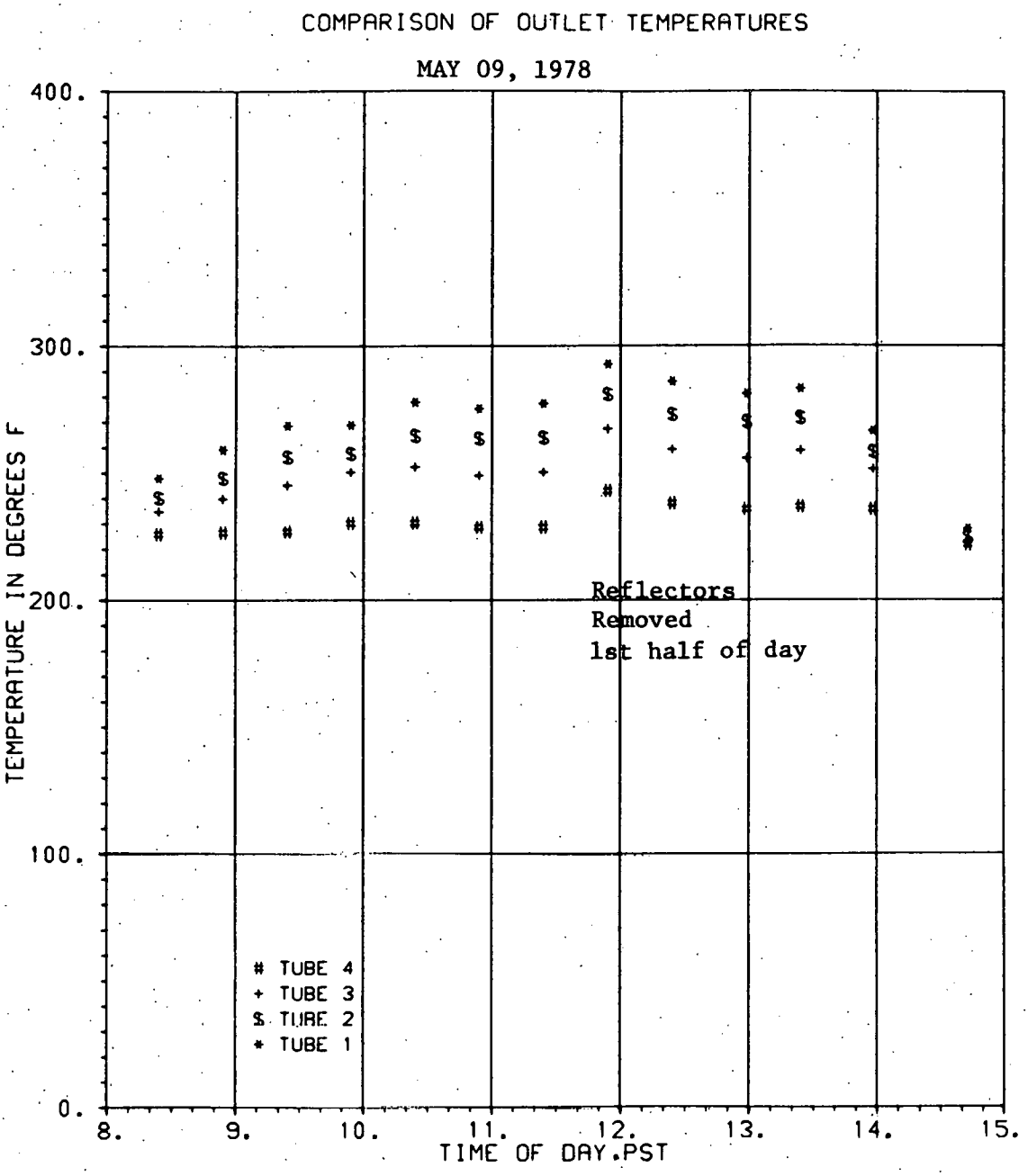
COMPARISON OF OUTLET TEMPERATURES
MAY 09, 1978
400.
300.
200.
100.
0.
TEMPERATURE IN DEGREES F
8.
9.
10.
11.
12.
13.
14.
15.
TIME OF DAY.PST
Reflectors
Removed
1st half of day
TUBE 4
+ TUBE 3
$ TUBE 2
* TUBE 1

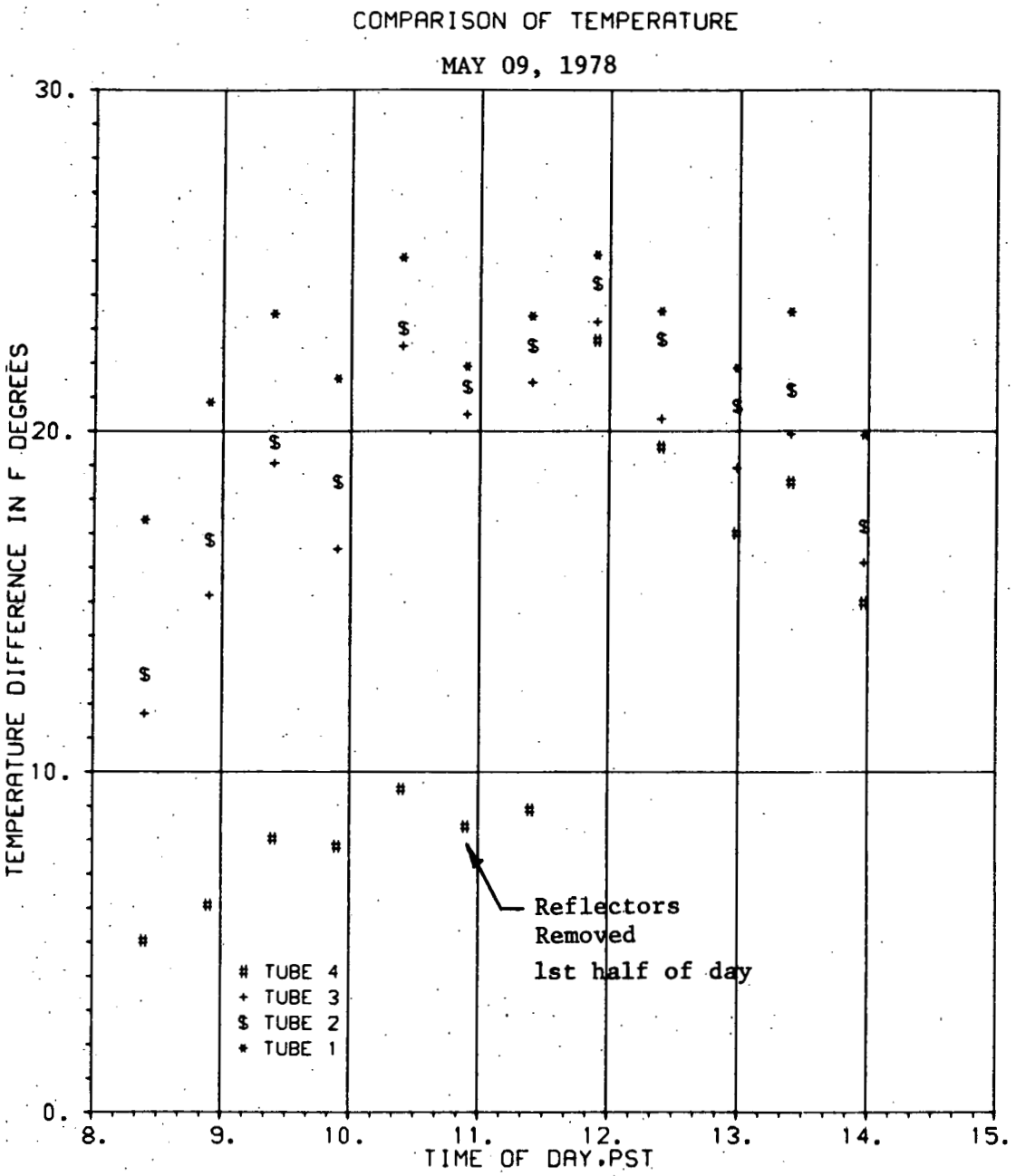
COMPARISON OF TEMPERATURE
MAY 09, 1978
TEMPERATURE DIFFERENCE IN F DEGREES
30.
20.
10.
0.
8.
9.
10.
11.
12.
13.
14.
15.
TIME OF DAY,PST
TUBE 4
+ TUBE 3
$ TUBE 2
* TUBE 1
Reflectors
Removed
1st half of day

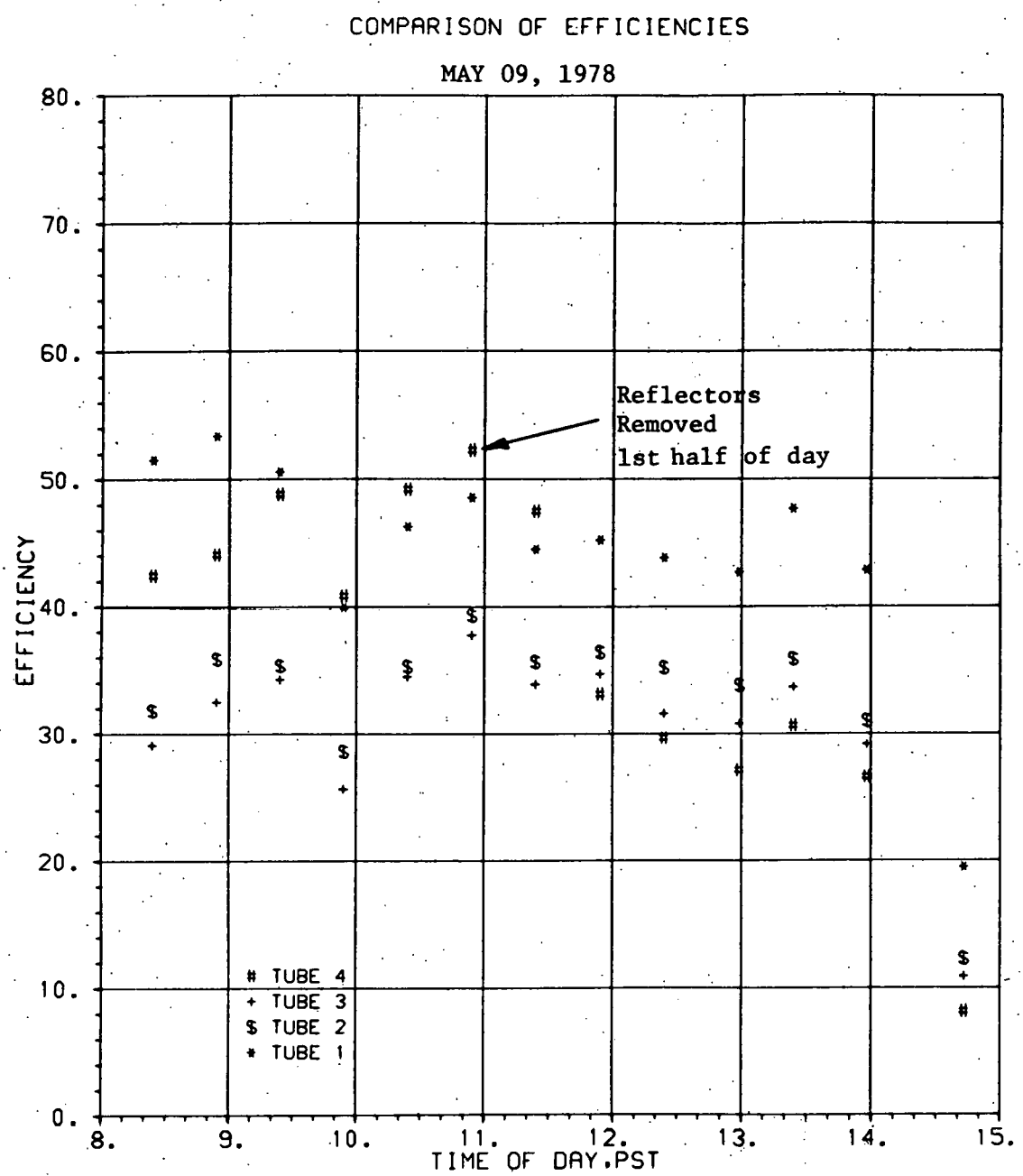
COMPARISON OF EFFICIENCIES
MAY 09, 1978
EFFICIENCY
80.
70.
60.
50.
40.
30.
20.
10.
0.
8.
9.
10.
11.
12.
13.
14.
15.
TIME OF DAY,PST
Reflectors
Removed
1st half of day
TUBE 4
+ TUBE 3
$ TUBE 2
* TUBE 1

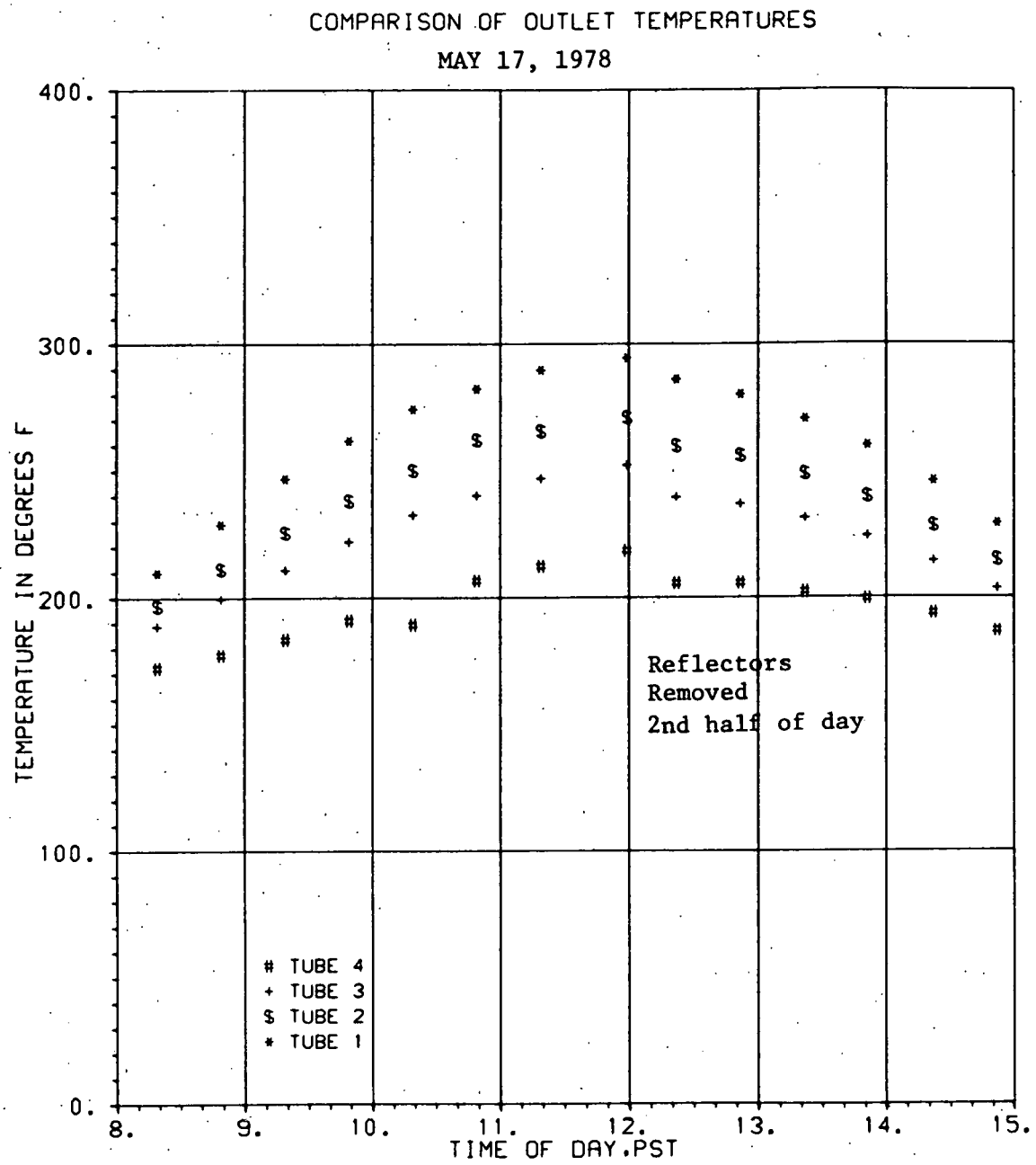
COMPARISON OF OUTLET TEMPERATURES
MAY 17, 1978
400.
300.
200.
100.
0.
TEMPERATURE IN DEGREES F
8.
9.
10.
11.
12.
13.
14.
15.
TIME OF DAY.PST
TUBE 4
+ TUBE 3
$ TUBE 2
* TUBE 1
Reflectors
Removed
2nd half of day

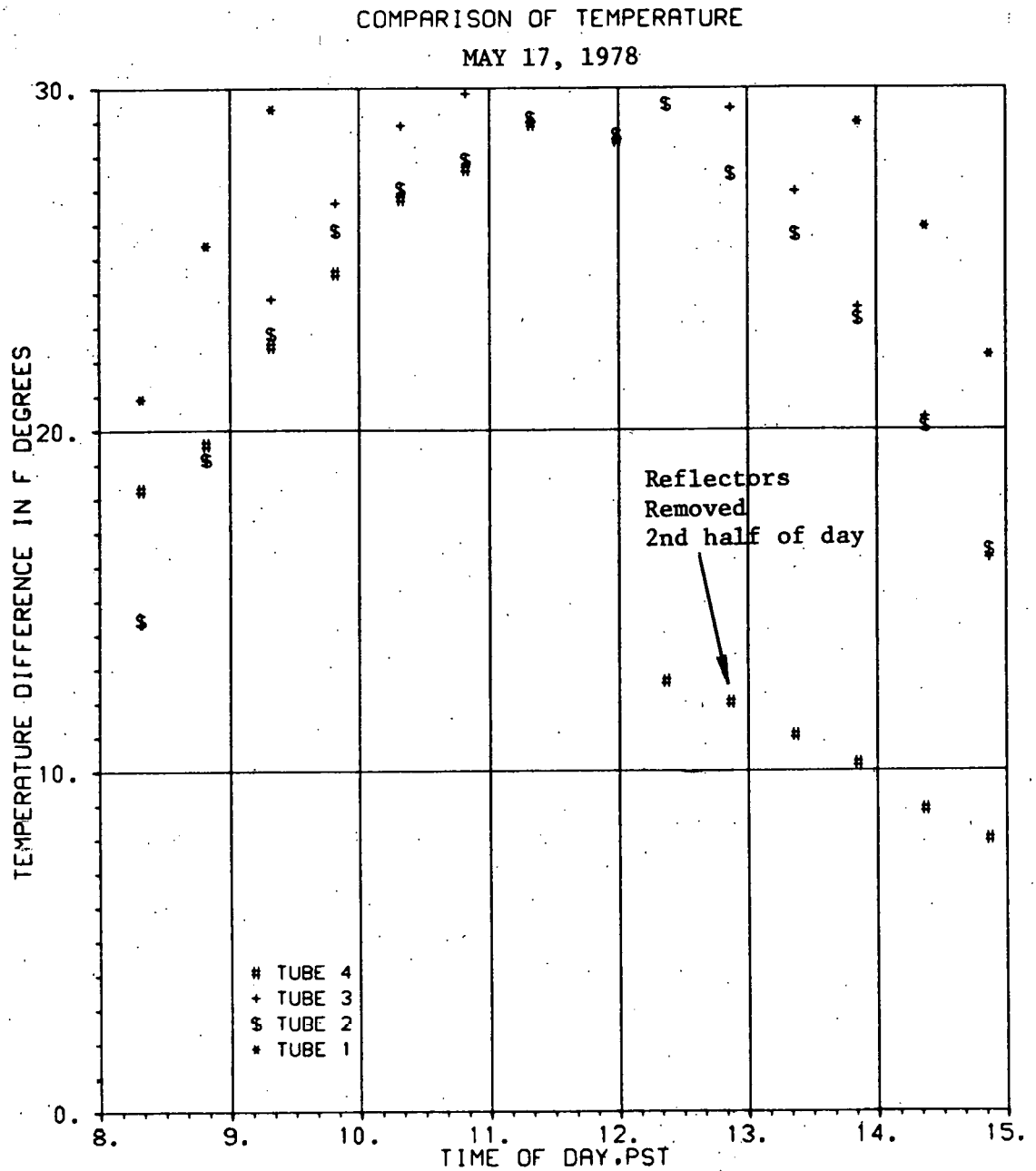
COMPARISON OF TEMPERATURE
MAY 17, 1978
TEMPERATURE DIFFERENCE IN F DEGREES
30.
20.
10.
0.
8.
9.
10.
11.
12.
13.
14.
15.
TIME OF DAY,PST
Reflectors
Removed
2nd half of day
TUBE 4
+ TUBE 3
$ TUBE 2
* TUBE 1

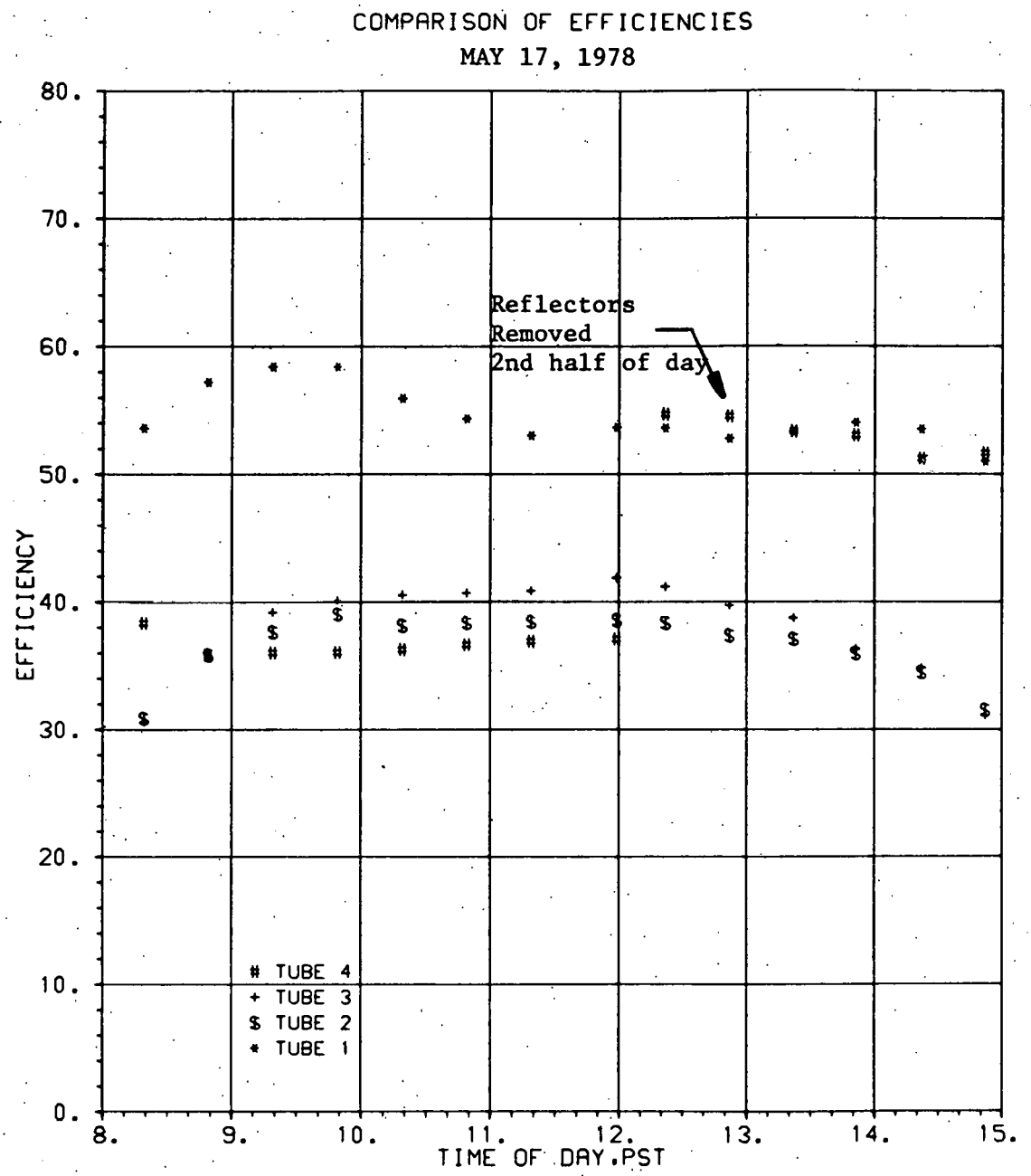
COMPARISON OF EFFICIENCIES
MAY 17, 1978
Reflectors
Removed
2nd half of day
EFFICIENCY
80.
70.
60.
50.
40.
30.
20.
10.
0.
8.
9.
10.
11.
12.
13.
14.
15.
TIME OF DAY,PST
TUBE 4
+ TUBE 3
$ TUBE 2
* TUBE 1

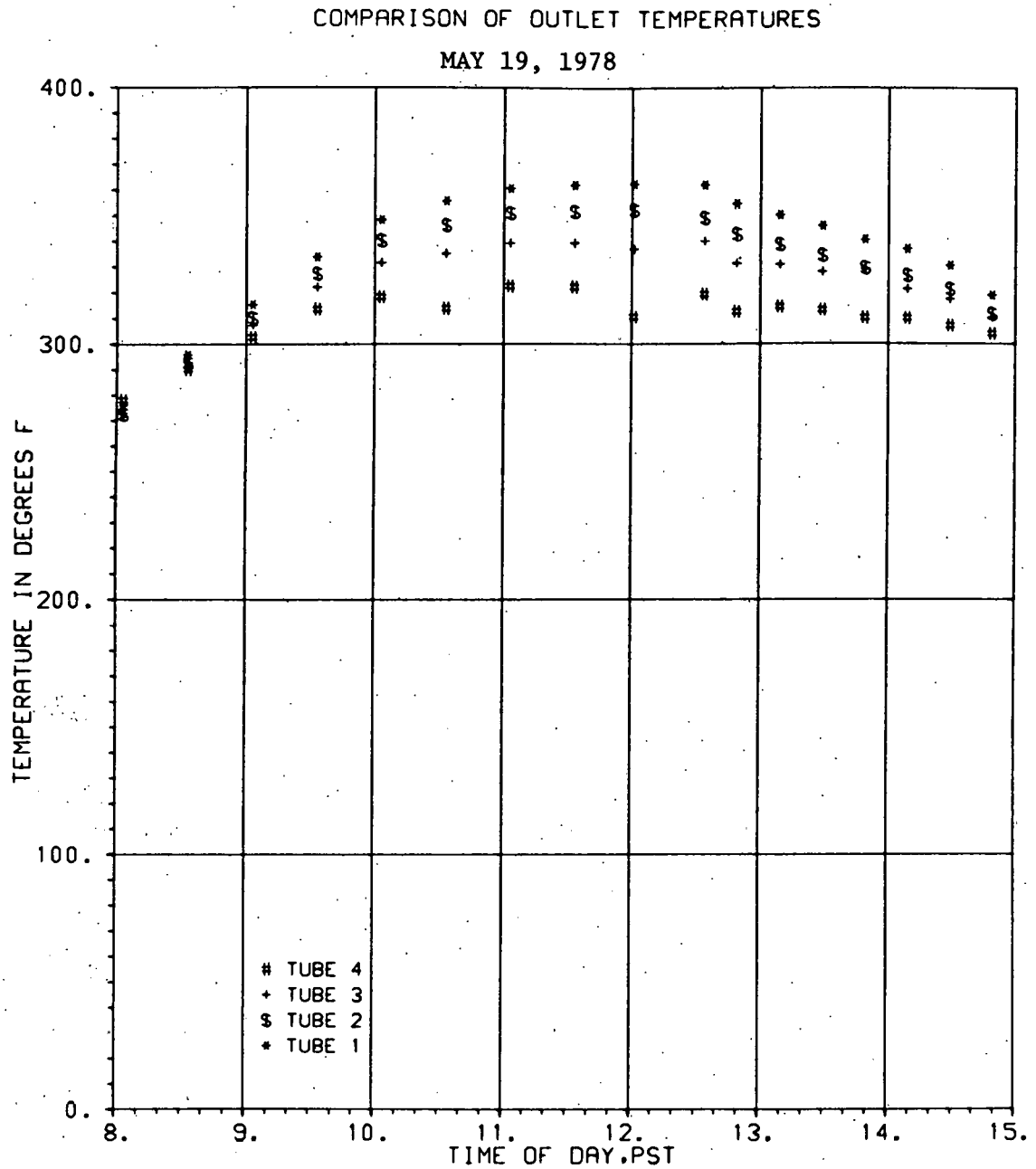
COMPARISON OF OUTLET TEMPERATURES
MAY 19, 1978
400.
300.
200.
100.
0.
TEMPERATURE IN DEGREES F
8.
9.
10.
11.
12.
13.
14.
15.
TIME OF DAY,PST
TUBE 4
+ TUBE 3
$ TUBE 2
* TUBE 1

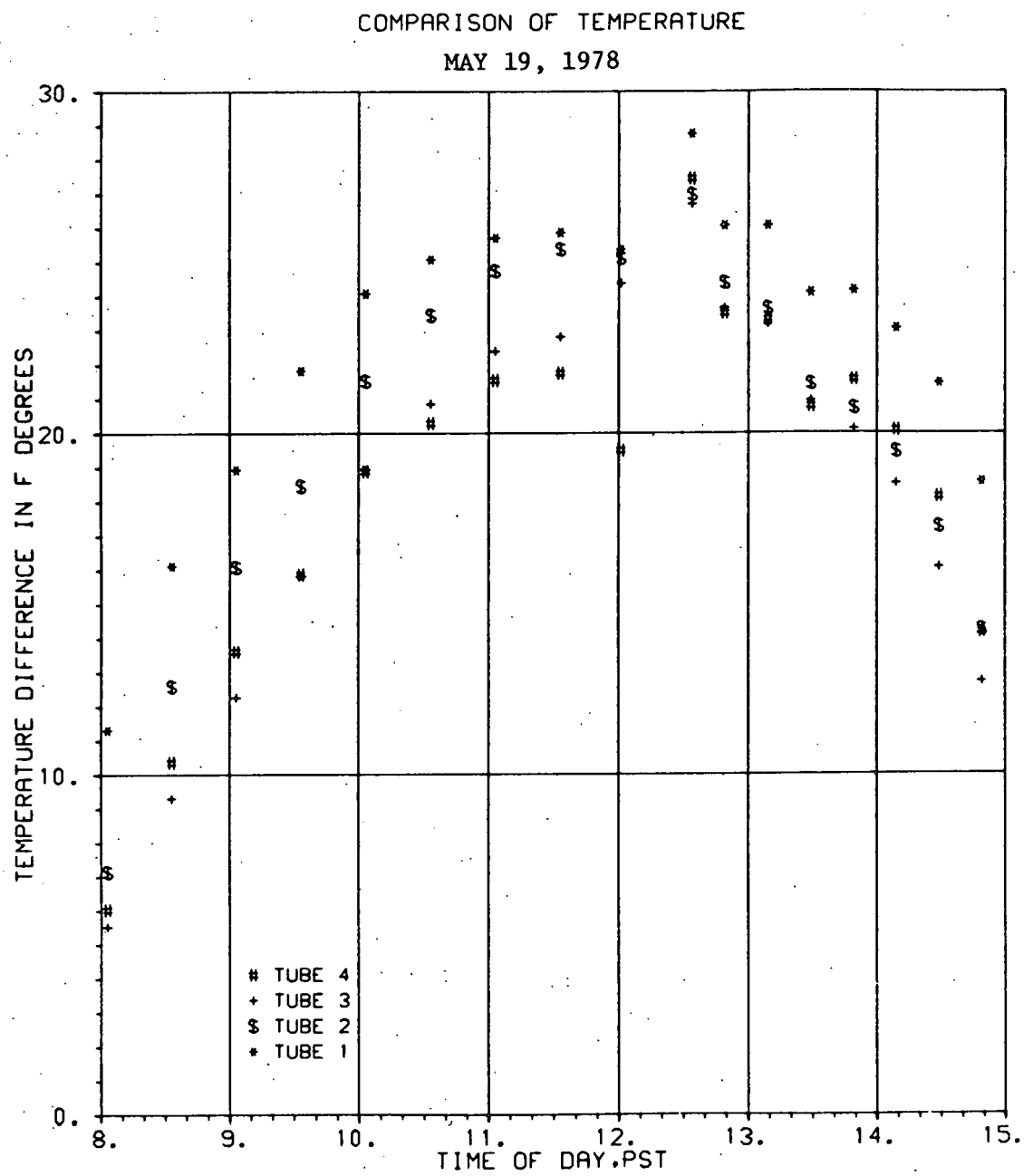
COMPARISON OF TEMPERATURE
MAY 19, 1978
TEMPERATURE DIFFERENCE IN F DEGREES
30.
20.
10.
0.
8.
9.
10.
11.
12.
13.
14.
15.
TIME OF DAY,PST
TUBE 4
+ TUBE 3
$ TUBE 2
* TUBE 1

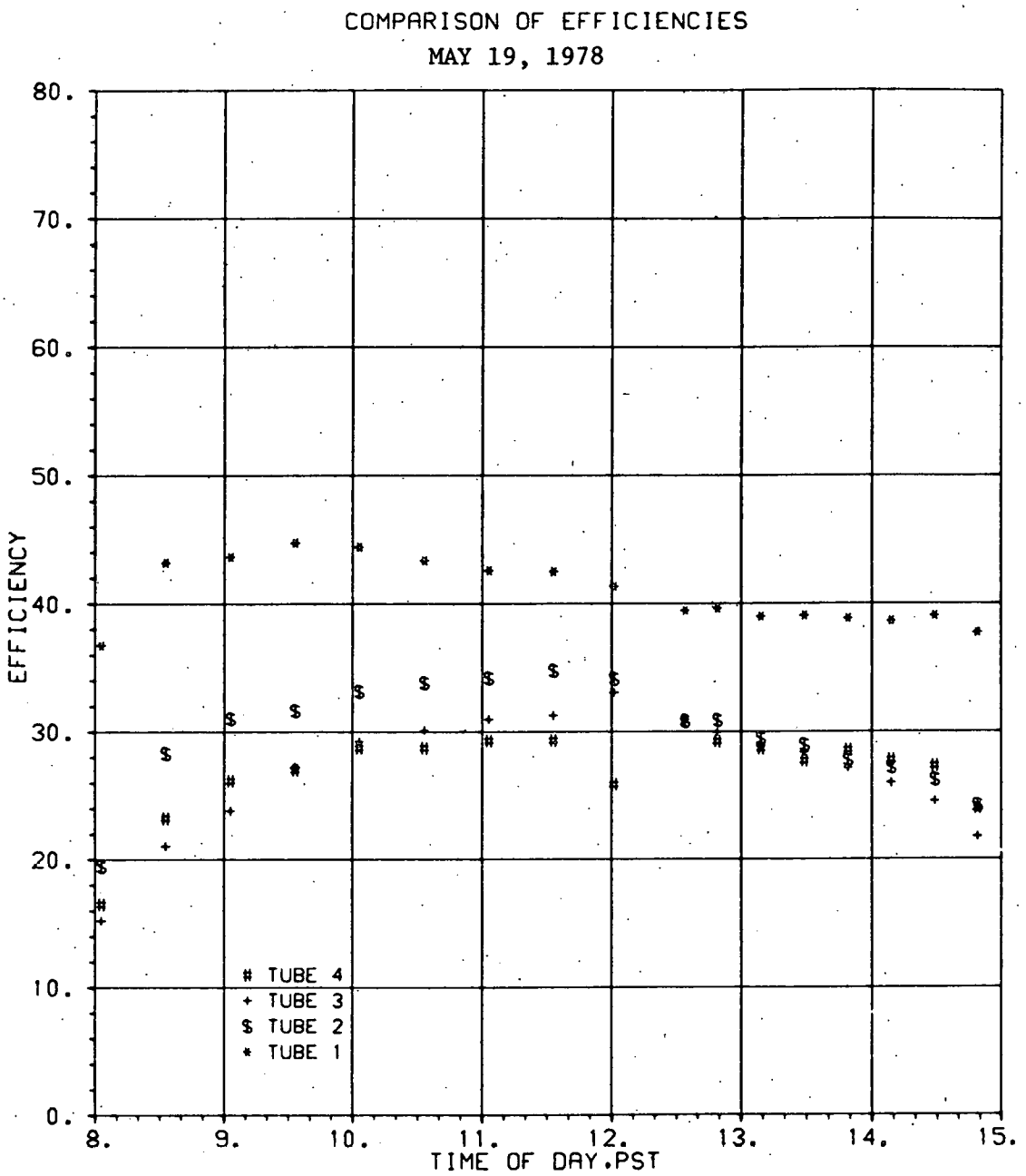
COMPARISON OF EFFICIENCIES
MAY 19, 1978
EFFICIENCY
80.
70.
60.
50.
40.
30.
20.
10.
0.
8.
9.
10.
11.
12.
13.
14.
15.
TIME OF DAY.PST
TUBE 4
+ TUBE 3
$ TUBE 2
* TUBE 1

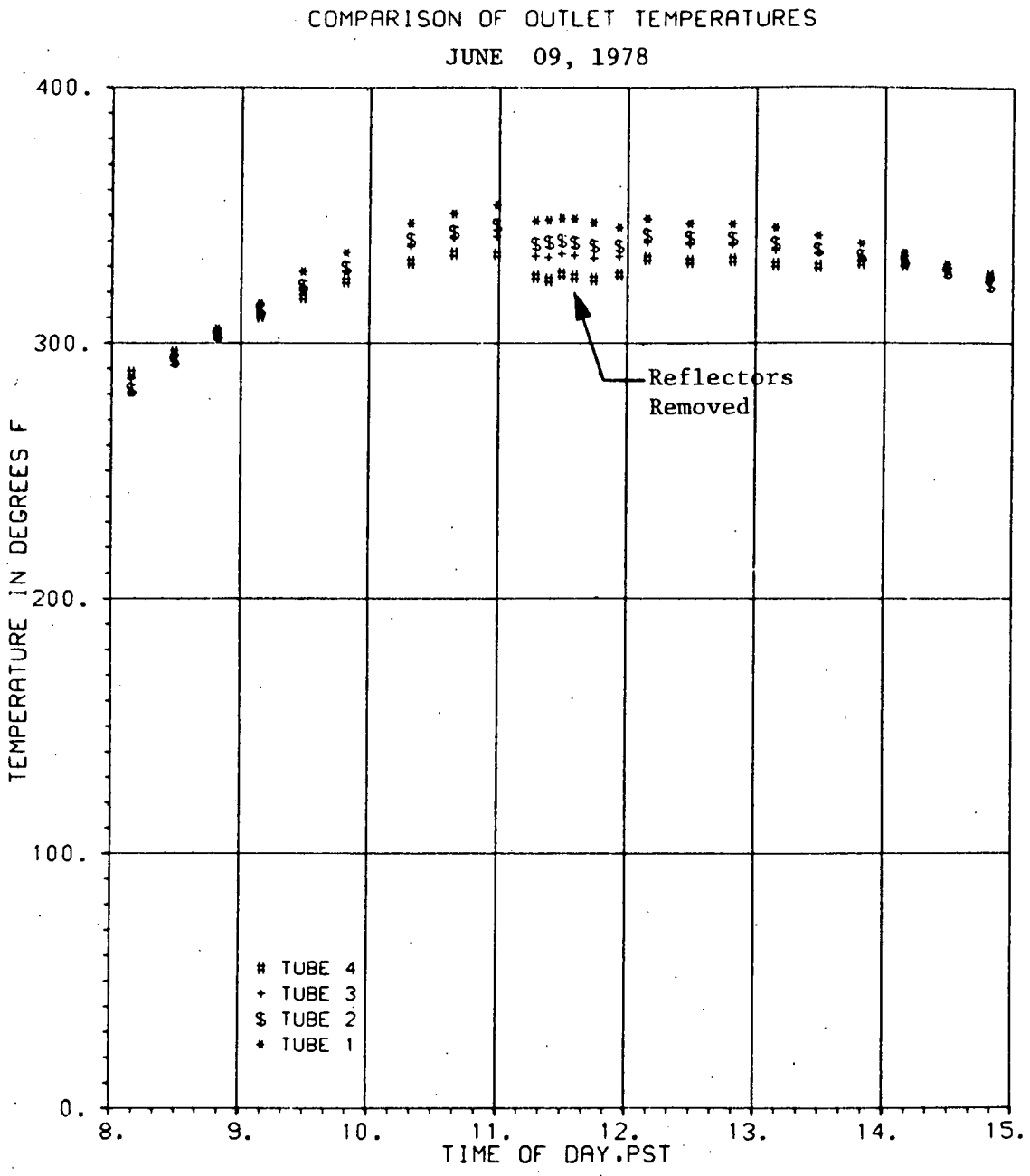
COMPARISON OF OUTLET TEMPERATURES
JUNE 09, 1978
400.
300.
200.
100.
0.
TEMPERATURE IN DEGREES F
Reflectors
Removed
TUBE 4
+ TUBE 3
$ TUBE 2
* TUBE 1
8.
9.
10.
11.
12.
13.
14.
15.
TIME OF DAY,PST

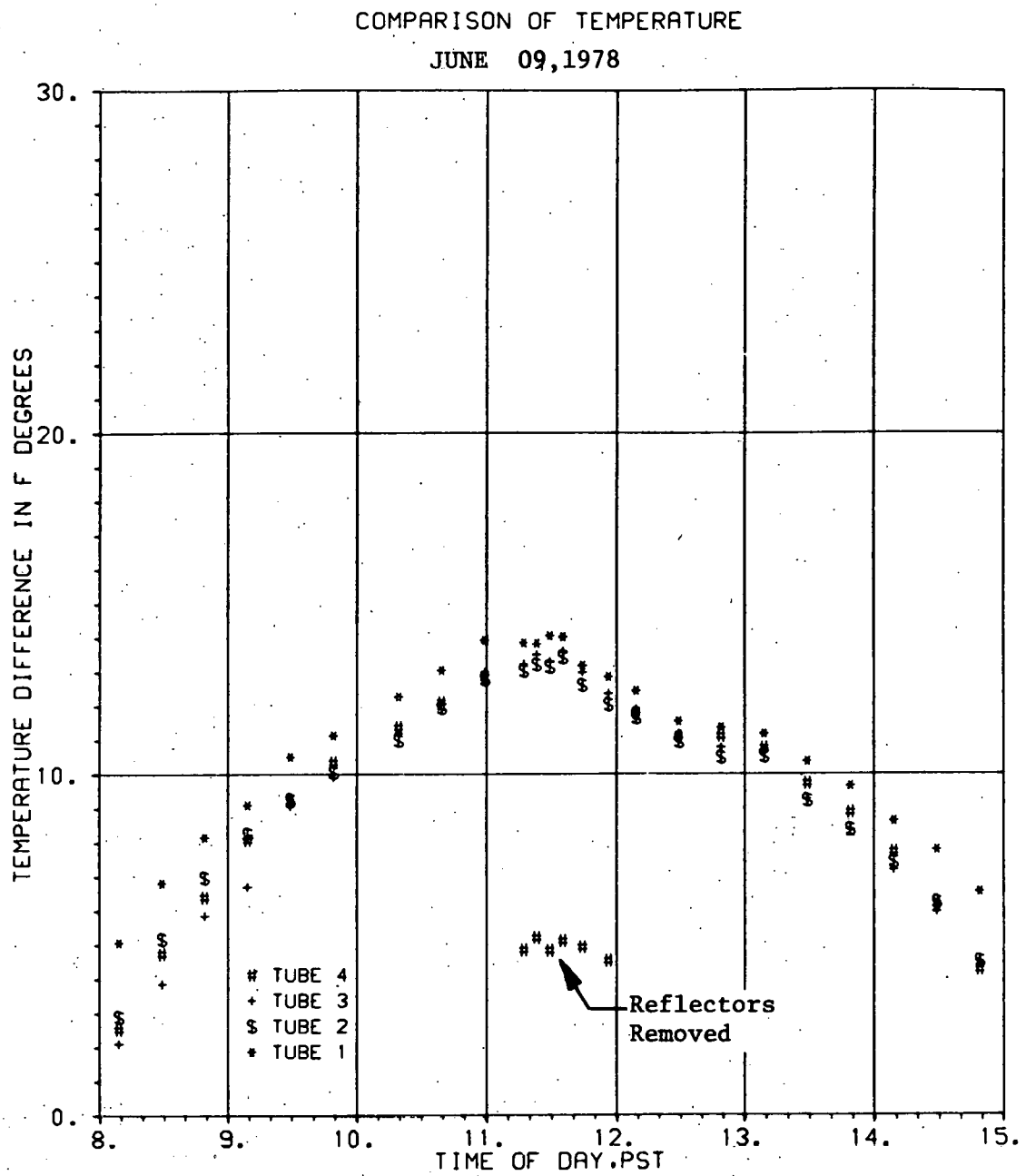
COMPARISON OF TEMPERATURE
JUNE 09,1978
TEMPERATURE DIFFERENCE IN F DEGREES
30.
20.
10.
0.
8.
9.
10.
11.
12.
13.
14.
15.
TIME OF DAY.PST
TUBE 4
+ TUBE 3
$ TUBE 2
* TUBE 1
Reflectors
Removed

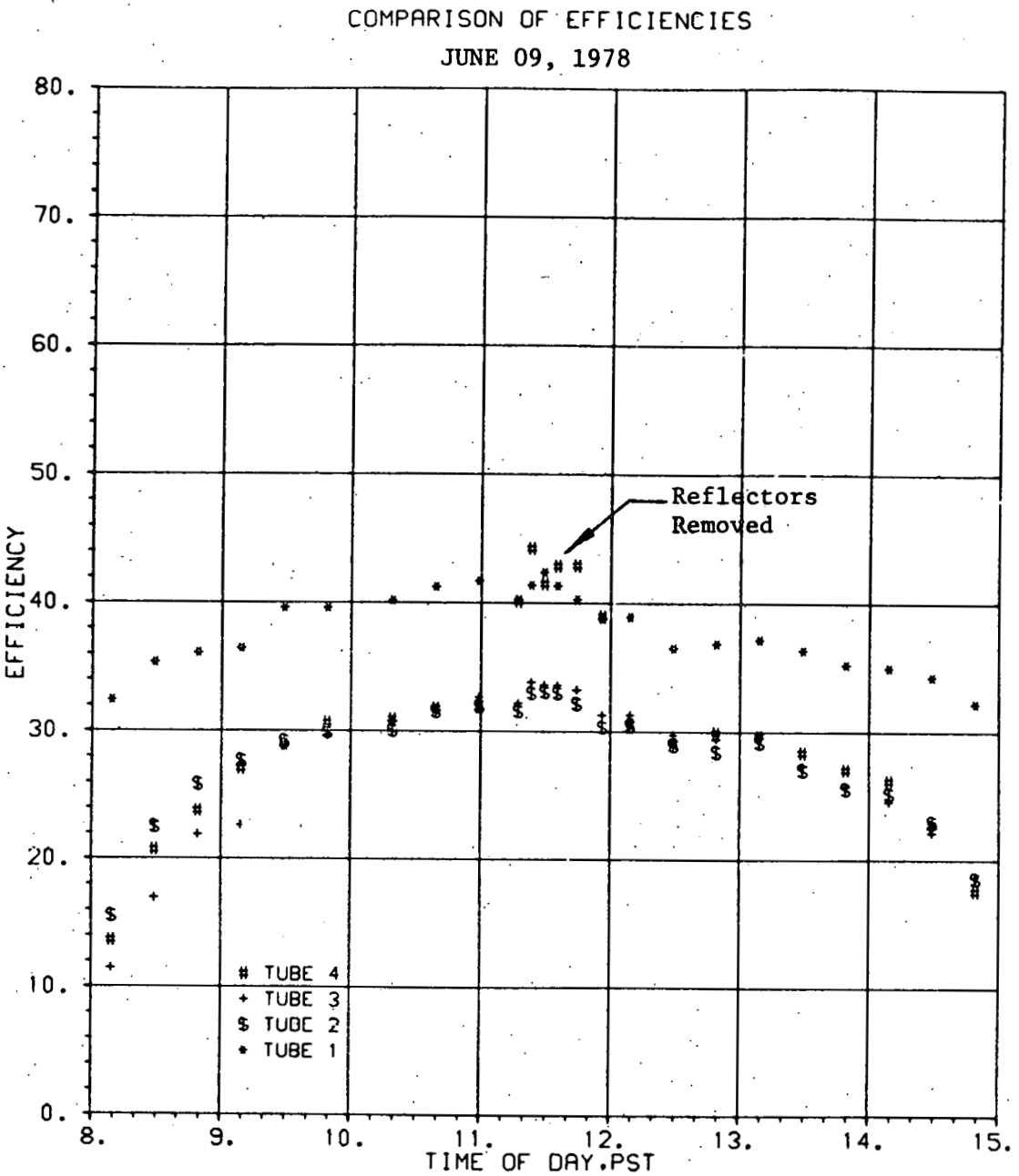
COMPARISON OF EFFICIENCIES
JUNE 09, 1978
EFFICIENCY
80.
70.
60.
50.
40.
30.
20.
10.
0.
8.
9.
10.
11.
12.
13.
14.
15.
TIME OF DAY,PST
Reflectors Removed
TUBE 4
+ TUBE 3
$ TUBE 2
* TUBE 1

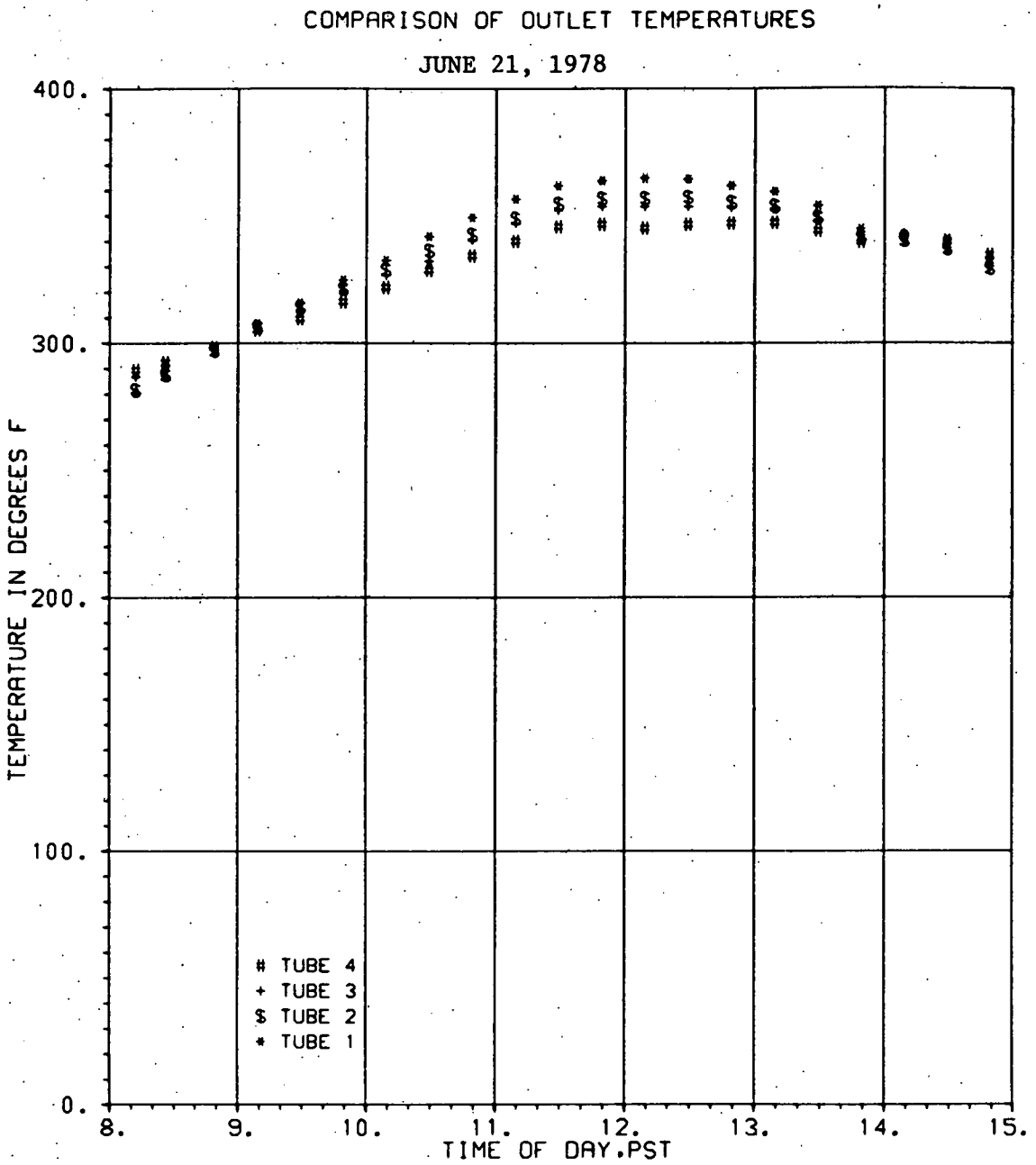
COMPARISON OF OUTLET TEMPERATURES
JUNE 21, 1978
400.
300.
200.
100.
0.
TEMPERATURE IN DEGREES F
8.
9.
10.
11.
12.
13.
14.
15.
TIME OF DAY.PST
TUBE 4
+ TUBE 3
$ TUBE 2
* TUBE 1

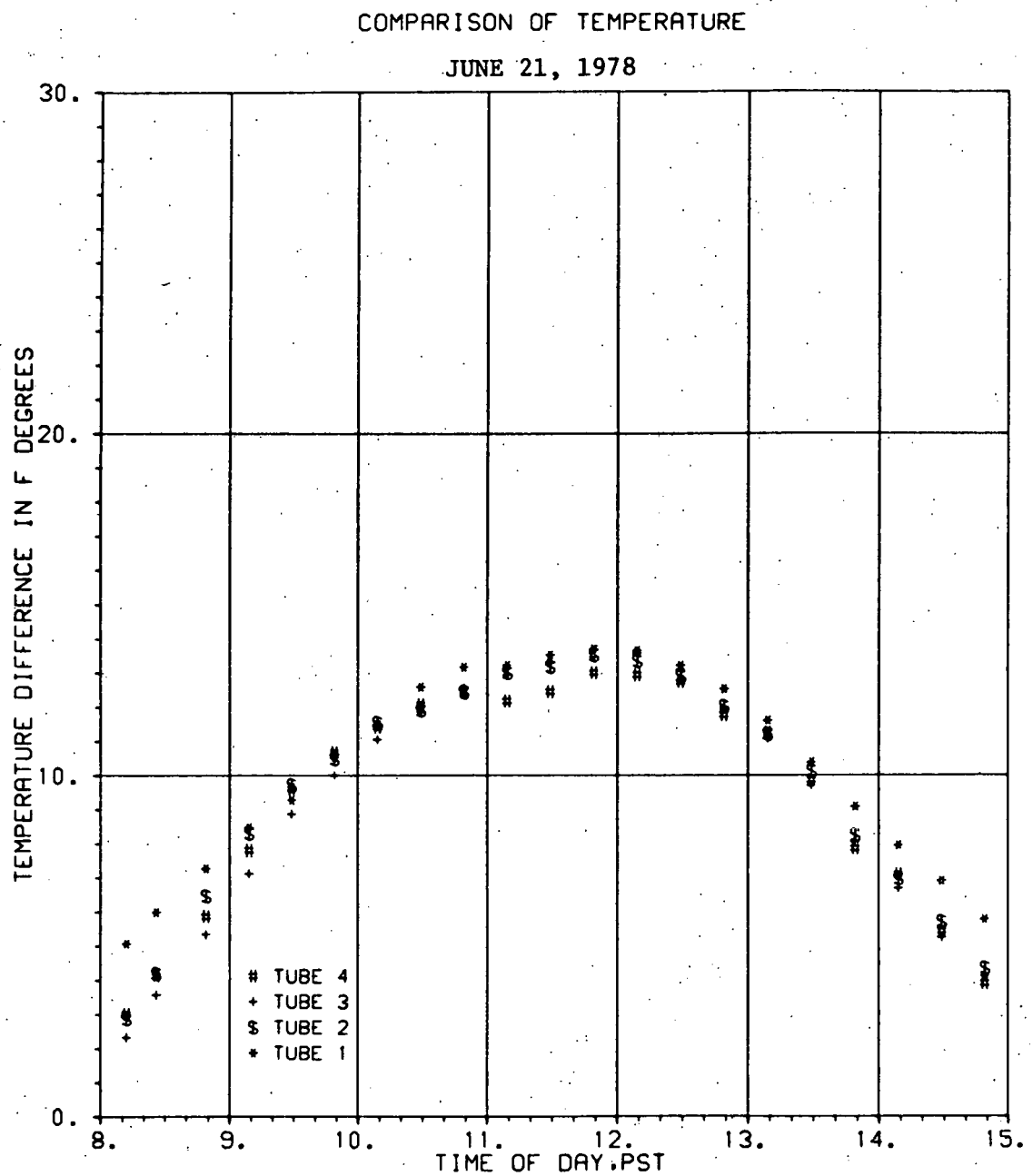
COMPARISON OF TEMPERATURE
JUNE 21, 1978
TEMPERATURE DIFFERENCE IN F DEGREES
30.
20.
10.
0.
8.
9.
10.
11.
12.
13.
14.
15.
TIME OF DAY,PST
TUBE 4
+ TUBE 3
$ TUBE 2
* TUBE 1

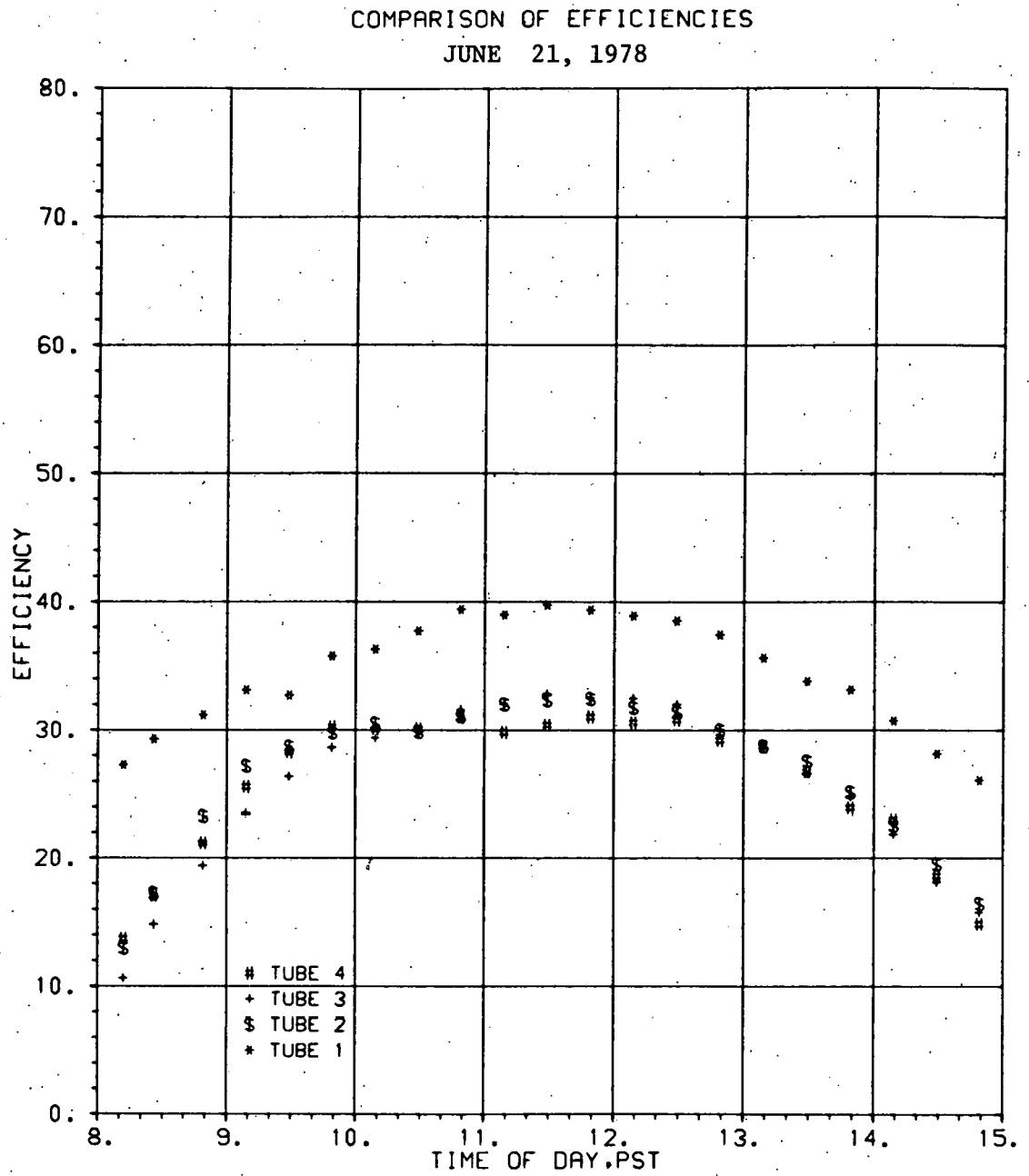
COMPARISON OF EFFICIENCIES
JUNE 21, 1978
EFFICIENCY
80.
70.
60.
50.
40.
30.
20.
10.
0.
8.
9.
10.
11.
12.
13.
14.
15.
TIME OF DAY,PST
TUBE 4
+ TUBE 3
$ TUBE 2
* TUBE 1

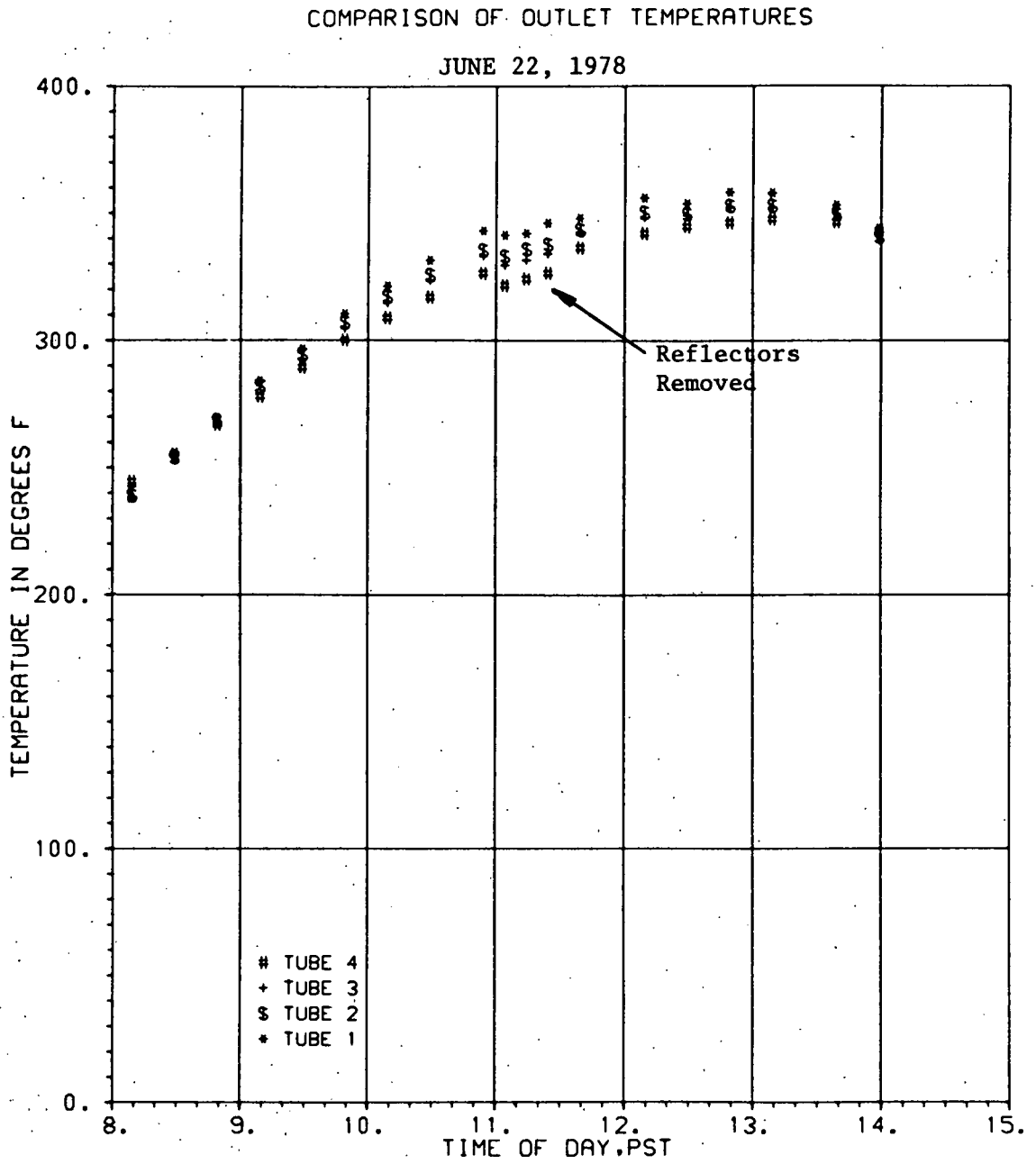
COMPARISON OF OUTLET TEMPERATURES
JUNE 22, 1978
400.
300.
200.
100.
0.
TEMPERATURE IN DEGREES F
Reflectors
Removed
TUBE 4
+ TUBE 3
$ TUBE 2
* TUBE 1
8.
9.
10.
11.
12.
13.
14.
15.
TIME OF DAY,PST

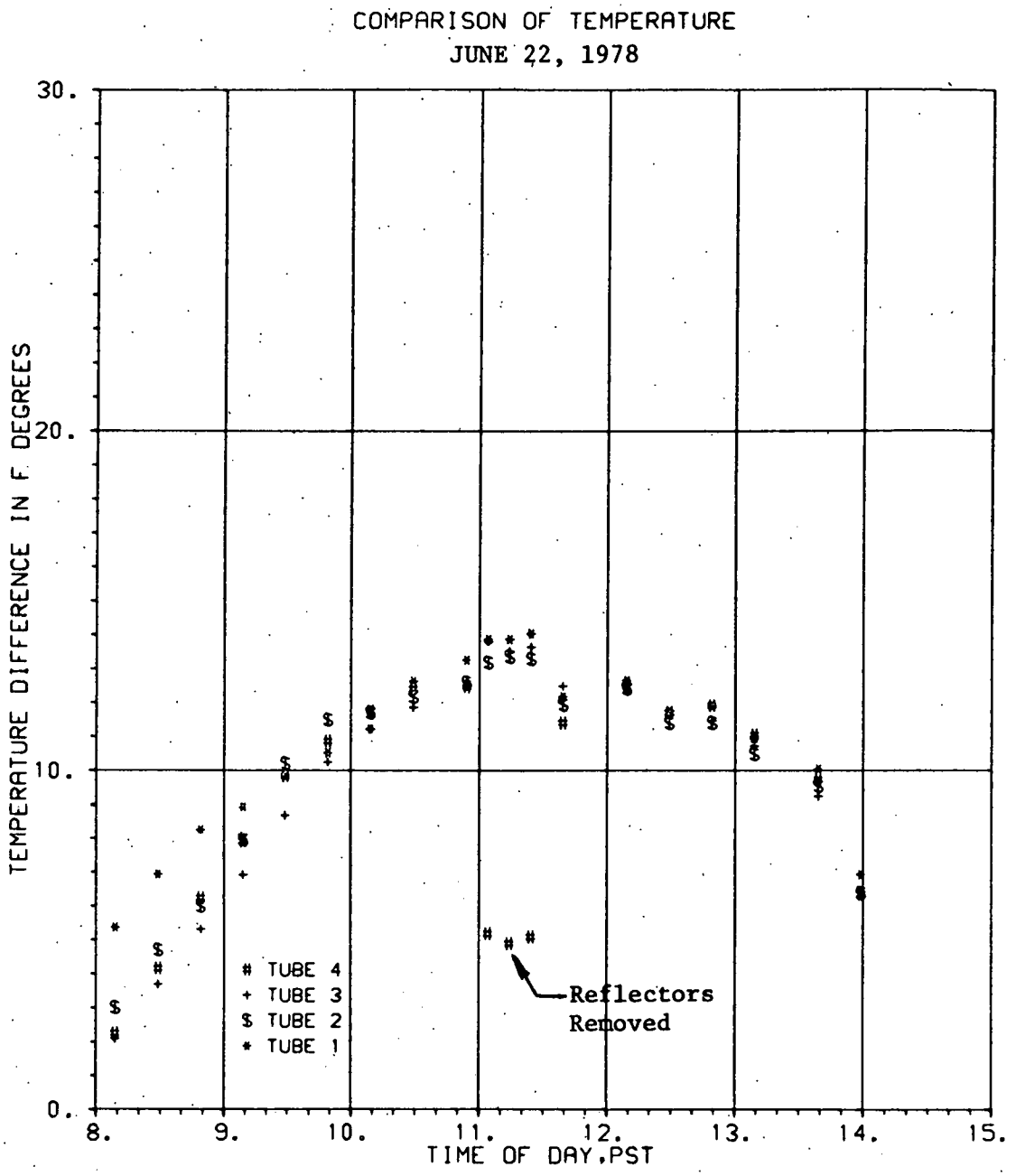
COMPARISON OF TEMPERATURE
JUNE 22, 1978
TEMPERATURE DIFFERENCE IN F DEGREES
30.
20.
10.
0.
8.
9.
10.
11.
12.
13.
14.
15.
TIME OF DAY,PST
TUBE 4
+ TUBE 3
$ TUBE 2
* TUBE 1
Reflectors
Removed

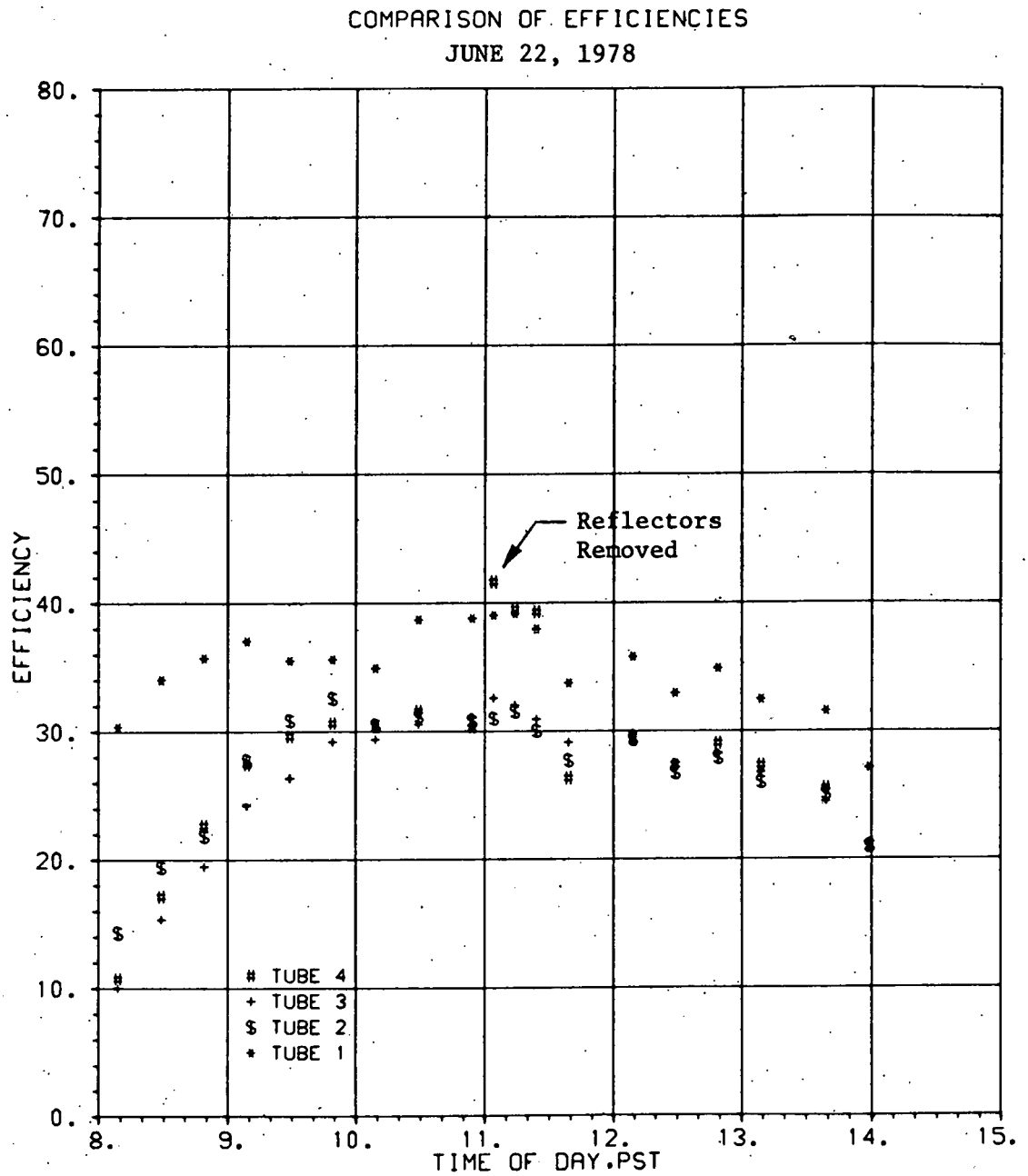
COMPARISON OF EFFICIENCIES
JUNE 22, 1978
EFFICIENCY
80.
70.
60.
50.
40.
30.
20.
10.
0.
8.
9.
10.
11.
12.
13.
14.
15.
TIME OF DAY.PST
Reflectors
Removed
TUBE 4
+ TUBE 3
$ TUBE 2
* TUBE 1

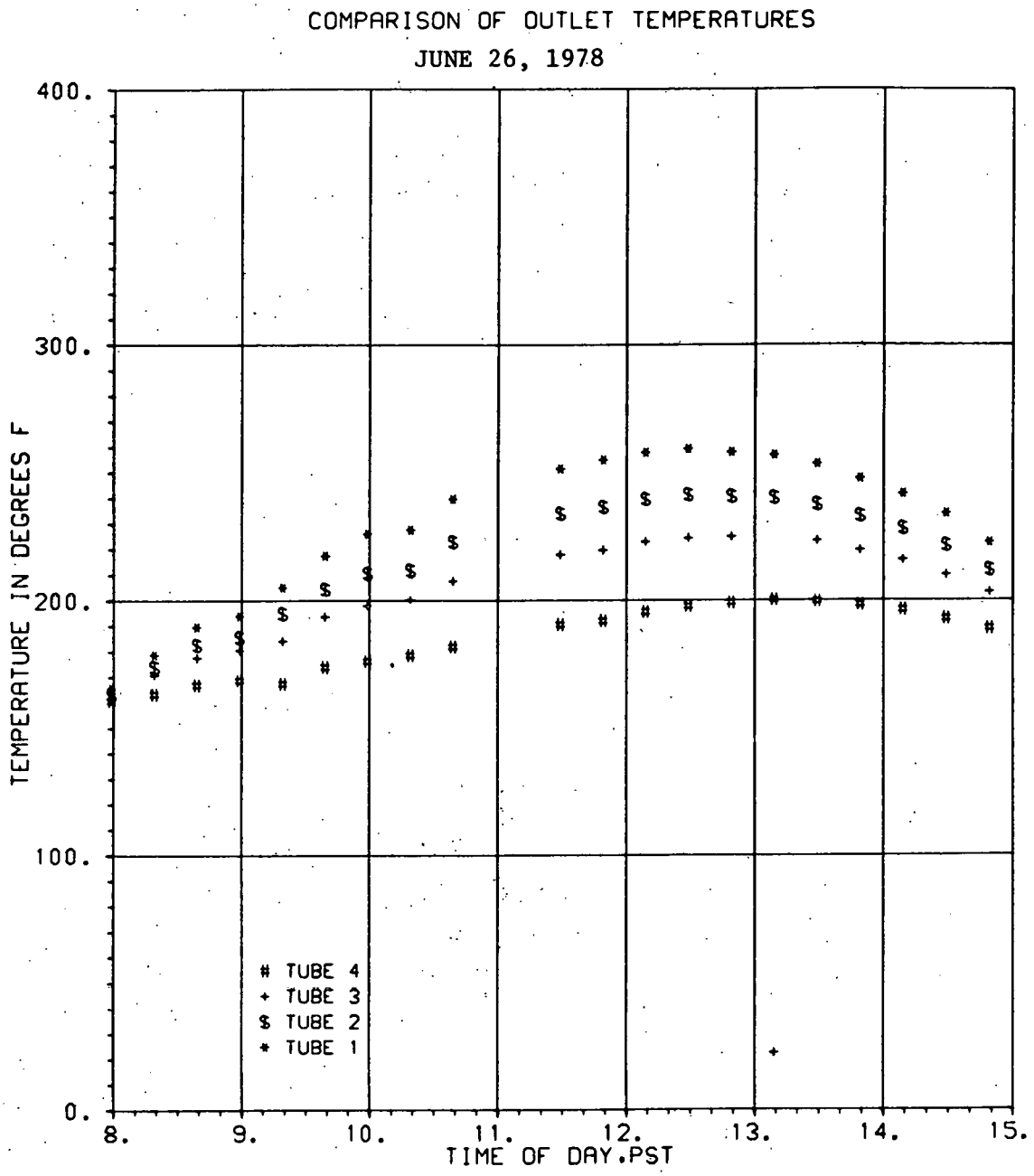
COMPARISON OF OUTLET TEMPERATURES
JUNE 26, 1978
400.
300.
200.
100.
0.
TEMPERATURE IN DEGREES F
8.
9.
10.
11.
12.
13.
14.
15.
TIME OF DAY.PST
TUBE 4
+ TUBE 3
$ TUBE 2
* TUBE 1

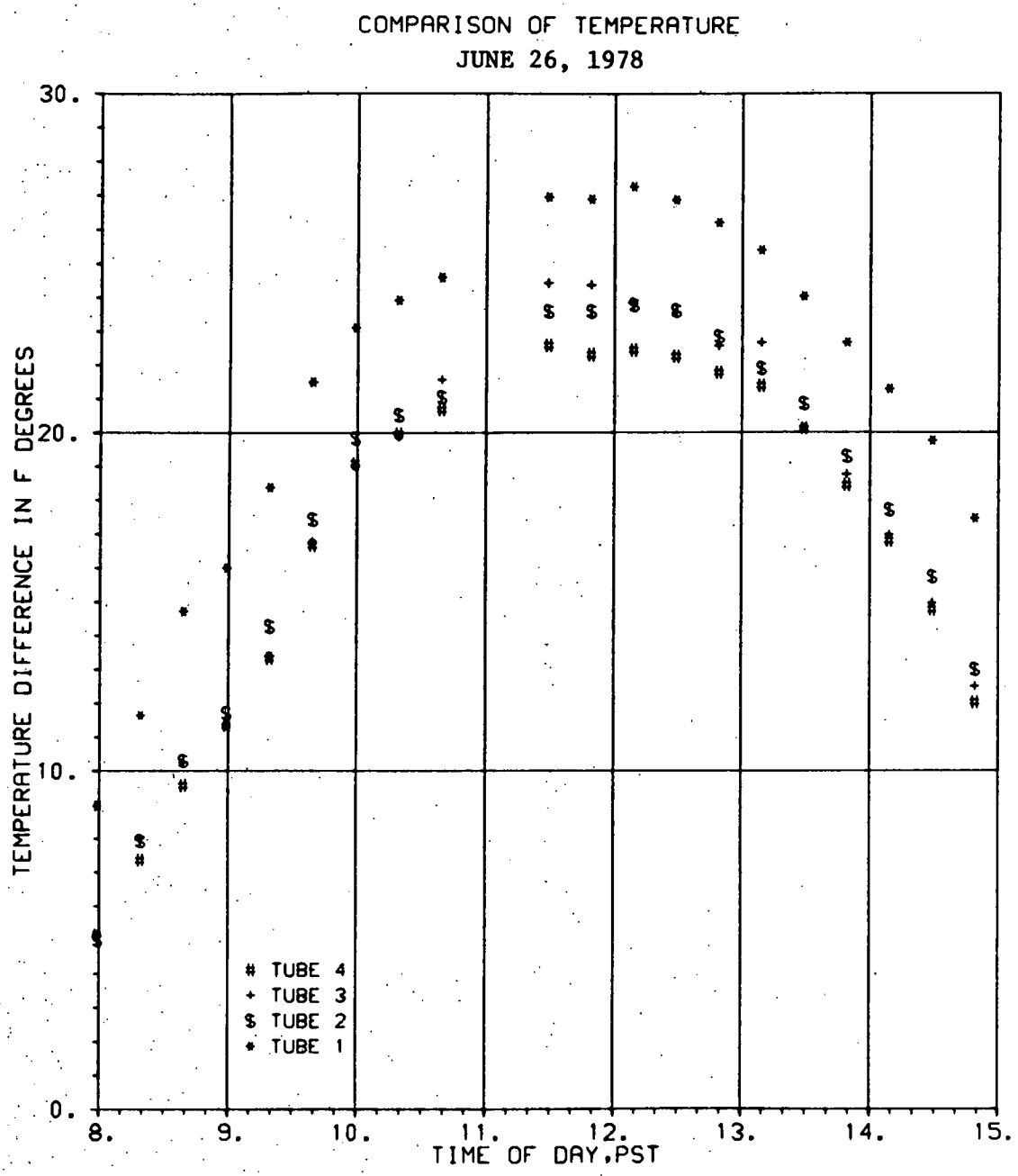
COMPARISON OF TEMPERATURE
JUNE 26, 1978
TEMPERATURE DIFFERENCE IN F DEGREES
30.
20.
10.
0.
8.
9.
10.
11.
12.
13.
14.
15.
TIME OF DAY,PST
TUBE 4
+ TUBE 3
$ TUBE 2
* TUBE 1

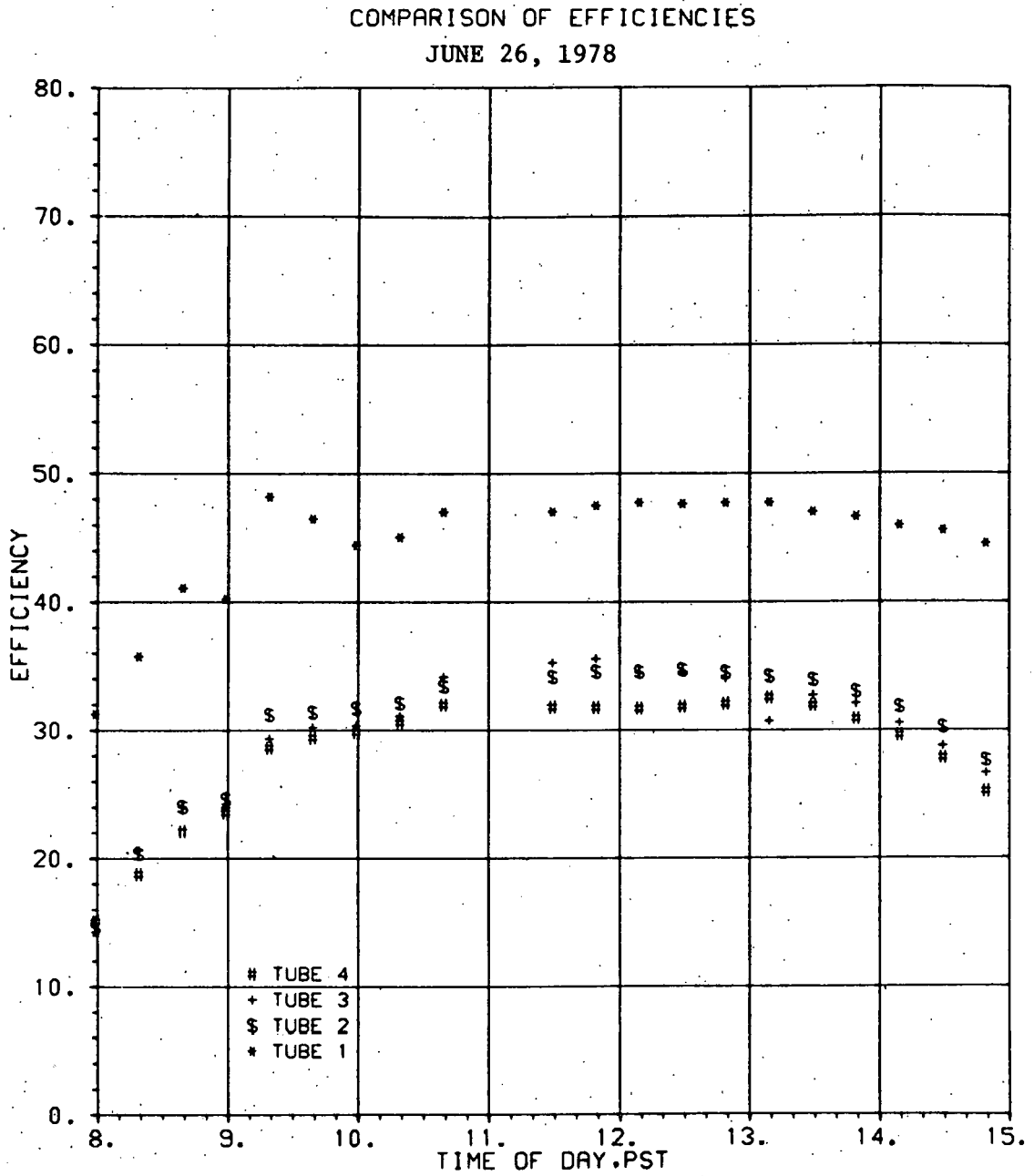
COMPARISON OF EFFICIENCIES
JUNE 26, 1978
EFFICIENCY
80.
70.
60.
50.
40.
30.
20.
10.
0.
8.
9.
10.
11.
12.
13.
14.
15.
TIME OF DAY.PST
TUBE 4
+ TUBE 3
$ TUBE 2
* TUBE 1

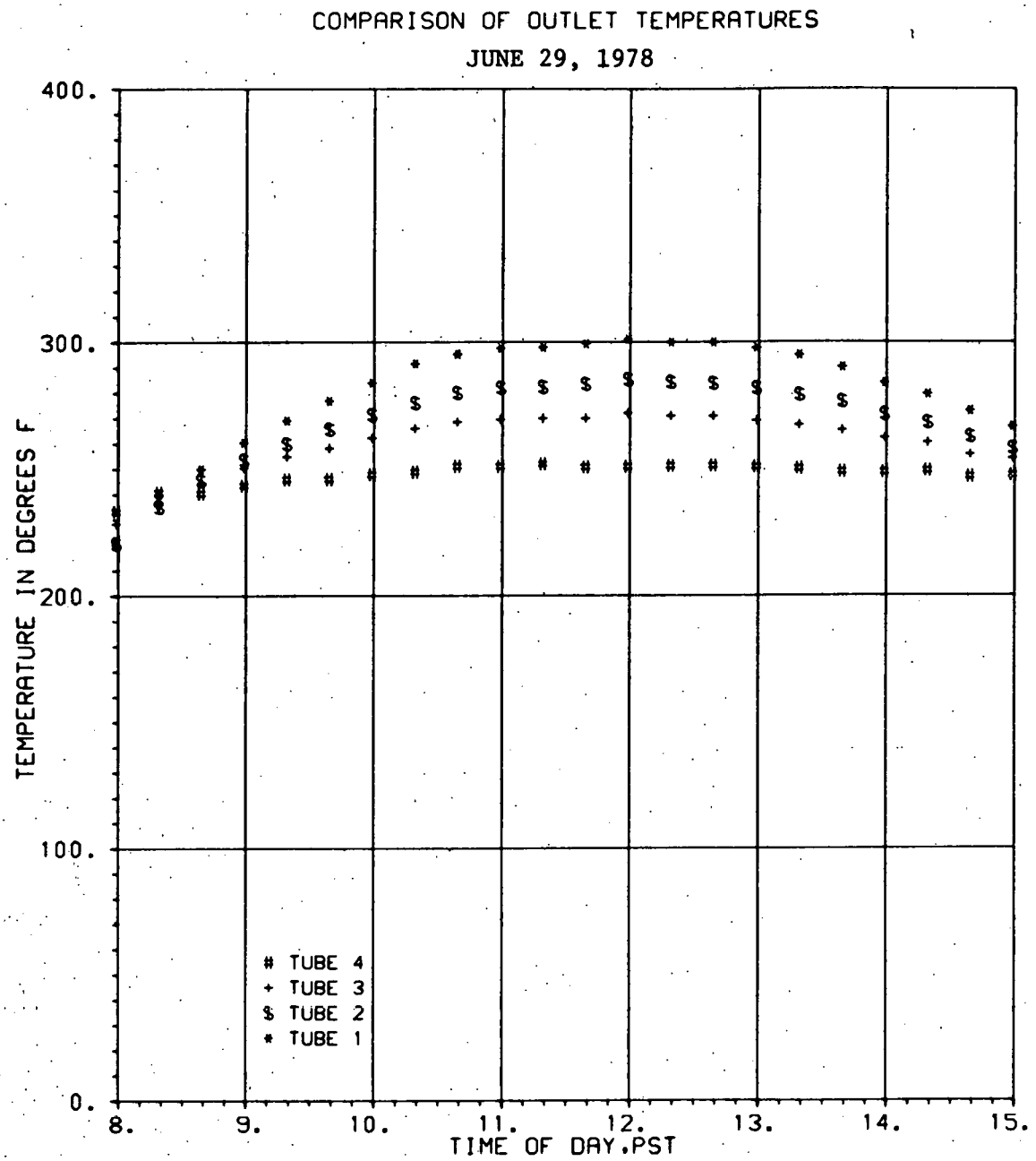
COMPARISON OF OUTLET TEMPERATURES
JUNE 29, 1978
400.
300.
200.
100.
0.
TEMPERATURE IN DEGREES F
8.
9.
10.
11.
12.
13.
14.
15.
TIME OF DAY.PST
TUBE 4
+ TUBE 3
$ TUBE 2
* TUBE 1

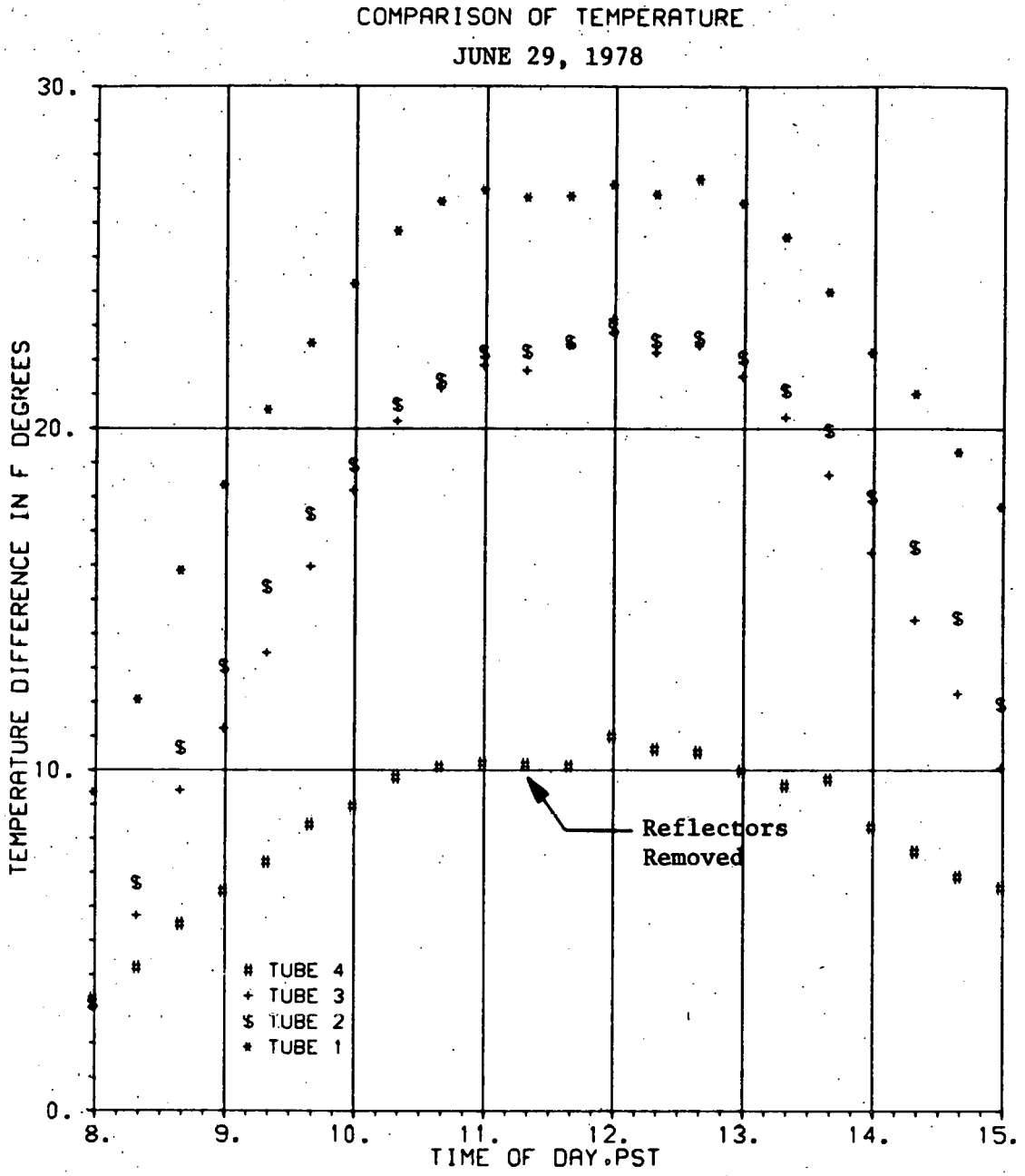
COMPARISON OF TEMPERATURE
JUNE 29, 1978
30.
20.
10.
0.
TEMPERATURE DIFFERENCE IN F DEGREES
8.
9.
10.
11.
12.
13.
14.
15.
TIME OF DAY,PST
Reflectors
Removed
TUBE 4
+ TUBE 3
$ TUBE 2
* TUBE 1

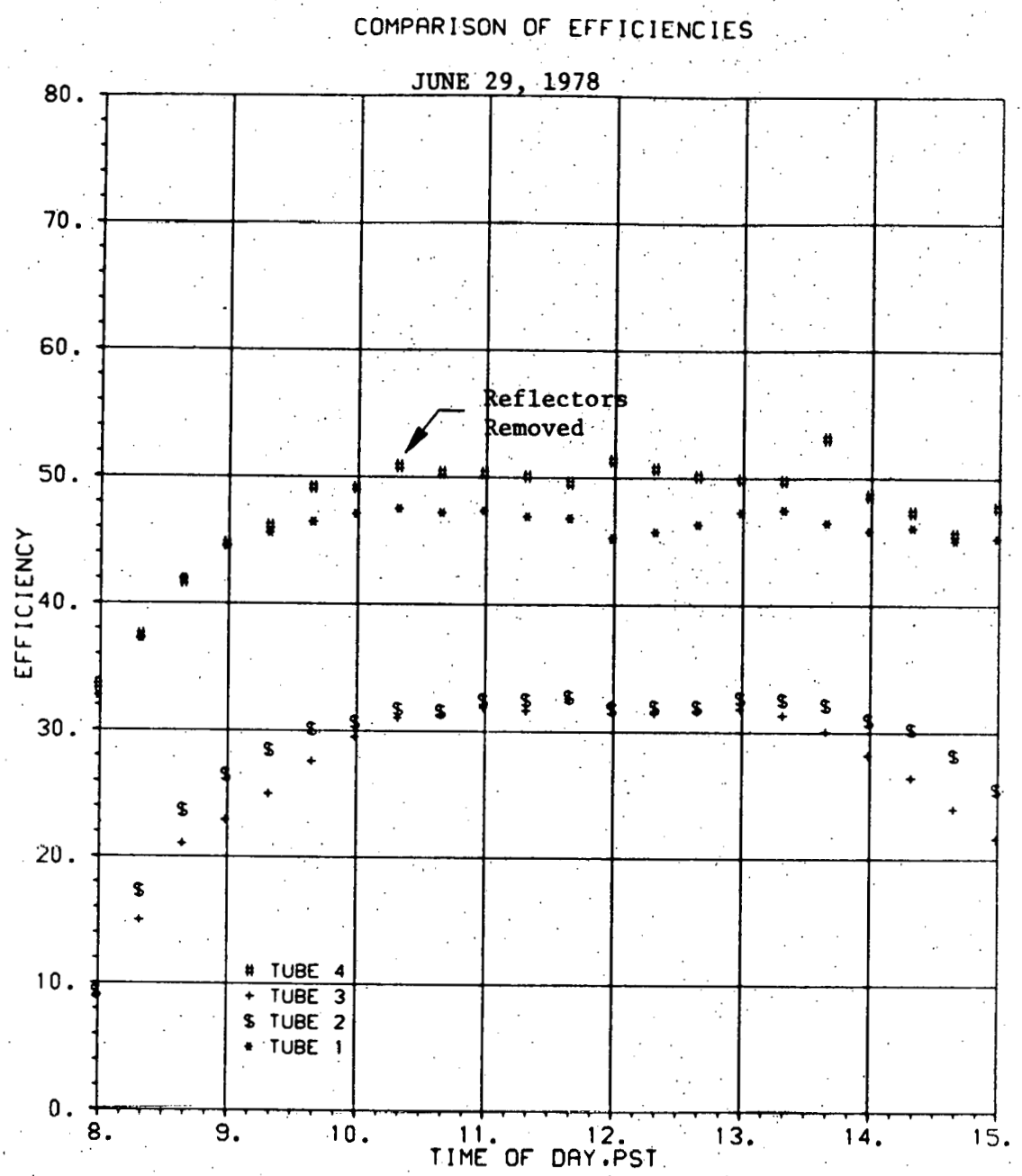
COMPARISON OF EFFICIENCIES
JUNE 29, 1978
80.
70.
60.
50.
40.
30.
20.
10.
0.
EFFICIENCY
Reflectors
Removed
TUBE 4
+ TUBE 3
$ TUBE 2
* TUBE 1
8.
9.
10.
11.
12.
13.
14.
15.
TIME OF DAY,PST

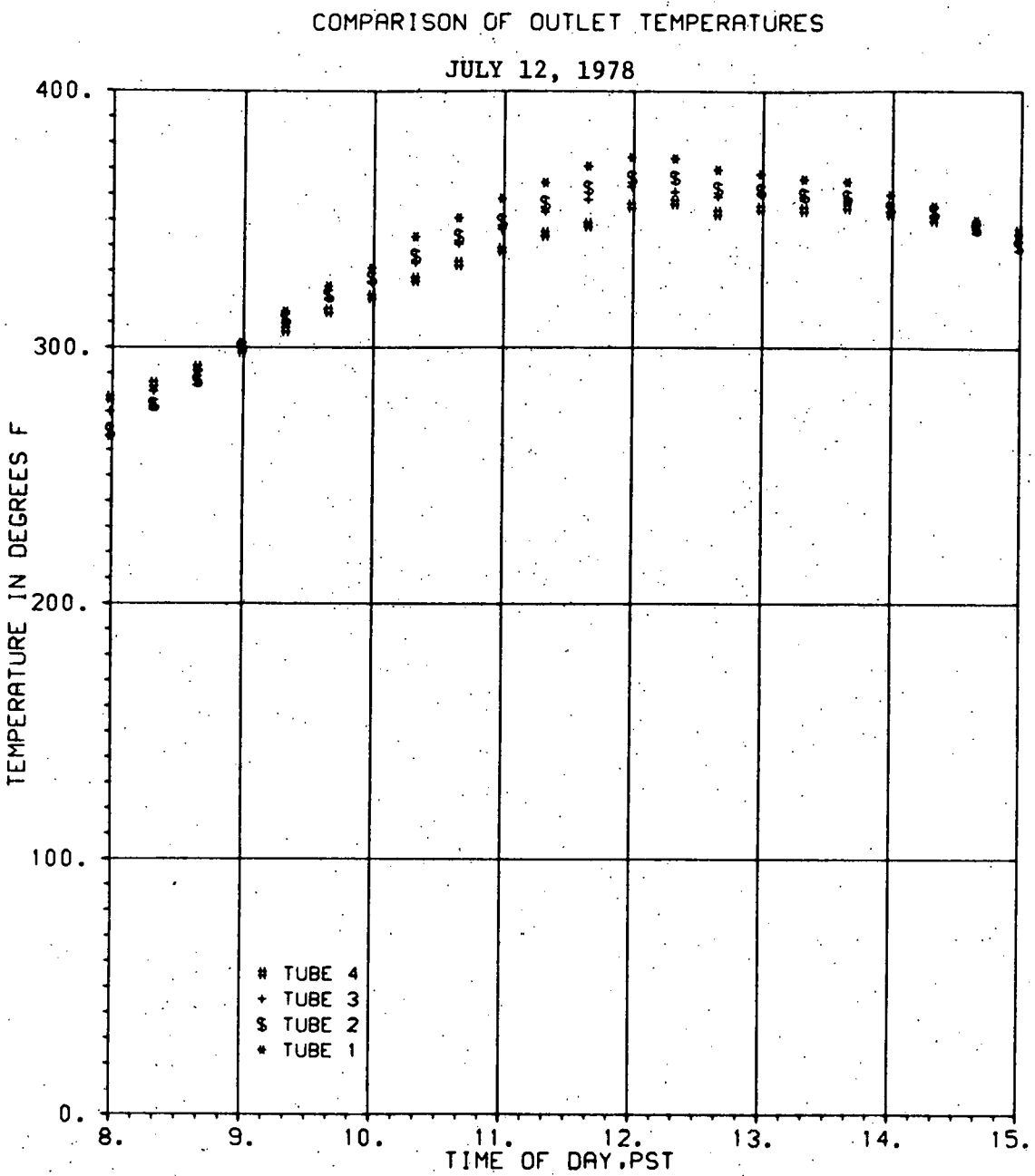
COMPARISON OF OUTLET TEMPERATURES
JULY 12, 1978
400.
300.
200.
100.
0.
TEMPERATURE IN DEGREES F
8.
9.
10.
11.
12.
13.
14.
15.
TIME OF DAY,PST
TUBE 4
+ TUBE 3
$ TUBE 2
* TUBE 1

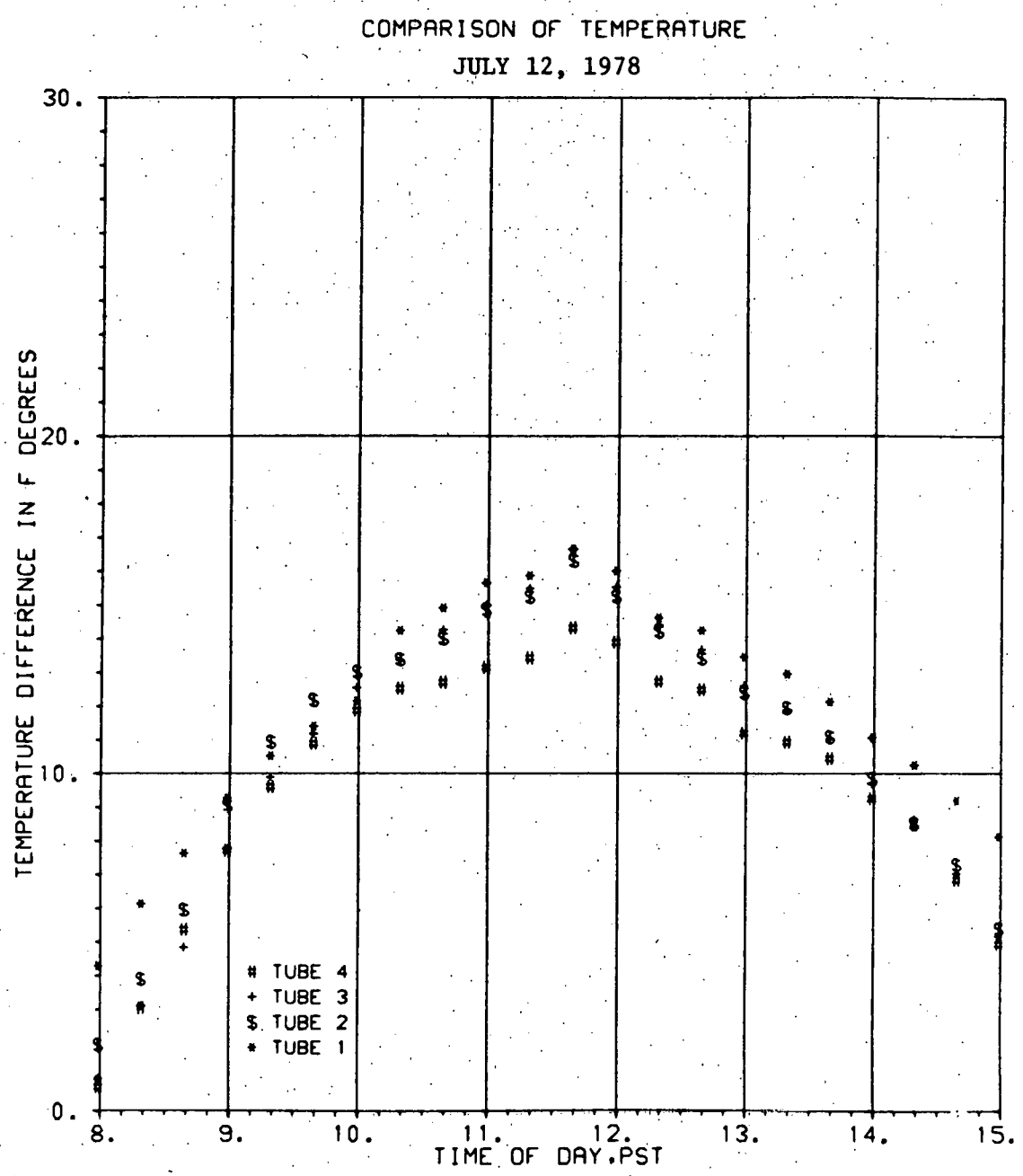
COMPARISON OF TEMPERATURE
JULY 12, 1978
TEMPERATURE DIFFERENCE IN F DEGREES
30.
20.
10.
0.
8.
9.
10.
11.
12.
13.
14.
15.
TIME OF DAY,PST
TUBE 4
+ TUBE 3
$ TUBE 2
* TUBE 1

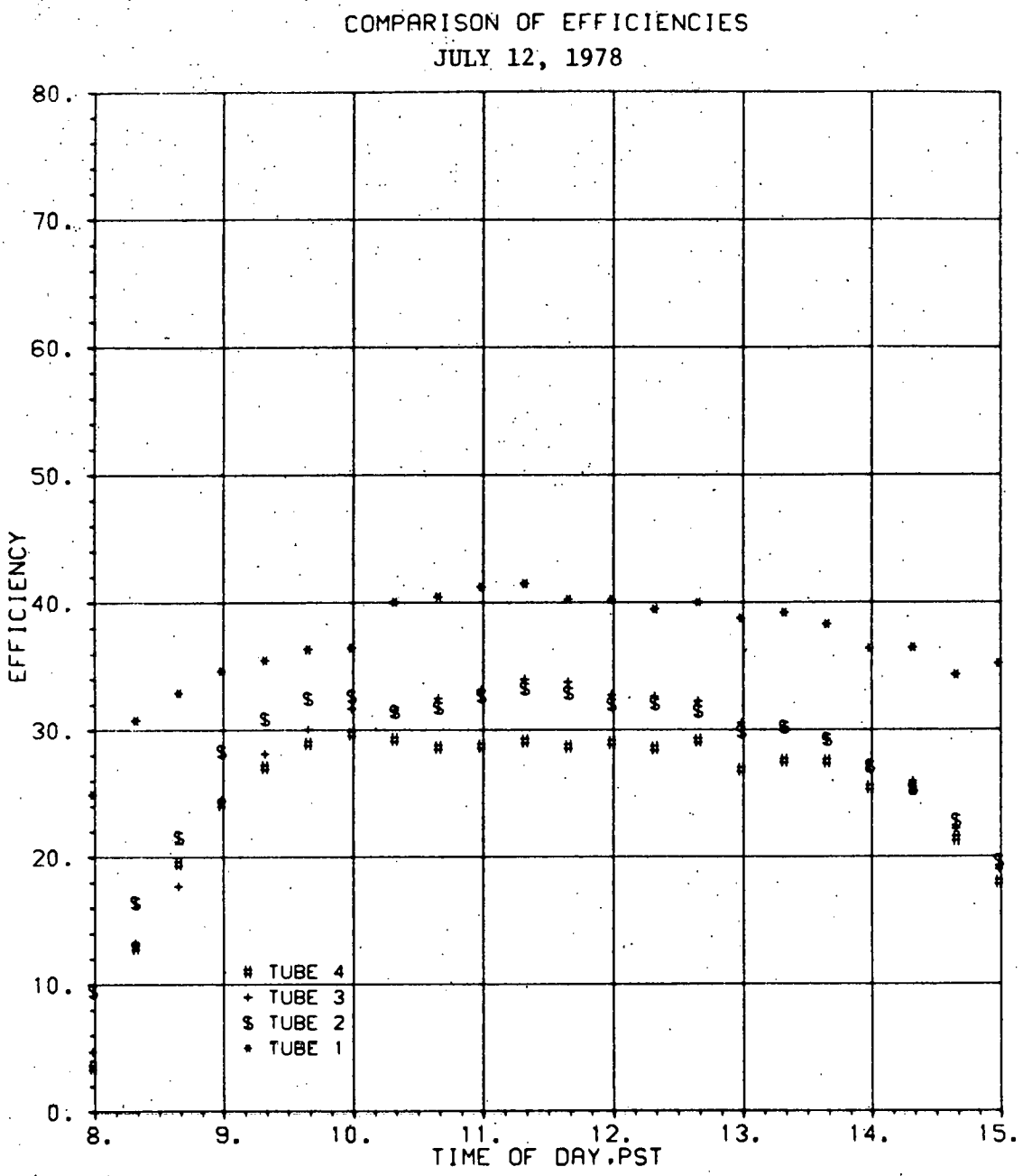
COMPARISON OF EFFICIENCIES
JULY 12, 1978
EFFICIENCY
80.
70.
60.
50.
40.
30.
20.
10.
0.
8.
9.
10.
11.
12.
13.
14.
15.
TIME OF DAY.PST
TUBE 4
+ TUBE 3
$ TUBE 2
* TUBE 1

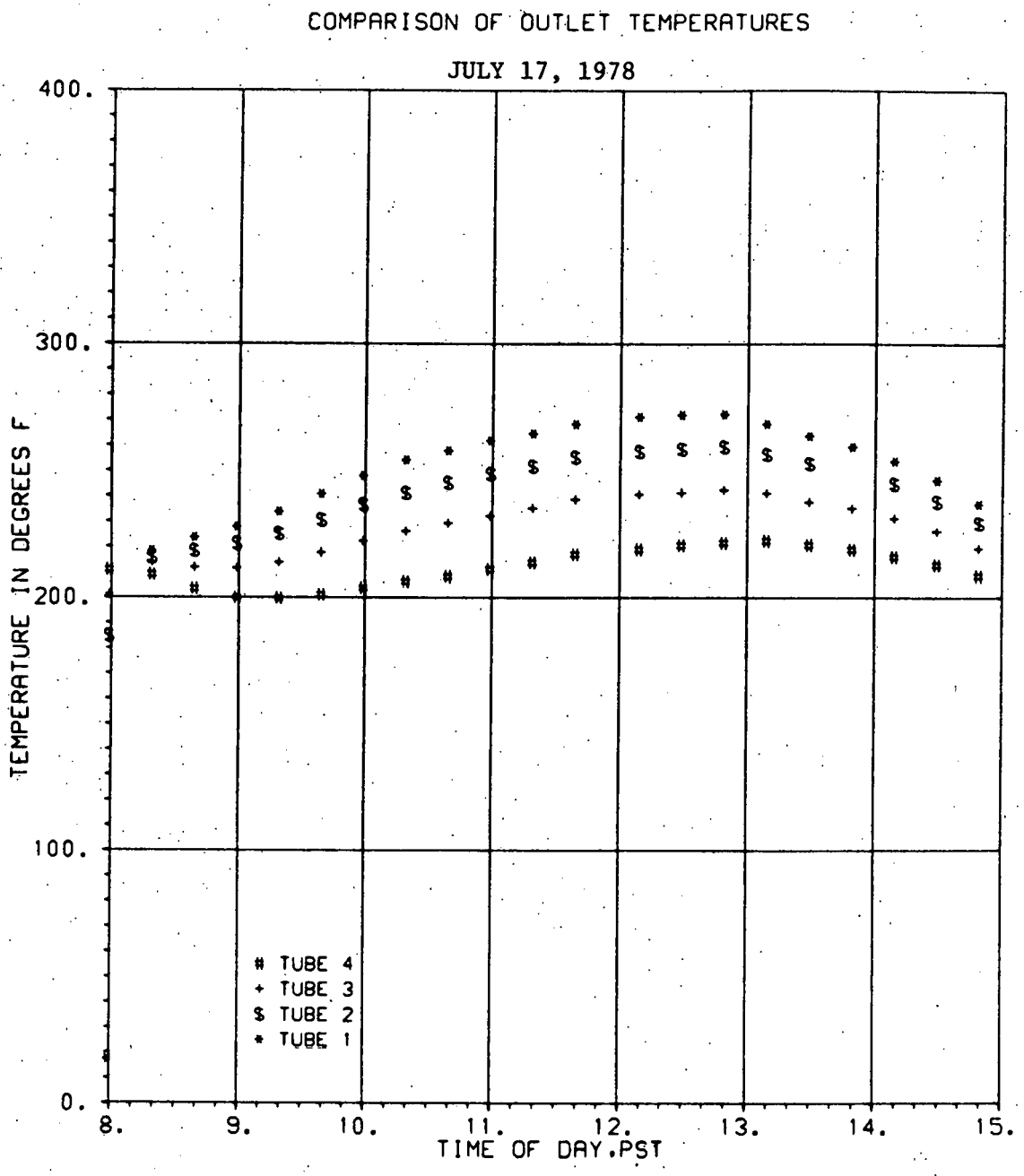
COMPARISON OF OUTLET TEMPERATURES
JULY 17, 1978
400.
300.
200.
100.
0.
TEMPERATURE IN DEGREES F
8.
9.
10.
11.
12.
13.
14.
15.
TIME OF DAY,PST
TUBE 4
+ TUBE 3
$ TUBE 2
* TUBE 1

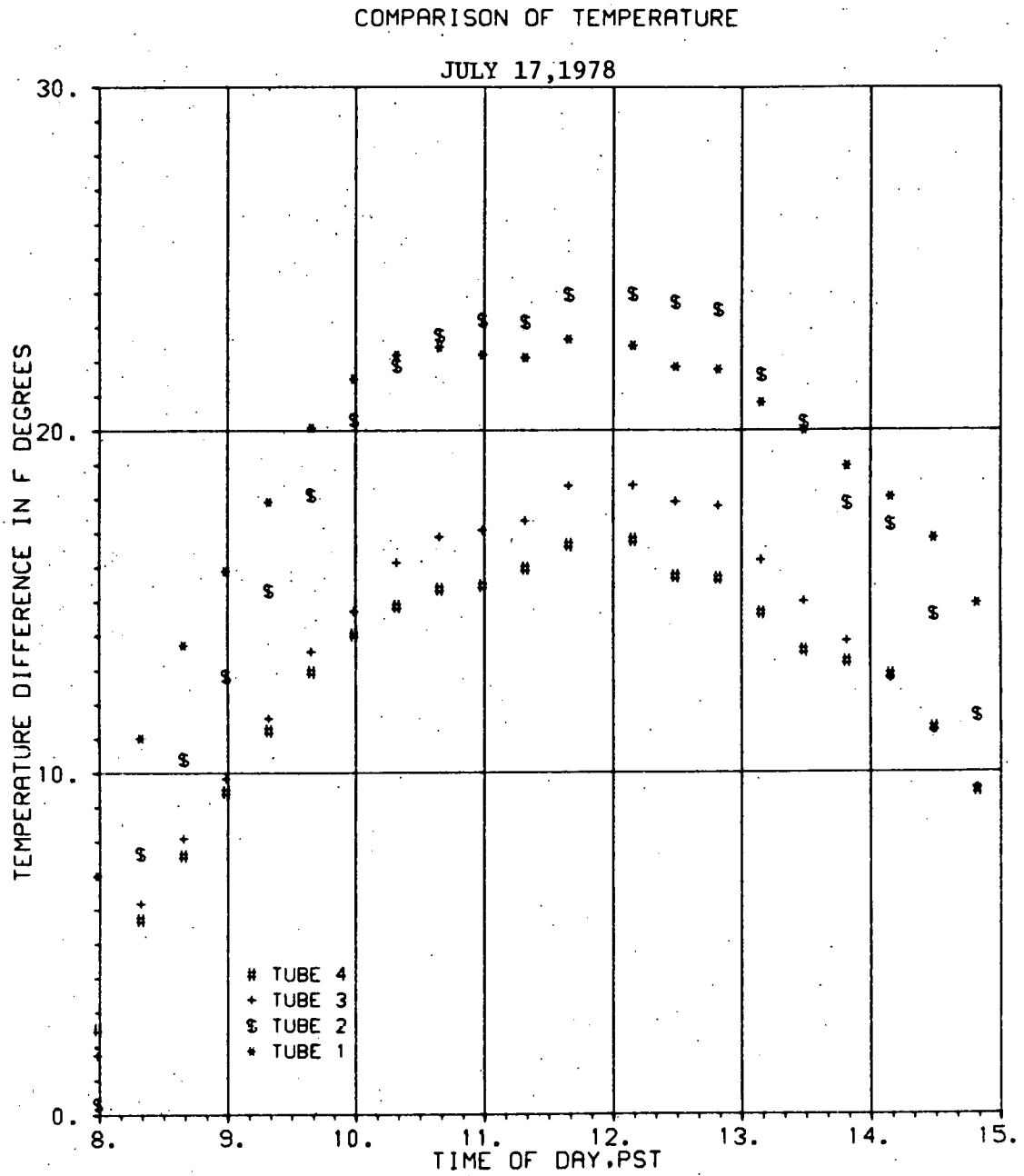
COMPARISON OF TEMPERATURE
JULY 17,1978
30.
20.
10.
0.
TEMPERATURE DIFFERENCE IN F DEGREES
8.
9.
10.
11.
12.
13.
14.
15.
TIME OF DAY,PST
TUBE 4
+ TUBE 3
$ TUBE 2
* TUBE 1

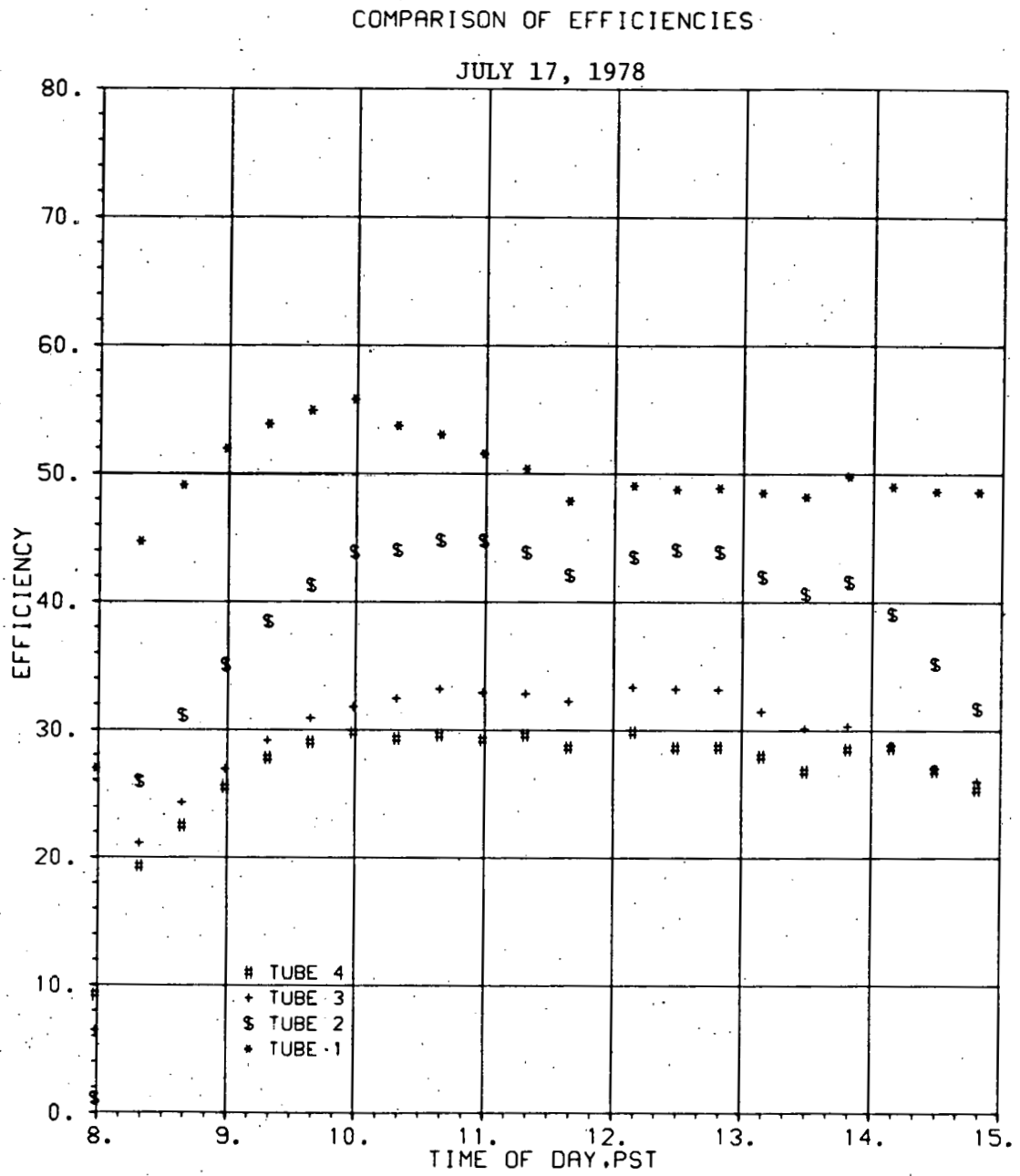
COMPARISON OF EFFICIENCIES
JULY 17, 1978
EFFICIENCY
80.
70.
60.
50.
40.
30.
20.
10.
0.
8.
9.
10.
11.
12.
13.
14.
15.
TIME OF DAY,PST
TUBE 4
+ TUBE 3
$ TUBE 2
* TUBE 1

APPENDIX B

TYPICAL CURVES AND DATA PRESENTED FOR DAILY TOTAL USEFUL HEATS AND AVERAGE DAILY EFFICIENCIES

The typical curves are based on weather data for the city of Burbank, California in 1962. These curves are generated using the Burbank weather data and a simplified thermal model, and are presented here to demonstrate the year-round trends. Direct comparison between these curves and the data points is not valid.

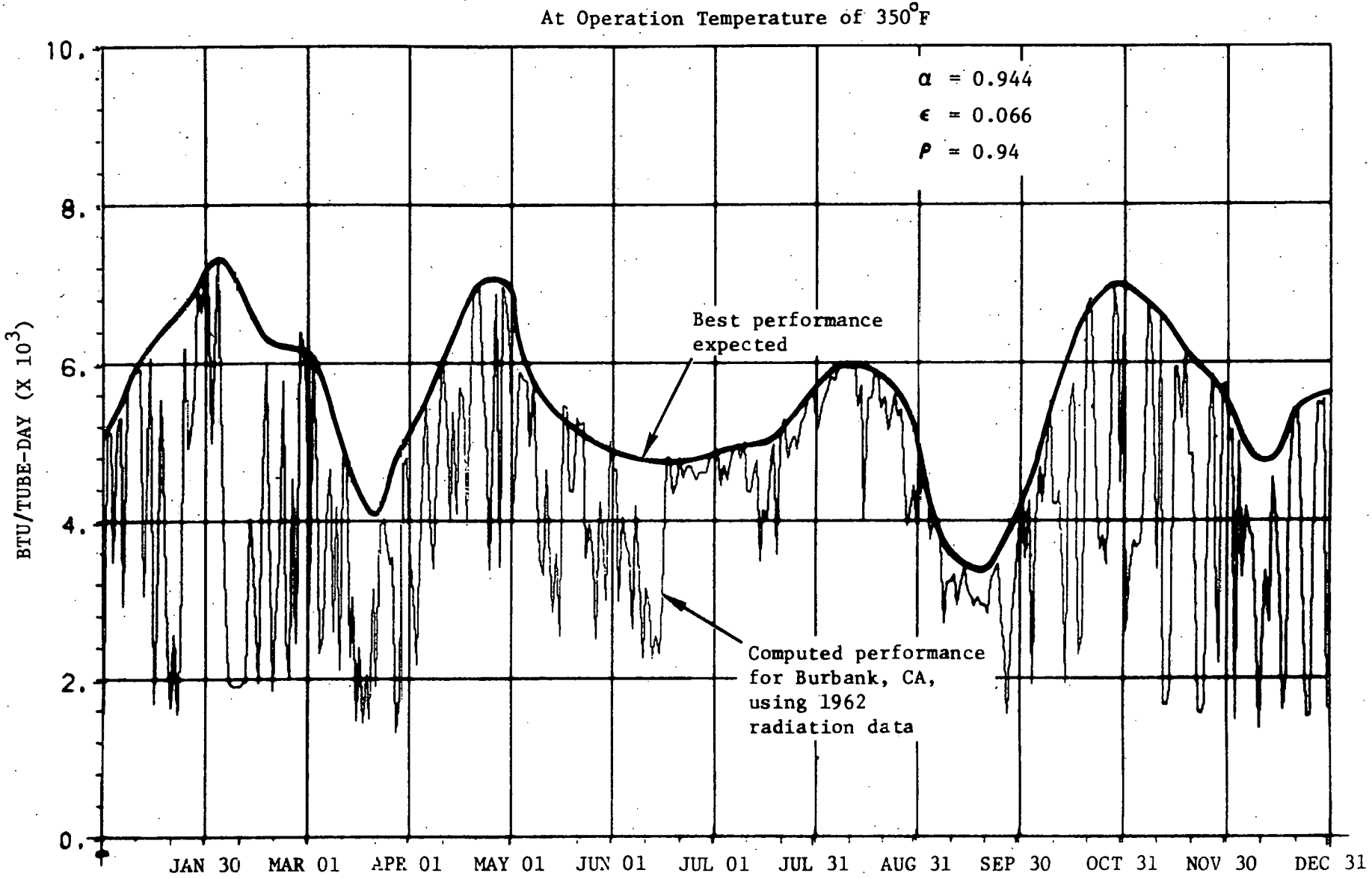

Figure B-1. Useful Heats; Typical Yearly Performance

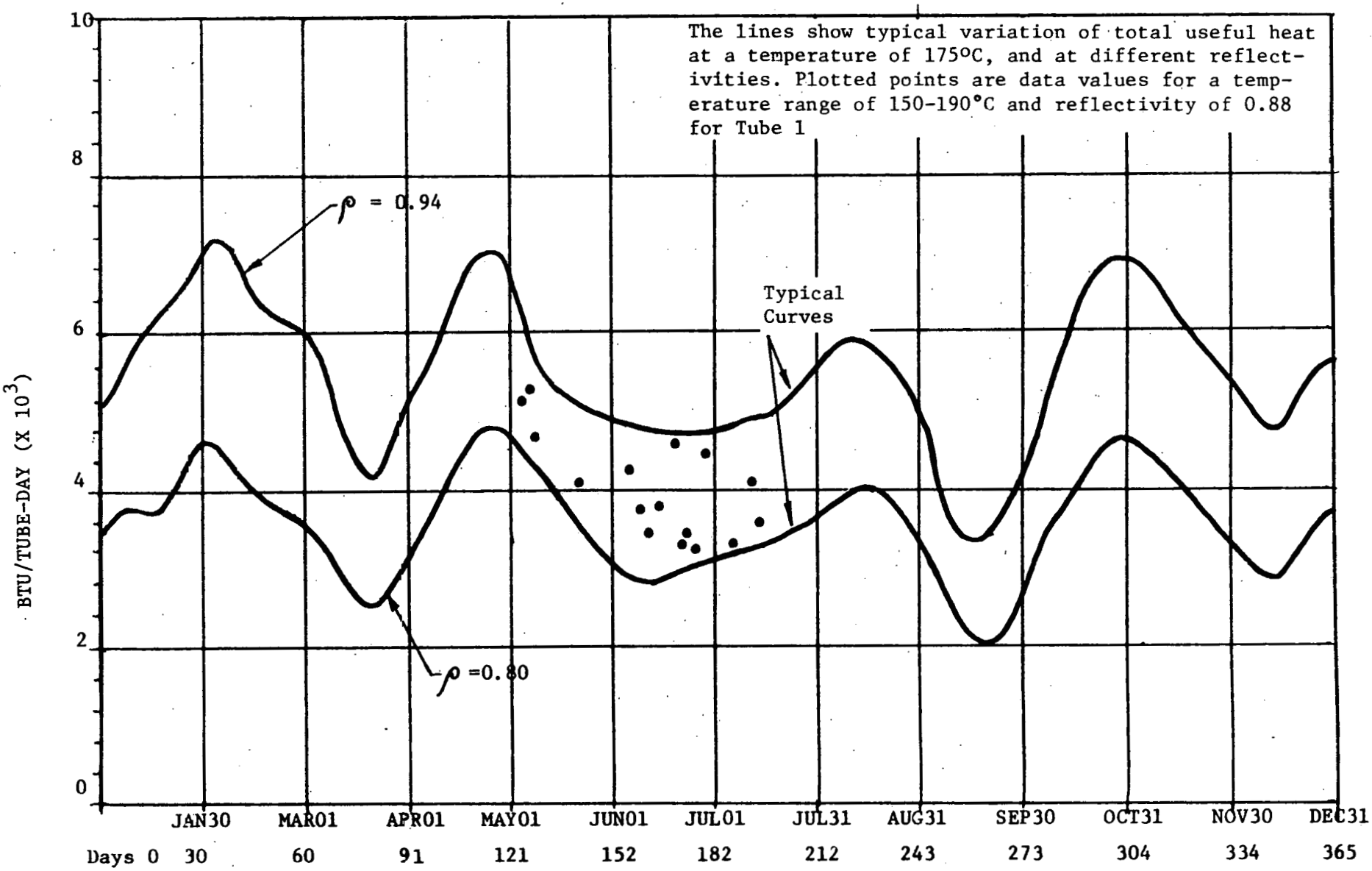

Figure B-2. Useful Heat for Tube 1

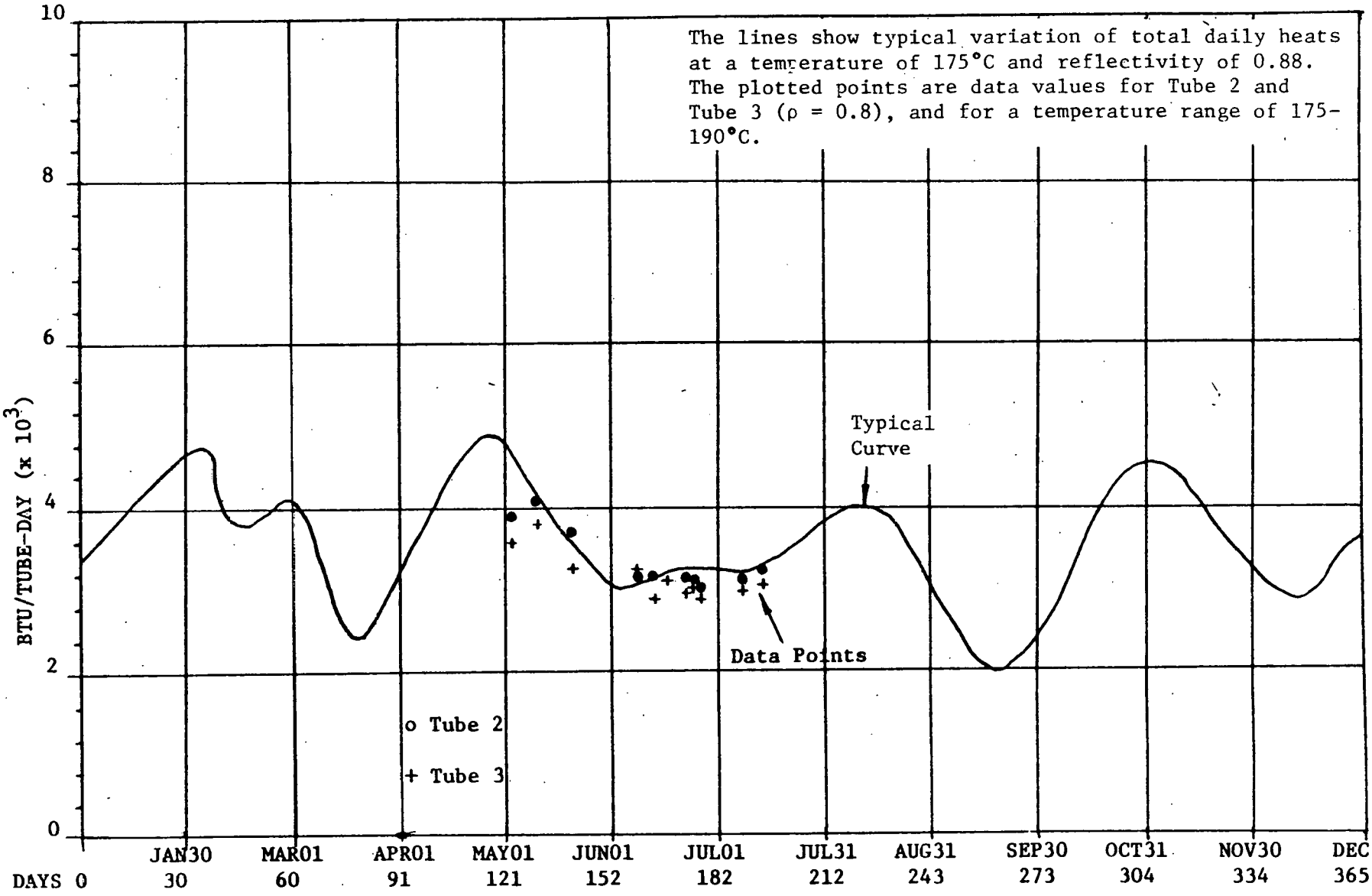

Figure B-3. Useful Heats for Tubes 2 and 3

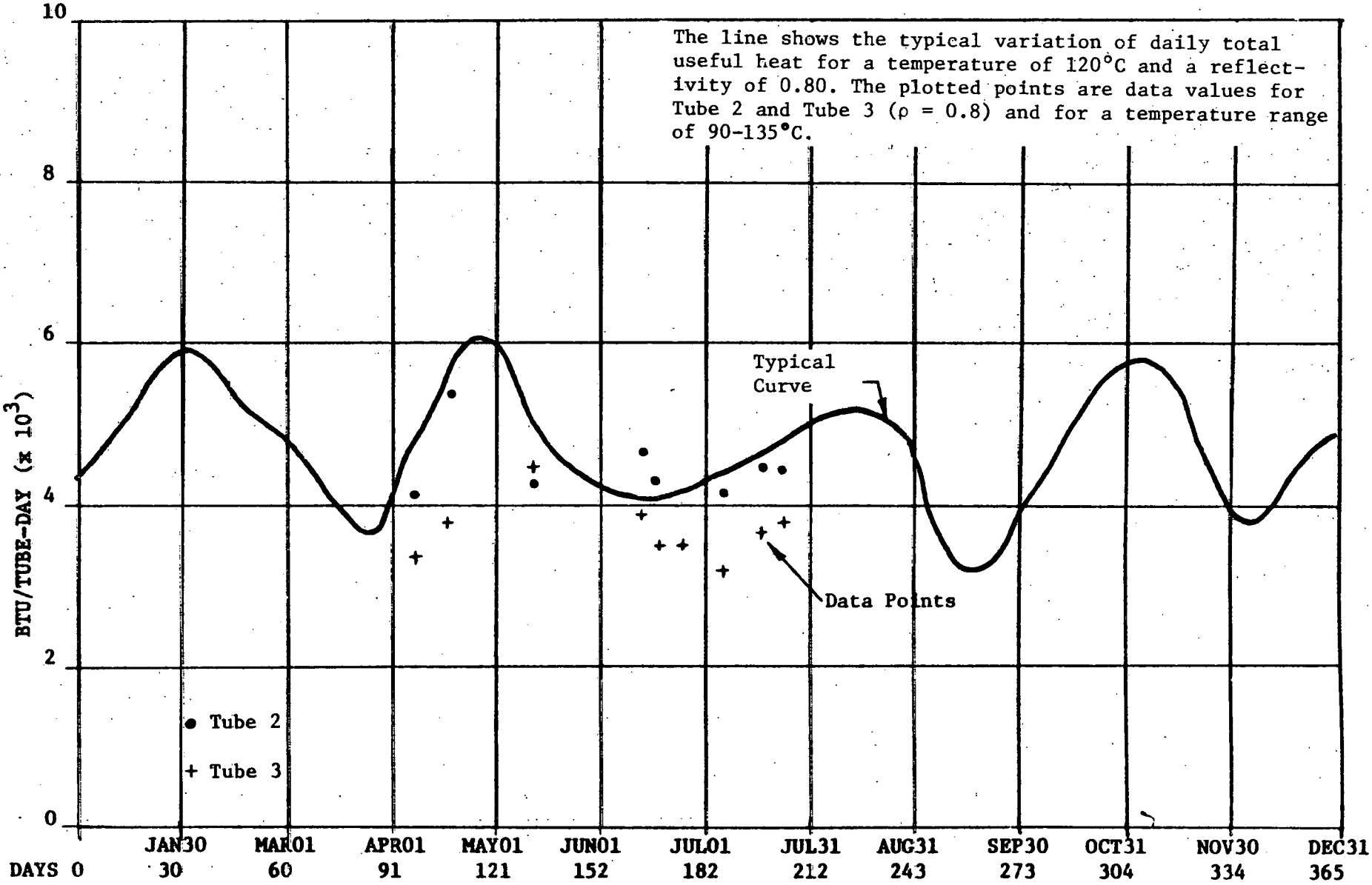

Figure B-4. Useful Heats for Tubes 2 and 3

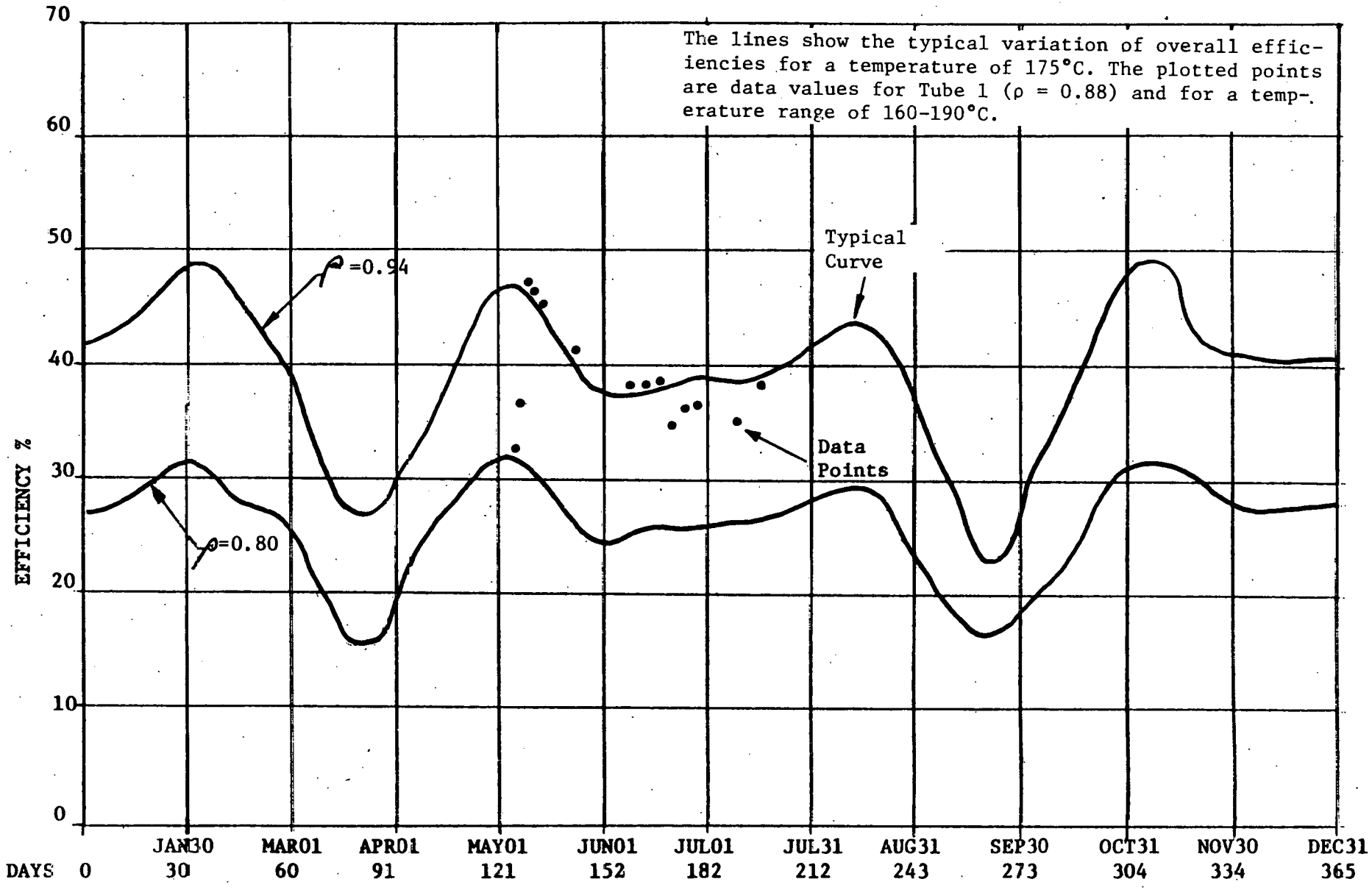

Figure B-5. Overall Collector Efficiency for Tube 1

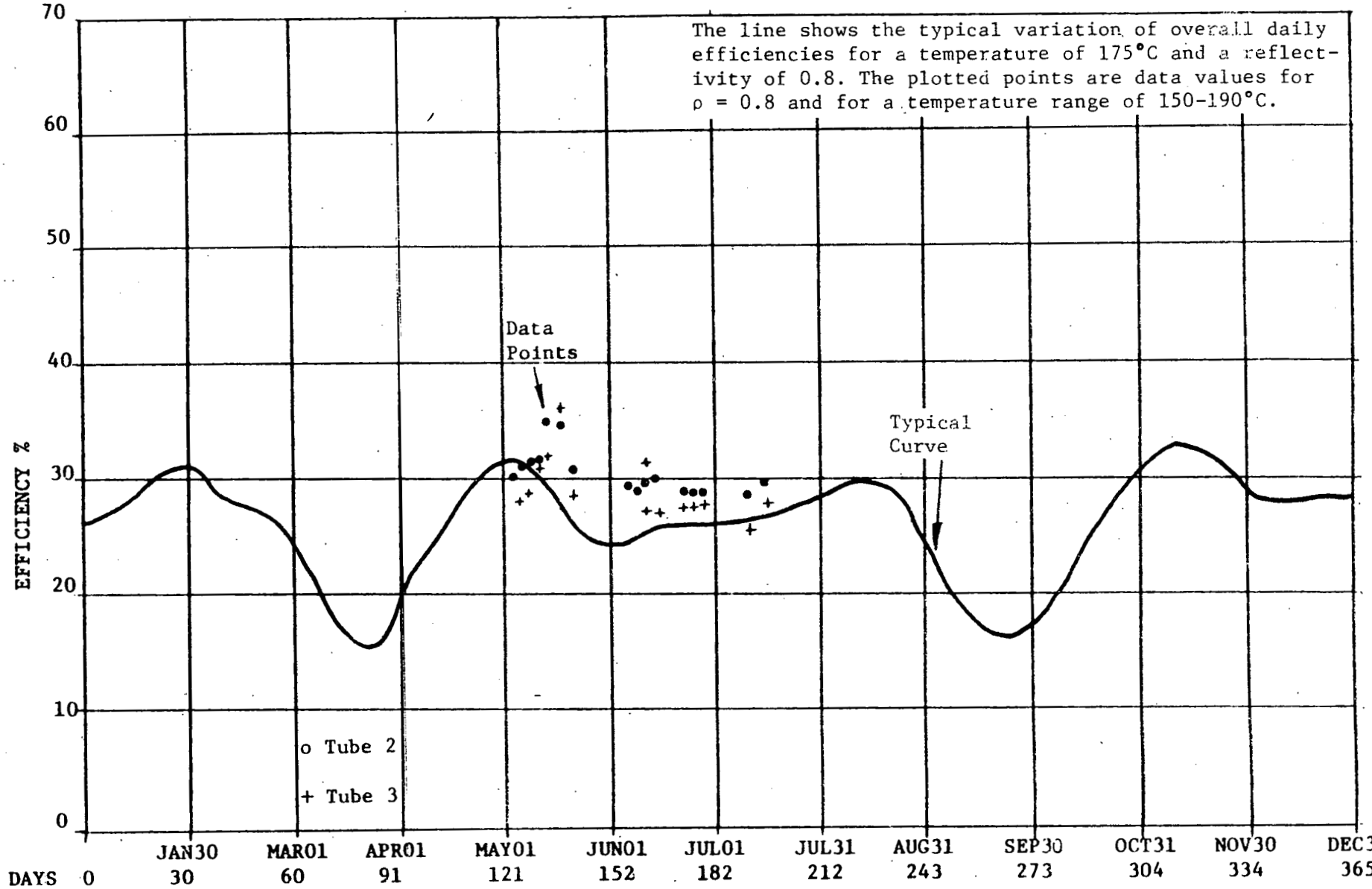

Figure B-6. Overall Collector Efficiency for Tubes 2 and 3

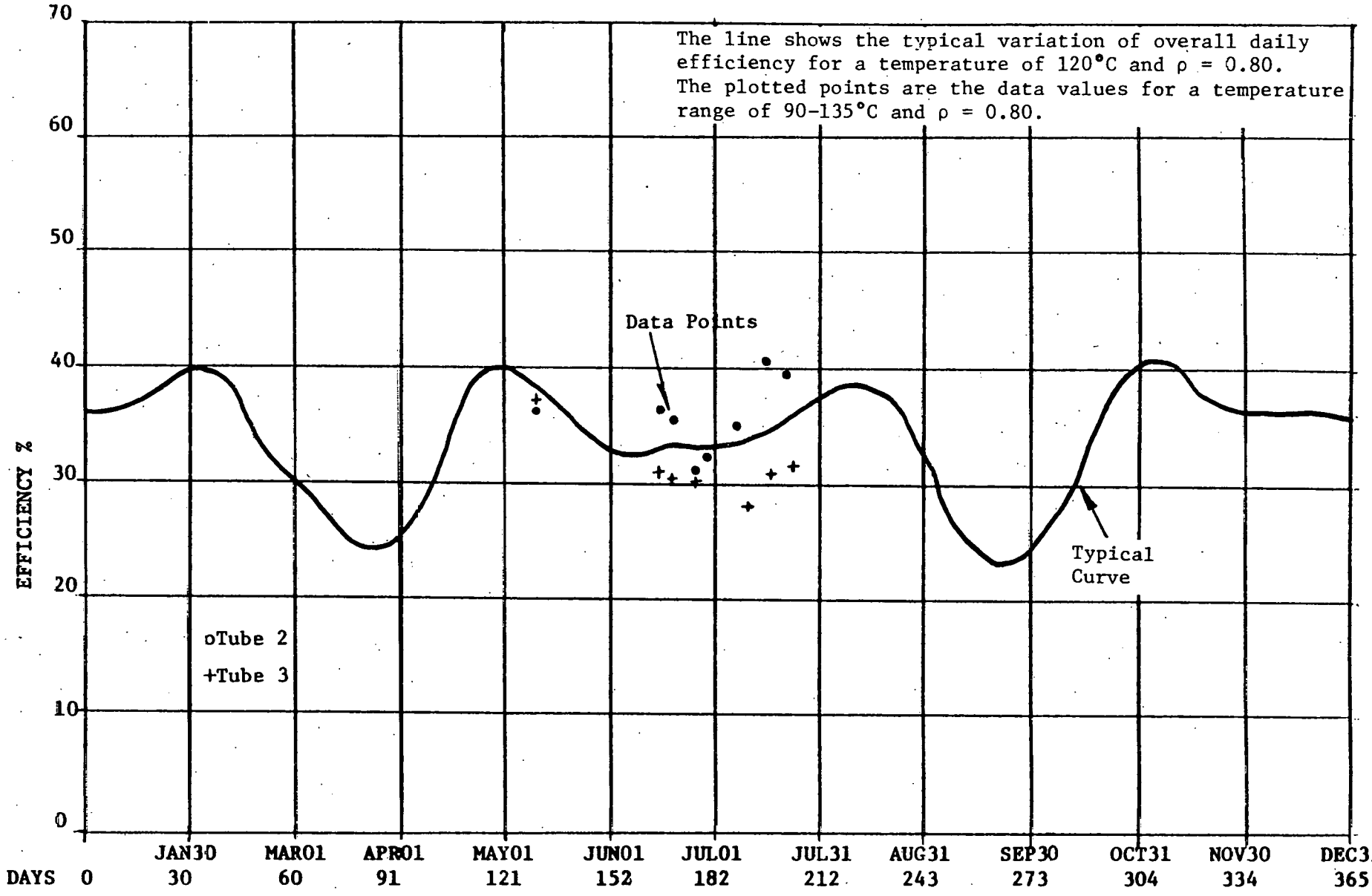

Figure B-7. Overall Collector Efficiency for Tubes 2 and 3

APPENDIX C

PROPERTIES OF THERMINOL 44

The following tables, charts and equations, give the properties of Therminol 44 as used in the calculations. The graphs and charts have been provided by Monsanto Chemicals.

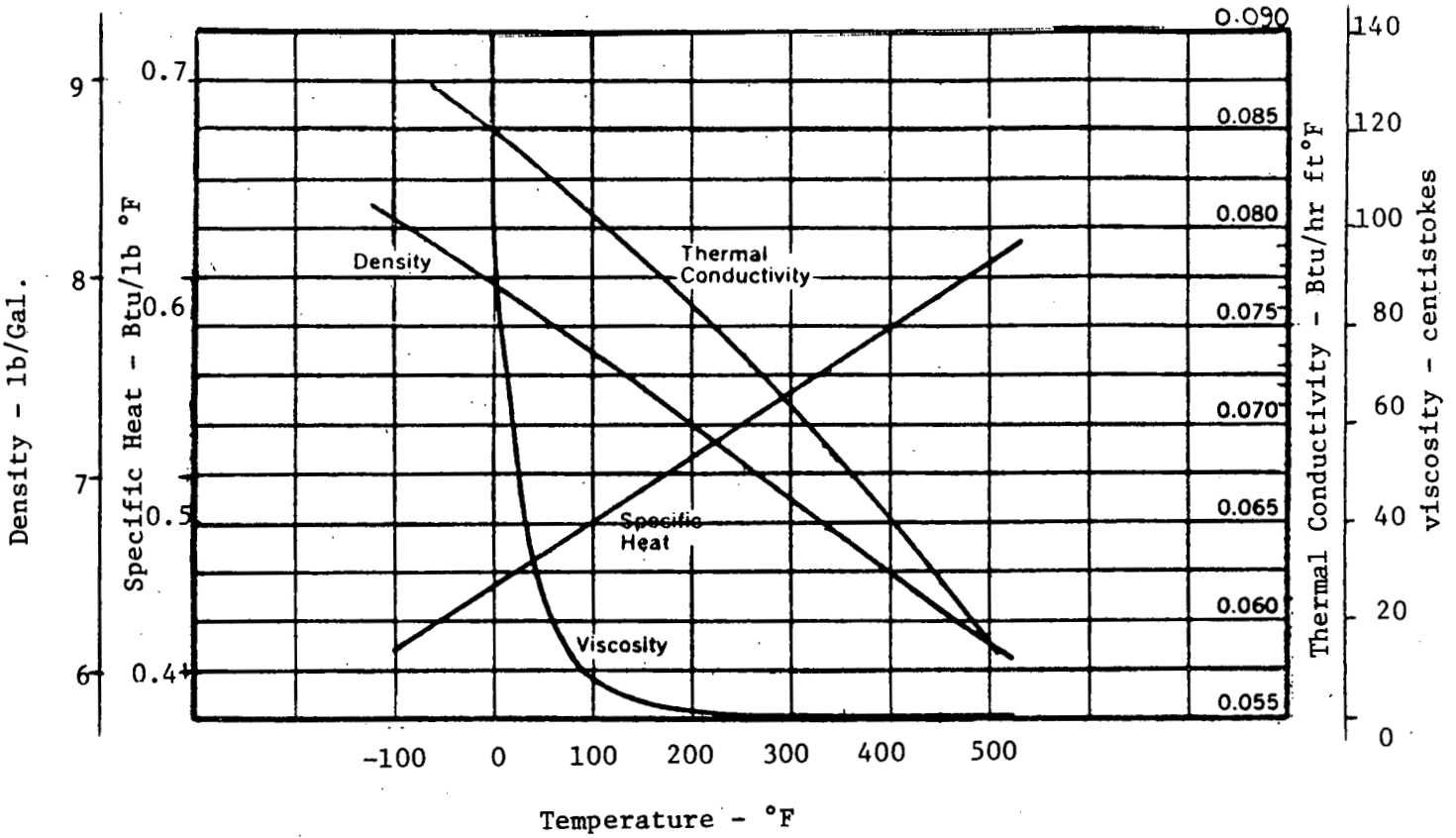

Therminol 44 - Physical Properties

Approximating equations for specific gravity and density, as functions of temperature are as follows:

$cp = 1.855 + .0028T$	(kJ/kg °C), T in °C
$cp = 0.443 + .0033T$	(Btu/lb°F), T in °F
$\rho = 952.8 - .88T$	(kg/m^2) , T in °C
$\rho = 59.48 - .0269T$	(lb/ft^3) , T in °F

TYPICAL PROPERTIES

Composition	Modified Ester Based Fluid
Appearance	Clear yellow liquid
Odor	Faint
Pour Point	−80° to −90°F. (−62° to −68°C.)
Density @ 75°F.	7.67 lbs./gal.
Flash Point, coc.	405°F. (207°C.)
Fire Point, coc.	438°F. (225°C.)
AIT	705°F. (374°C.)
Coefficient of Expansion	0.0008 cc/cc/°C.
Boiling Range:	
10%	638°F. (337°C.)
90%	734°F. (390°C.)
Average Molecular Weight	367

VARIATION OF PROPERTIES WITH TEMPERATURE

Temperature		Density			Specific Heat		Thermal Conductivity		Viscosity		Vapor Pressure	
°F	°C	lbs./gal.	lb./ft.³	Kg./m.³	BTU/lb. °F	Kcal./Kg. °C	BTU/ft. hr. °F	Kcal./m. hr. °C	μ lb./hr. ft.	ν cs	mmHg. absolute	Kg./cm.²
−65	−53.8	8.18	61.2	980	0.421	0.421	0.0874	0.1301	6321	6450	—	—
−50	−45.6	8.13	60.8	974	0.426	0.426	0.0866	0.1290	1948	2000	—	—
0	−17.8	7.95	59.5	953	0.443	0.443	0.0847	0.1261	119	125	—	—
50	10.0	7.78	58.2	932	0.459	0.459	0.0828	0.1233	22.8	24.5	—	—
100	37.8	7.63	57.1	915	0.476	0.476	0.0806	0.1200	8.05	8.80	—	—
150	66	7.43	55.6	890	0.492	0.492	0.0782	0.1164	3.92	4.40	—	—
200	93	7.23	54.1	867	0.508	0.508	0.0760	0.1132	2.34	2.70	—	—
250	121	7.05	52.8	845	0.524	0.524	0.0736	0.1096	1.54	1.82	<0.2	—
300	149	6.88	51.5	825	0.542	0.542	0.0709	0.1056	1.07	1.30	0.6	—
350	177	6.69	50.1	802	0.558	0.558	0.0680	0.1013	0.84	1.05	2.0	0.0027
400*	204	6.51	48.7	780	0.574	0.574	0.0651	0.0969	0.66	0.85	5.5	0.0075
450	232	6.32	47.3	757	0.590	0.590	0.0620	0.0923	0.52	0.69	20	0.027
500	260	6.14	46.0	736	0.607	0.607	0.0587	0.0874	0.42	0.57	47	0.064

This data is based upon samples tested in the laboratory and is not guaranteed for all samples.

APPENDIX D

PUBLICATIONS AND PRESENTATIONS RELATED TO THE VEE-TROUGH EVACUATED COLLECTOR

1. Selçuk, M. K., "A Fixed Collector Employing Reversible Vee-Trough Concentrator and a Vacuum Tube for High Temperature Solar Energy Systems," Proceedings 11th Intersociety Energy Conversion Engineering Conference, 1976, State Line, Nevada, Paper No. 769222.

2. Selçuk, M. K., "Fixed Flat Plate Collector with a Reversible Vee-Trough Concentrator," ASME Paper No. 76-WA/HT-12, New York, N.Y., December 1976.

3. Selçuk, M. K., "A Vacuum Tube Vee-Trough Collector for Solar Heating and Air Conditioning Applications," ERDA, U. of Miami Forum on Solar Heating and Cooling, Miami Beach, FL, December 1976.

4. Selçuk, M. K., "A Fixed Moderately Concentrating Collector with Reversible Asymmetric Vee-Trough and Vacuum Tube Receiver, "ERDA Concentrating Collectors Conference, Atlanta, GA, September 1977.

5. Selçuk, M. K., "Experimental Evaluation of a Fixed Collector Employing Vee-Trough Concentrator and Vacuum Tube Receivers," for Presentation at the American Society of Mechanical Engineers 1977 Winter Annual Meeting, Atlanta, GA.

6. Selçuk, M. K., "A Fixed Tilt Solar Collector Employing Reversible Vee-Trough Reflectors and Vacuum Tube Receivers," Presentation Only ERDA Contractors Meeting Solar Heating and Cooling Branch, Reston, Virginia, Aug. 8-10, 1977.

7. Selçuk, M. K., "A Fixed Tilt Solar Collector Employing Reversible Vee-Trough Reflectors and Vacuum Tube Receivers for Solar Heating and Cooling Systems," Phase I Final Report DOE/JPL/1024-1, January 1978.